1

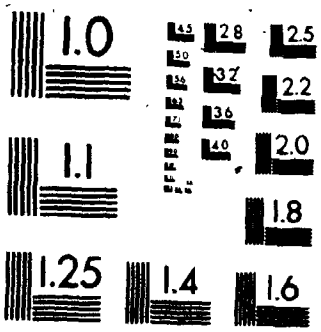

0-315-01652-5

National Library of Canada | Bibliothèque nationale du Canada | CANADIAN THESES ON MICROFICHE | THÈSES CANADIENNES SUR MICROFICHE

49539

NAME OF AUTHOR/NOM DE L'AUTEUR Mohamed EL-Said Said Issa

TITLE OF THESIS/TITRE DE LA THÈSE "Application of Boundary Element Method to Certain Elasticity problems."

UNIVERSITY/UNIVERSITÉ Carleton University

DEGREE FOR WHICH THESIS WAS PRESENTED/ GRADE POUR LEQUEL CETTE THÈSE FUT PRÉSENTÉE M. Eng.

YEAR THIS DEGREE CONFERRED/ANNÉE D'OBTENTION DE CE DEGRÉ 1980

NAME OF SUPERVISOR/NOM DU DIRECTEUR DE THÈSE J. L. Humar

Permission is hereby granted to the NATIONAL LIBRARY OF CANADA to microfilm this thesis and to lend or sell copies of the film.

The author reserves other publication rights, and neither the thesis nor extensive extracts from it may be printed or otherwise reproduced without the author's written permission.

L'autorisation est, par la présente, accordée à la BIBLIOTHÈQUE NATIONALE DU CANADA de microfilmer cette thèse et de prêter ou de vendre des exemplaires du film.

L'auteur se réserve les autres droits de publication; ni la thèse ni de longs extraits de celle-ci ne doivent être imprimés ou autrement reproduits sans l'autorisation écrite de l'auteur.

DATED/DATÉ Aug. 15, 1980 SIGNED/SIGNÉ Mohamed Issa

PERMANENT ADDRESS/RÉSIDENCE FIXE 10 street 72 - Cairo - Egypt
AL-MAADY

NL-91 (11-78)

National Library of Canada
Collections Development Branch

Canadian Theses on
Microfiche Service

Bibliothèque nationale du Canada
Direction du développement des collections

Service des thèses canadiennes
sur microfiche

NOTICE

The quality of this microfiche is heavily dependent upon the quality of the original thesis submitted for microfilming. Every effort has been made to ensure the highest quality of reproduction possible.

If pages are missing, contact the university which granted the degree.

Some pages may have indistinct print especially if the original pages were typed with a poor typewriter ribbon or if the university sent us a poor photocopy.

Previously copyrighted materials (journal articles, published tests, etc.) are not filmed.

Reproduction in full or in part of this film is governed by the Canadian Copyright Act, R.S.C. 1970, c. C-30. Please read the authorization forms which accompany this thesis.

THIS DISSERTATION
HAS BEEN MICROFILMED
EXACTLY AS RECEIVED

AVIS

La qualité de cette microfiche dépend grandement de la qualité de la thèse soumise au microfilmage. Nous avons tout fait pour assurer une qualité supérieure de reproduction.

S'il manque des pages, veuillez communiquer avec l'université qui a conféré le grade.

La qualité d'impression de certaines pages peut laisser à désirer, surtout si les pages originales ont été dactylographiées à l'aide d'un ruban usé ou si l'université nous a fait parvenir une photocopie de mauvaise qualité.

Les documents qui font déjà l'objet d'un droit d'auteur (articles de revue, examens publiés, etc.) ne sont pas microfilmés.

La reproduction, même partielle, de ce microfilm est soumise à la Loi canadienne sur le droit d'auteur, SRC 1970, c. C-30. Veuillez prendre connaissance des formules d'autorisation qui accompagnent cette thèse.

LA THÈSE A ÉTÉ
MICROFILMÉE TELLE QUE
NOUS L'AVONS REÇUE

Ottawa, Canada
K1A 0N4

NL 339 (Rev. 8/80)

APPLICATION OF BOUNDARY ELEMENT METHOD TO CERTAIN ELASTICITY PROBLEMS

by

M. E. Said Issa, B.Sc. Eng.

A thesis submitted to the
Faculty of Graduate Studies and Research
in partial fulfillment of the requirements for the degree of
MASTER OF ENGINEERING

Department of Civil Engineering
Faculty of Engineering
Carleton University
Ottawa, Canada

July 1980

The undersigned recommend to the

Faculty of Graduate Studies and Research acceptance of the thesis:

"APPLICATION OF BOUNDARY ELEMENT METHOD TO

CERTAIN ELASTICITY PROBLEMS"

submitted by M. E. Said Issa, B.Sc. Eng., in

partial fulfillment of the requirements for the degree of

MASTER OF ENGINEERING

Thesis Supervisor

Chairman,
Department of Civil Engineering

Carleton University

Ottawa, Canada

August 1980

ABSTRACT

The mathematical basis for the formulation of the boundary element method is reviewed. The method is then applied to certain elasticity problems such as a disc with internal pressure and a circular cavity under internal pressure in an infinite medium. The results are compared with known classical solutions.

A combined boundary element - finite element method is then developed to study the behaviour of a beam on elastic half-space. The effect of certain parameters on the displacements of the beam and on the distribution of bending moments and shearing forces is studied.

It is noted that since the boundary element method involves discretization of only the boundary, the time required to prepare input data for any analysis is much less than would be required for a comparable analysis by domain methods, e.g. the finite elements. The method also provides a convenient way of modelling infinite domains without the need for truncating it at an arbitrary distance away from the region of interest. Another feature of the method is that the values of the function under consideration are calculated at only those internal points of the domain where they are needed. Finally, the method can be combined with the finite element method to deal with situations where neither the boundary element method nor the finite element method is appropriate by itself.

ACKNOWLEDGEMENTS

The author is grateful for the guidance and encouragement offered by his supervisor, Professor J. L. Humar, throughout the course of this research programme. Professor Humar made himself available for consultation and discussions at all times. The author expresses his unbounded gratitude to him.

The author is also grateful to Professors W. H. Bowes and A. P. S. Selvadurai, for their assistance and their many valuable suggestions.

This research would not have been possible without the scholarship awarded to the author by Carleton University.

The author appreciates the care and attention of Miss Diane Dodds for typing the manuscript.

Grateful thanks are also due to the author's family and friends, especially Mr. M. O. Faruque and Mr. H. A. Khattab, for their support and encouragement during the preparation of the thesis.

Last but not the least, special thanks are due to the author's fiancee for her encouragement throughout the duration of this study.

To my mother

TABLE OF CONTENTS

Abstract

Acknowledgements

List of Figures

List of Tables

CHAPTER 1: INTRODUCTION 1

1.1 General 1
1.2 Boundary Element Method 2
1.3 Review of Past Work 4
1.4 Scope of the Present Study 7
1.5 Format of the Thesis 8

CHAPTER 2: FORMULATION OF THE BOUNDARY ELEMENT METHOD 11

2.1 Introduction 11
2.2 Linear Theory of Elasticity 11
2.3 Basic Relationships 14
2.4 Fundamental Solution 16
2.5 Boundary Element Discretization 20

2.5.1 Constant Boundary Element 21

2.5.1.1 Solution Technique 24
2.5.1.2 Body Forces 27
2.5.1.3 Numerical Solution of the Integral Equation 29

2.5.2 Linear Boundary Element 31

2.5.2.1 Numerical Solution of the Integral Equation 37

CHAPTER 3: APPLICATION OF BOUNDARY ELEMENT METHOD TO CERTAIN ELASTICITY PROBLEMS 51

3.1 Finite Domain Problems 51

3.1.1 Disc Under Internal Pressure 51
3.1.2 Bodies with More Than One Surface 55

3.2 Infinite Medium Problem 57
3.3 Comments 58

CHAPTER 4: COMBINATION OF BOUNDARY AND FINITE ELEMENTS IN ELASTOSTATICS 74

4.1 Introduction 74
4.2 The Relationship Between Finite and Boundary Elements 75

4.2.1 Equivalent Finite Element Approach 75
4.2.2 Equivalent Boundary Element Approach 82

4.3 Applications 84

CHAPTER 5: COMBINATION OF BOUNDARY AND FINITE ELEMENT FOR THE ANALYSIS OF BEAMS RESTING ON HOMOGENEOUS ELASTIC HALF-SPACE 92

5.1 Introduction 92
5.2 Relationship Between Soil Parameters and Coefficient of Subgrade Reaction 93
5.3 Relative Rigidity of the Beam 95
5.4 Finite Element Representation of the Beam Element 96
5.5 Equivalent Finite Element Approach 99
5.6 Computer Program for the Equivalent Finite Element Approach 100
5.7 Equivalent Boundary Element Approach 102
5.8 Computer Program for the Equivalent Boundary Element Approach 104
5.9 Analytical Results 106

5.9.1 Comparison Between the Equivalent Finite Element and Boundary Element Approach 106
5.9.2 Effect of the Finite Representation of Infinite Boundary 107
5.9.3 Effect of Relative Rigidity 107
5.9.4 Effect of Load Location 108

5.10 Comments 109

CHAPTER 6: SUMMARY AND CONCLUSIONS 131

6.1 Summary and Conclusions 131
6.2 Recommendation for Future Work 133

Appendix A 134

Appendix B 139

Appendix C 141

Appendix D 144

REFERENCES 148

LIST OF FIGURES

1.1	Nodes for the Representation of Functions	10
2.1	Notations for Force, Stress and Displacement	40
2.2	Definitions of the Domain and the Boundary	41
2.3	Fundamental Solution for the Three Dimensional Case (Kelvin Solution)	42
2.4	Geometrical Definitions for the Points P and Q	43
2.5	Two Dimensional Body Divided into Boundary Element	44
2.6a	Point (P) Approach a Flat Boundary	45
2.6b	Representation of Boundary Surface S* by a Semi-Circle for the Purposes of Integration	45
2.7	Two-Dimensional Body Divided into Boundary Elements and Internal Cells	46
2.8a	Element Definitions	47
2.8b	Geometrical Definitions for an Element and its Terminal Points	47
2.9a	Procedure for (P) Approaching Boundary Corner of Included Angle α	48
2.9b	Boundary Surface Γ_{s*} Assumed Part of Circle for Integration Purposes	48
2.10	Linear Boundary Element	49
2.11	A Typical Boundary Modelled by Linear Boundary Element	50
2.12	Geometrical Definition for the Points M and F	51
3.1	Thin Disc with Internal Pressure	59
3.2	Finite Element Mesh	60
3.3	Constant Boundary Element Discretization	61
3.4	Linear Boundary Element Discretization	62
3.5	Comparison of Exact Solution with Finite Element and Boundary Element Solution	63
3.6	Body with Holes	64
3.7	Boundary Element Discretization	65
3.8	Stress in a Disc with Internal Pressure	66
3.9	Circular Cavity Under Internal Pressure	67
3.10	Boundary Element Discretization for Circular Cavity	68
3.11	Radial Stress in an Infinite Medium Subjected to Internal Stresses in a Circular Cavity	69
4.1	Representation of Boundary Elements Domain and Finite Elements Domain	87
4.2	Body Divided into Finite Elements and Boundary Elements	88
4.3	Interpolation Functions for Boundary Elements	89
4.4	Boundary Element Region	90

5.1	Beam Element	111
5.2	Geometry of the Problem Solved by Using Equivalent Finite Element Approach and Equivalent Boundary Element Approach	112
5.3	Comparison of Displacement	113
5.4	Comparison of Shearing Force	114
5.5	Comparison of Bending Moment	115
5.6	Geometry of the Problem Solved by Equivalent Finite ELement Approach	116
5.7	Effect of Finite Representation of Infinite Boundary on Central Displacement	117
5.8	Effect of Relative Rigidity $\lambda\ell$ on Beam-Displacements	118
5.9	Effect of Relative Rigidity on Moment	119
5.10	Effect of Relative Ridigity on Shear	120
5.11	Effect of Relative Rigidity on Beam-Displacements	121
5.12	Variation of Displacement for Different Position of Load	122
5.13	Variation of Shear for Different Position of Load	123
5.14	Variation of Shear for Different Position of Load	124
5.15	Variation of Displacement for Different Load Position	125
5.16	Variation of Bending Moment for Different Load Position	126
5.17	Variation of Shear for Different Position of Load	127

LIST OF TABLES

3.1	Comparison of Radial and Hoop Stresses in a Disc Segment Obtained by the Classical and the Numerical Methods	70
3.2	Comparison of Data Input and Run Time Required	71
3.3	Comparison of Radial and Hoop Stresses in a Disc Obtained by Classical and Numerical Methods	72
3.4	Radial Stresses in an Infinite Medium Subjected to Internal Stresses in a Circular Cavity	73
4.1	Comparison of the Results Obtained by Brebbia and Present Work by Using Constant Boundary Elements	90
4.2	Comparison of the Results Obtained From Boundary Element Method and Equivalent Finite Element Approach, Using Linear Boundary Elements	91
5.1	Combined Effect of Flexural Stiffness and the Shape of Foundation	128
5.2	Comparison of the Displacements Obtained by Using Equivalent Finite Element Approach and Equivalent Boundary Element Approach	129
5.3	Effect of Finite Representation of Infinite Boundary	130

CHAPTER 1

INTRODUCTION

1.1 General

In the past twenty years, various numerical techniques have been developed for the solution of the differential or integral equations encountered in many engineering problems of stress analysis. These numerical methods can be categorized as domain or boundary methods, depending on whether the numerical analysis involves a discretization of the domain or of the boundary.

Domain type methods most commonly used are finite element methods and the finite difference methods. A brief description of these methods follows.

The basic concept of the finite element method is the discretization of the continuum into elements of finite size and the assumption of a displacements or stresses distribution within each element expressed in terms of a set of unknown nodal values. The minimization of the global potential energy yields a set of linear algebraic equations whose solution determines these unknown values. In regions where field gradients are expected to change rapidly, either smaller elements or higher order elements are used [30,2].

The finite difference method replaces the governing differential equations by the corresponding difference equations. The solution proceeds

by solving the resulting set of simultaneous equations, thereby evaluating the unknown functions at specific internal and boundary points. The number of equations involved in the solution is proportional to the number of nodes chosen for the approximation of the function. The choice of this number is governed by the fact that the accuracy is improved with the decrease in nodal spacing [24].

Domain type methods give rise to a large number of simultaneous equations because each node whether on the boundary or inside the domain contributes one or more unknown values, and a sufficient number of such nodes must be used for obtaining reasonably accurate results. However, the resulting matrices are usually banded and contain many zero elements. In some cases the domain methods prove to be inaccurate and/or unsuitable techniques. For example, problems involving infinite domains cannot be dealt with efficiently by these methods. The finite element method also requires special care in the data preparation and errors are frequent. On the other hand, complicated geometry cannot be dealt with easily when the finite difference method is used. These difficulties associated with domain type methods can be overcome in some situations by using the "Boundary Element Method".

1.2 Boundary Element Method

The term "boundary elements" originated within the Civil Engineering Department of Southampton University. It is used to indicate a method whereby the external surface of a domain is divided into a series of

elements over which the function under consideration can vary in different ways, in much the same manner as it varies over the domain in the finite element method [4]. The tractions and displacements over the elements are represented in terms of unknown nodal values of these quantities. For constant elements these nodes are taken to be in the middle of each segment. As an alternative one can use linear elements (i.e. elements for which the nodes are at the intersection of elements) or curved elements such as quadratic and the cubic elements, as shown in Figure 1.1.

When the body forces are taken into consideration the body volume has to be divided into a series of internal cells as shown in Figure 2.7. These cells resemble finite elements but are used only for the purpose of evaluation of the volume integrals and do not introduce any internal unknowns.

The boundary element method offers the following advantages over the domain type methods. Since the problem is transformed from one over the domain to one over the boundary the dimension of the problem is reduced by one (e.g. in elasticity the solution of equation over the body is replaced by the study of behaviour on the surface). This greatly simplifies the development and coding of computer programs especially in the specification of data and interpretation of results, and also reduces the number of the system of simultaneous equations to be solved.

The boundary element method is also well suited to solve problems with infinite domain such as those occuring in soil mechanics, hydraulics

and hydrodynamics, for which the classical "domain" methods are unsuitable. Another ~~important~~ advantage of the boundary element method is that the values of the functions under consideration are calculated for internal points of the domain only where they are needed.

The boundary element also has a few disadvantages. Boundary element matrices are usually fully populated. This may make the method computationally less efficient than other methods in certain applications. The boundary element method is also inefficient in handling problems where the material is anisotropic or non-homogeneous.

The boundary element method can be combined with other methods such as the finite element method to deal with situations where the boundary element method are appropriate. This implies that the weakness of one approach can be offset by the strengths of the other to form a combination more powerful than either approach. This also applies to the problem which involves infinite domain or non-homogeneous material properties.

1.3 Review of Past Work

Historically, the integral methods are a development of the method of Fredholm which consists of the application of potential theory in conjunction with the theory of linear integral equations.

Fredholm was also the first to apply the method to elasticity [9]. After this development, numerous publications on the application of Fredholm's equations appeared, but today most of these are considered to be of no

interest, because only special problems were analysed, and the mathematical treatment lacked rigor.

The early implementations of the boundary element method by Jawson and Ponter [13] and Symm [25] were, inexplicably, not followed up by further research until considerably later. Rizzo [22] and Cruse [7] applied the method to problems of elasticity. These authors demonstrated that the method could in many situations be more efficient than the finite difference or finite element methods. They pointed out that by transforming the partial differential equation to a boundary integral equation the dimension of the problem was reduced by one.

Boissenot, Lachat and Watson [1] also applied the boundary element method to plane elasticity problems. They defined the variation of displacements and tractions by linear, quadratic or cubic shape functions. The equations for unknown nodal displacements and tractions were constructed in non-dimensional form, to avoid possible numerical instability inherent in mixed systems. Brady and Bray [6] applied the method to determine the stress distribution which would exist in a rock medium after excavation of openings, and the displacements which would be introduced by excavation in the stressed medium. Cruse and Vanburen [8] applied the integral equation method to three dimensional analysis of a fracture specimen with an edge crack. In 1971, Swedlow and Cruse [26] presented an elastoplastic analysis for an isotropic compressible material subjected to strain-hardening, but gave no numerical examples. In addition, they did not present expressions for internal values of stress or strains,

which are of fundamental importance for the stepwise plasticity analysis.

Since then Mendelson[19] has presented analysis of the elastoplastic problem, accompanied by numerical results, he also gives an expression for stress and strain for two and three dimensional problems, including thermal strains. As pointed out by Mukherjee [20,15] some of these expressions are however, incorrect due to the way in which Mendelson considers the plain strain case.

J. C. F. Telles and C. A. Brebbia [27] have developed a complete formulation for the boundary element method applied to two and three dimensional plasticity problems. The correct expressions for the internal stresses are given including the derivatives of the singular integral.

The development work on the boundary element method was followed by the use of a combination of the boundary element method with the finite element method. The idea of combining both techniques can be attributed to Wexley [17], who started to use integral equation solutions to represent the unbounded field problem early in 1970.

The first combination of the two methods for elastostatics is attributed to Osies[21], although he applied the methods to wave propagation problems. A combination of the methods was used by Mei [18] in 1975 who explained the procedure for combining the two methods by using variational techniques. Brebbia and Georgiou [5] have applied this technique on two models to illustrate how the combination can be set up. To the author's knowledge this technique has not been applied

to study practical problems in soil-structure interaction, for example to the case of a beam on elastic half-space. These problems have been studied in this thesis.

1.4 Scope of the Present Study

The main objectives of this thesis can be summarized as follows:

1. To review the mathematical basis and formulation of the boundary element method; with particular reference to its application in elastostatics.

2. To develop a computer program for the solution of two dimensional elastostatic problems by the use of linear boundary element method. Application of the program to the solution of certain problems in elastostatics.

3. A review of the methods for the application of a combination of boundary element methods and finite element methods.

4. Development of a procedure and a computer program to obtain the behaviour of a beam on elastic half-space, using a combination of the boundary element methods and the finite element methods.

5. Parametric study of beams resting on half-space.

The basic formulation of the boundary element method and significant amount of information on its application to elastostatic problems exist in the literature. The author's contribution is in the study of the application of linear elements to certain problems in elastostatics and comparison of the results obtained with these obtained

by constant boundary elements and the finite element method.

The above study forms the groundwork for the more important part of this work namely the application of finite element-boundary element methods to simple problems of soil-structure interaction. The study on beams resting on half-space by the use of the above procedure is new and demonstrates the feasibility of using the approach in such cases.

1.5 Format of the Thesis

The thesis has been divided into six chapters as follows:

Chapter 1 introduces the boundary element methods as a numerical technique and presents its advantages over the domain methods such as the finite element and the finite difference methods. The possible disadvantages of the method are also described. The Chapter then presents the scope of the present study and the format of the thesis.

Chapter 2 deals with the mathematical basis of the formulation of the boundary element method as applied to elasticity problems. The formulation is presented for both the constant and the linear boundary elements.

Chapter 3 is devoted to the application of the boundary element method in the solution of the following problems:

i) Finite domain problems

ii) Circular cavity under internal pressure in an infinite medium.

The results obtained for both the constant and the linear elements are compared with known classical solutions. The agreement of results

is found to be satisfactory.

Chapter 4, investigates two approaches for the combination of the boundary element method with the finite element method. These approaches are:

i) Equivalent finite element approach

ii) Equivalent boundary element approach.

This investigation is followed by one application, which shows that the results obtained by using the equivalent finite element approach are in excellent agreement with the corresponding results obtained from the boundary element method.

Chapter 5 is devoted to a study of the behaviour of beams on elastic half-space. It starts by describing the solution of beam problem by using the two approaches. A comparison between the results obtained by the two approaches is found to be quite satisfactory. This is followed by a parametric study of the beam behaviour in which the equivalent finite element approach is used.

Chapter 6 contains a summary, conclusions of the present study, and recommendations for future work.

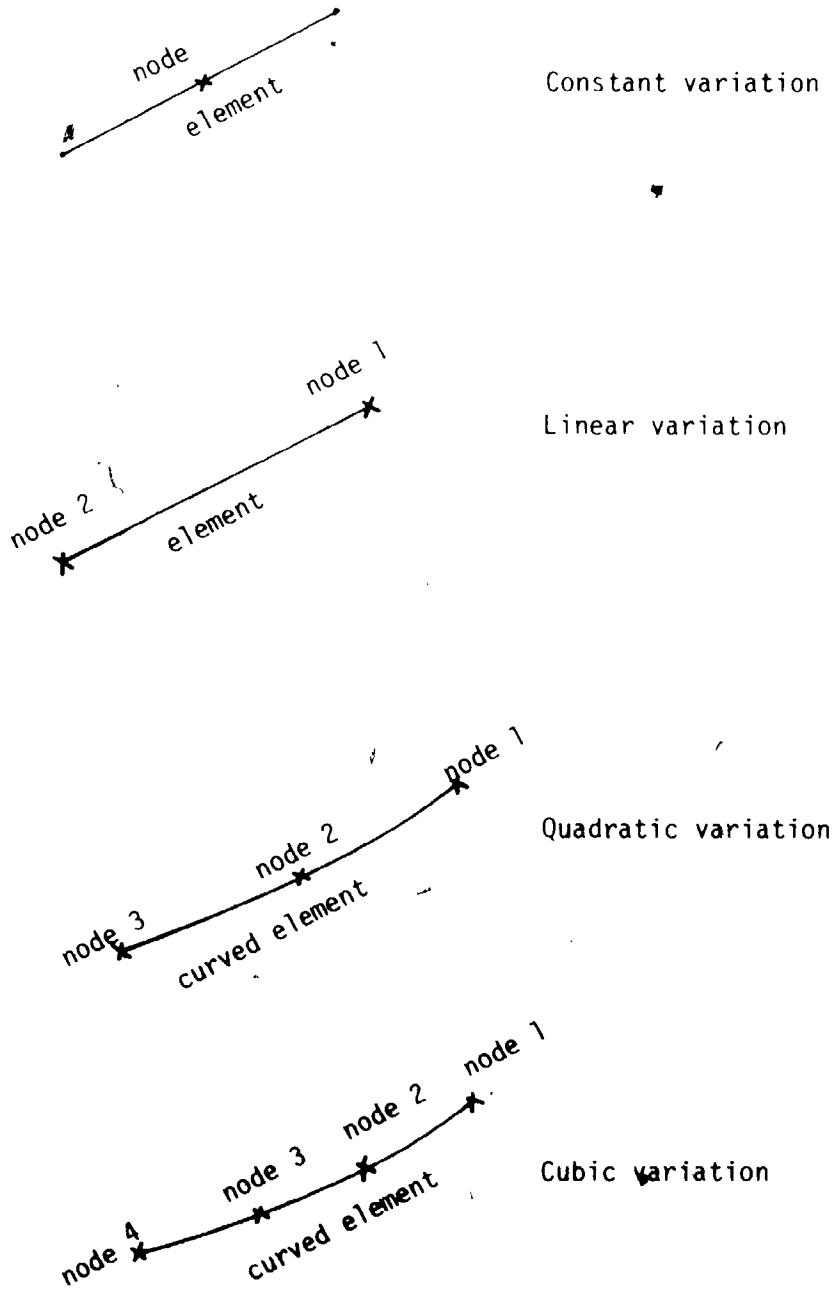

Figure 1.1 Nodes for the Representation of Functions

CHAPTER 2

FORMULATION OF THE BOUNDARY ELEMENT METHOD

2.1 Introduction

The mathematical formulation of the boundary element method is developed in this chapter. The development presented here is based on the following assumptions:

1. The material has a linear stress-strain relationship
2. The change in orientation of a body due to displacements is negligible.

These assumptions lead to linear load-displacement relations and also permit forming the equilibrium relations with reference to the undeformed geometry.

Two types of formulation have been presented here:

1. Constant element formulation
2. Linear element formulation

In the constant element formulation the traction and displacement are assumed to be constant over the element, while in the linear element they are considered to vary linearly along the element.

2.2 Linear Theory of Elasticity

The state of stress at a point (Figure 2.1) is completely defined by specifying six components. These can be grouped together in a stress tensor of the following form:

$$\begin{bmatrix} \sigma_{11} & \sigma_{12} & \sigma_{13} \\ \sigma_{21} & \sigma_{22} & \sigma_{23} \\ \sigma_{31} & \sigma_{32} & \sigma_{33} \end{bmatrix}$$

where:

$$\sigma_{21} = \sigma_{12}, \quad \sigma_{31} = \sigma_{13}, \quad \sigma_{32} = \sigma_{23}$$

These stress components must satisfy the equilibrium equations throughout the interior of the body,

$$\frac{\partial \sigma_{ij}}{\partial x_j} + b_i = 0 \ , \quad i = 1,2,3 \quad j = 1,2,3 \tag{2.1}$$

where:

σ_{ij} are the components of the stress tensor,

b_i are the body forces.

Equation 2.1 has been written in the indicial notation. In this notation (used throughout the remainder of this chapter) repeated occurrence of an index implies summation over the entire range of that index. Thus equation 2.1 means:

$$\sum_{j=1}^{3} \frac{\partial \sigma_{ij}}{\partial x_j} + b_i = 0 \quad , \quad i = 1,2,3$$

Using the indical notation defined above, the tractions boundary conditions can be written as,

$$p_i = \sigma_{ij} \cdot n_j = \bar{p}_i \quad , \quad i = 1,2,3 \tag{2.2}$$

where:

p_i are the tractions on the boundary,

n_j are the direction cosines of outward normal to the boundary and the bar indicates a known quantity

The state of strain at a point is defined by the following strain tensor:

$$\begin{bmatrix} \varepsilon_{11} & \varepsilon_{12} & \varepsilon_{13} \\ \varepsilon_{21} & \varepsilon_{22} & \varepsilon_{23} \\ \varepsilon_{31} & \varepsilon_{32} & \varepsilon_{33} \end{bmatrix}$$

where:

$$\varepsilon_{21} = \varepsilon_{12} \ , \ \varepsilon_{31} = \varepsilon_{13} \ , \ \varepsilon_{32} = \varepsilon_{23}$$

The relations between the strain and the displacements can be expressed as follows:

$$\varepsilon_{ij} = \frac{1}{2} \left(\frac{\partial u_i}{\partial x_j} + \frac{\partial u_j}{\partial x_i} \right) , \quad i = 1,2,3 \quad j = 1,2,3 \tag{2.3}$$

The relationship between stress and strain is given by

$$\sigma_{ij} = E_{ijk\ell} \cdot \varepsilon_{k\ell} \quad k = 1,2,3 \ , \ \ell = 1,2,3 \tag{2.4}$$

where coefficients $E_{ijk\ell}$ depend on material properties and are called rigidity coefficients.

It should be noted that Equation 2.4 has also been written in the indicial form and implies summation over k and ℓ for each set of values of i and j.

There are 21 material constants for an elastic material.

The number of independent constants is reduced when the material structure has one or more planes of symmetry. If the material has three orthogonal planes of symmetry it is said to be orthotropic, and the number

of independent constants reduces to 9. An isotropic material has only two independent constants (Young's modulus and Poisson's ratio).

2.3 Basic Relationships

Referring to Figure 2.2 the boundary conditions of any problem can be divided into two types:

a) boundary on which displacements are prescribed, such as

$u = \bar{u}$ on Γ_1

b) boundary on which tractions are prescribed, such as $p = \bar{p}$ on Γ_2

The total boundary is $\Gamma = \Gamma_1 + \Gamma_2$

Having defined the boundary conditions, the principle of virtual displacements for a linearly elastic material can be written as:

$$\int_{\Omega} (\sigma_{ij,j} + b_i)\, u_i^* \, d\Omega = \int_{\Gamma_2} (p_i - \bar{p}_i)\, u_i^* \, d\Gamma \qquad (2.5)$$

where:

$$(\ \ ),j = \frac{\partial(\ \ )}{\partial x_j}$$

u_i^* are the virtual displacements satisfying the homogeneous boundary conditions,

$$\bar{u}^* = 0, \quad \text{on } \Gamma_1$$

σ_{ij} and b_i are defined as in Equation 2.1 and p_i and $\bar{p}_i$ are defined as in Equation 2.2.

If u_i^* is interpreted as a weighting function which does not

identically satisfy the boundary conditions on Γ_1, Equation 2.5 becomes:

$$\int_\Omega (\sigma_{ij,j} + b_i)\, u_i^* \, d\Omega = \int_{\Gamma_2} (p_i - \bar{p}_i)\, u_i^* \, d\Gamma + \int_{\Gamma_1} (\bar{u}_i - u_i)\, p_i^* \, d\Gamma \tag{2.6}$$

where $p_i^* = \sigma_{ij}^* \cdot n_j$ are the surface tractions corresponding to the u_i^* system of displacements.

Integration by parts of the left hand side of Equation 2.6 gives

$$\int_\Omega (\sigma_{ij,j} + b_i)\, u_i^* \, d\Omega = -\int_\Omega \sigma_{ij} \cdot u_{i,j}^* \, d\Omega + \int u_i^* \cdot \sigma_{ij} \cdot n_j \, d\Gamma + \int_\Omega b_i \, u_i^* \, d\Omega \tag{2.7}$$

or

$$\int_\Omega (\sigma_{ij,j} + b_i)\, u_i^* \, d\Omega = -\int_\Omega \sigma_{ij} \cdot u_{i,j}^* \, d\Omega + \int p_i \cdot u_i^* \, d\Gamma + \int_\Omega b_i \, u_i^* \, d\Omega \tag{2.8}$$

Now if the material properties are linear, the following equality holds,

$$\int_\Omega \sigma_{ij} \cdot \varepsilon_{ij}^* \, d\Omega = \int_\Omega \sigma_{ij}^* \, \varepsilon_{ij} \, d\Omega \tag{2.9}$$

Equation 2.8 therefore becomes:

$$\int_\Omega (\sigma_{ij,j} + b_i)\, u_i^* \, d\Omega = -\int_\Omega \sigma_{ij}^* \cdot u_{i,j} \, d\Omega + \int p_i \, u_i^* \, d\Gamma + \int_\Omega b_i \cdot u_i^* \, d\Omega \tag{2.10}$$

On integrating by parts the first integral on the right hand side, Equation 2.10 reduces to the following form

$$\therefore \int_{\Omega} (\sigma_{ij,j} + b_i)\, u_i^* \, d\Omega = \int_{\Omega} u_i \cdot \sigma^*_{ij,j} \, d\Omega - \int u_i \cdot \sigma^*_{ij} \cdot n_j \, d\Gamma$$

$$+ \int p_i \cdot u_i^* \, d\Gamma + \int b_i \, u_i^* \, d\Omega$$

Thus the final form of the left hand side of Equation 2.6 is as below:

$$\int_{\Omega} u_i \cdot \sigma^*_{ij,j} \, d\Omega - \int p_i^* \cdot u_i \, d\Gamma + \int p_i \cdot u_i^* \, d\Gamma + \int_{\Omega} b_i \, u_i^* \, d\Omega$$

Substitution of this value in Equation 2.6 gives

$$\int_{\Omega} \sigma^*_{ij,j} \cdot u_i \, d\Omega = \int_{\Gamma_2} p_i^* \cdot u_i \, d\Gamma - \int_{\Gamma_1} p_i \cdot u_i^* \, d\Gamma + \int_{\Gamma_2} p_i \, u_i^* \, d\Gamma - \int_{\Gamma_2} \bar{p}_i \, u_i^* \, d\Gamma$$

$$+ \int_{\Gamma_1} \bar{u}_i \, p_i^* \, d\Gamma - \int_{\Gamma_1} u_i \, p_i^* \, d\Gamma - \int_{\Omega} b_i \, u_i^* \, d\Omega \qquad (2.11)$$

or

$$\int_{\Omega} \sigma^*_{ij,j} \, u_i \, d\Omega = - \int_{\Gamma_2} \bar{p}_i \cdot u_i^* \, d\Gamma - \int_{\Gamma_1} p_i \, u_i^* \, d\Gamma + \int_{\Gamma_1} \bar{u}_i \, p_i^* \, d\Gamma$$

$$+ \int_{\Gamma_2} u_i \, p_i^* \, d\Gamma - \int_{\Omega} b_i \cdot u_i^* \, d\Omega \qquad (2.12)$$

2.4 Fundamental Solution

So far nothing has been stated about the form of weighting function u^*. If this function is appropriately chosen, the domain integral on the left hand side of Equation 2.12 can be eliminated. The equation is then reduced to a form involving integrals only on the boundary with the exception of

the integral containing the known body forces. The reduced equation can be solved numerically by the discretization of the boundary into elements. This is the basis of the boundary element method.

The particular u^* function which converts the domain problem into a boundary problem is called the fundamental solution.

The fundamental solution should satisfy the following equation [3]

$$\sigma^*_{ij,i} + \Delta^P_j = 0 \tag{2.13}$$

where Δ^P_j is the Dirac delta function and represents a unit load at the internal point (P) in the 'j' direction. This type of solution will produce for each direction 'j' the following equation:

$$u^P_j + \int_{\Gamma_1} \bar{u}_i \, p^*_i \, d\Gamma + \int_{\Gamma_2} u_i \, p^*_i \, d\Gamma = \int_{\Omega} b_i \, u^*_i \, d\Omega + \int_{\Gamma_1} p_i \, u^*_i \, d\Gamma + \int_{\Gamma_2} \bar{p}_i \, u^*_i \, d\Gamma \tag{2.14}$$

where u^P_j represents the displacement of (P) in the 'j' direction. In general one can write for point (P):

$$u^P_j + \int_{\Gamma} u_i \, p^*_i \, d\Gamma = \int_{\Gamma} p_i \, u^*_i \, d\Gamma + \int_{\Omega} b_i \, u^*_i \, d\Omega \tag{2.15}$$

where u^*_i and p^*_i are the fundamental solutions, i.e. the displacements and tractions due to a concentrated unit load at point (P) in the direction 'j'.

Equation 2.15 applies for each of the three values of j. In its general form it can therefore be written as

$$u^P_j + \int_{\Gamma} u_i \, p^*_{ji} \, d\Gamma = \int_{\Gamma} p_i \, u^*_{ji} \, d\Gamma + \int_{\Omega} b_i \, u^*_{ji} \, d\Omega \tag{2.16}$$

$$j = 1,2,3$$

where p^*_{ji} and u^*_{ji} represent the tractions and displacements in the 'i' direction due to a unit force in the 'j' direction. Equation 2.16 is valid for the particular point (P) where such a force is applied.

The fundamental solution for a three-dimensional isotropic body for the plain strain case is available in the literature and is known as the Kelvin solution [16]. The Kelvin solution represents the effect of a point load applied at any point of an infinite space on other points in the same space. It is represented in Figure 2.3. The resultant u^*_{ji} and p^*_{ji} values are given by known formula [3].

The fundamental solution for a two-dimensional plain strain case [3] is given by

$$u^*_{ji} = \frac{1}{8\pi G(1-\nu)} \left[(3-4\nu) \ln \frac{1}{r} \Delta_{ji} + \frac{\partial r}{\partial x_j} \cdot \frac{\partial r}{\partial x_i}\right]$$

$$p^*_{ji} = \frac{-1}{4\pi(1-\nu)r} \left[\frac{\partial r}{\partial n} \{(1-2\nu)\Delta_{ji} + 2 \frac{\partial r}{\partial x_i} \cdot \frac{\partial r}{\partial x_j}\}\right.$$

$$\left. - (1-2\nu)\{ \frac{\partial r}{\partial x_j} \cdot n_i - \frac{\partial r}{\partial x_i} \cdot n_j\} \right] \tag{2.17}$$

where

- n is the normal to the surface of the body,
- Δ_{ji} is the Kronecker delta (Δ_{ji} = 1.0 when j = i and = 0 when j ≠ i),
- r is the distance from the point of application of the load (P) to the point under consideration (Q),

$\frac{\partial r}{\partial x_i} = \frac{r_i}{r}$

G shear modulus,

ν Poisson's ratio,

n_i, n_j direction cosines of outward normal n.

The case of plane stress can be handled through the use of an effective Poisson's ratio given by $\bar{\nu} = \frac{\nu}{1+\nu}$ and a modified value of the Young's modulus given by $\bar{E} = E(1-\nu^2)$.

If we neglect the effect of body forces, Equation 2.16 for the two dimensional case becomes:

$$u_j^P + \int_\Gamma u_i \, p_{ji}^* \, d\Gamma = \int_\Gamma p_i \, u_{ji}^* \, d\Gamma \qquad j = 1,2 \tag{2.18}$$

Equation 2.18 relates the value of the function under consideration 'u' in the direction 'j' at point (P) to its values on the boundary of the domain. It can be seen that the integrations contained in Equation 2.18 are to be carried out only on the boundary of the domain.

2.5 Boundary Element Discretization

In order to evaluate the integral contained in Equation 2.18 it is assumed that the boundary of the domain is divided into N boundary elements as shown in Figure 2.5. The points where the unknown values are considered are called 'nodes'. The position of the nodes differs according to the type of the boundary elements used. For constant elements the nodes are taken to be at the middle of each element (Figure 2.5a); for linear elements they are taken to be at intersections of the adjacent elements (Figure 2.5b).

The essence of the boundary-integral technique is to allow the internal point 'P' to pass to an arbitrary surface point 'z' as shown in Figure 2.6, yielding a set of integral equations which can be solved for the unknown boundary tractions and displacements.

It should be noted that the fundamental solutions exhibit singularities as (P) approaches (Q) (Figure 2.4), so that the resulting set of integral equations are singular, and that the values of the integral in Equation 2.18 are discontinuous as (P) passes through surface.

Details of the boundary element procedure for the following two types of elements are described next.

1. Constant Boundary Elements.
2. Linear Boundary Elements.

2.5.1 Constant Boundary Element

In this solution, the boundary is approximated by a number of straight elements, over which the tractions and displacements are assumed to be constant. The nodal points to which the constant values of traction and displacement apply are located at the center of each element. Thus a boundary point can be assumed to lie on a flat portions of the boundary rather than at corners as shown in Figure 2.6a.

To deal with the singularity in Equation 2.18, the surface Γ is divided into two parts as shown in Figure 2.6a, one part is denoted by s* and is a small portion of the surface surrounding point (P). The remaining surface is denoted by Γ-s*. Now,

$$\lim_{P \to z} u_j^P = u_j^z \qquad j = 1,2$$

and as shown in Appendix A

$$\lim_{P \to z} \int_\Gamma u_i \, p_{ji}^* \, d\Gamma = -\frac{1}{2} u_j^z + \lim_{s^* \to 0} \int_{\Gamma - s^*} u_i \, p_{ji}^* \, d\Gamma \qquad j = 1,2 \tag{2.19}$$

also

$$\lim_{P \to z} \int_\Gamma p_i \, u_{ji}^* \, d\Gamma = \lim_{s^* \to 0} \int_{\Gamma - s^*} p_i \, u_{ji}^* \, d\Gamma \qquad j = 1,2$$

Substituting Equation 2.19 in Equation 2.18 and taking the limiting value as s* shrinks to zero.

$$\frac{1}{2} u_j^z + \int_\Gamma u_i \, p_{ji}^* \, d\Gamma = \int_\Gamma p_i \, u_{ji}^* \, d\Gamma \quad , \quad j = 1,2 \tag{2.20}$$

The integrals in the above equation can be broken down into sum of the integrals over each element. Then since the tractions and displacements have been assumed to be constant on the boundary elements, Equation 2.20 becomes,

$$\frac{1}{2} u_j^z + \sum_{J=1}^{N} u_i^J \int_{\Gamma_J} p_{ji}^{\star} (J,z)\, d\Gamma (J) = \sum_{J=1}^{N} p_i^J \int_{\Gamma_J} u_{ji}^{\star} (J,z)\, d\Gamma (J) \qquad j=1,2 \qquad (2.21)$$

where:

N is the number of boundary elements (total number of nodes),

Γ_J denotes the surface of the jth boundary element,

u_i^J and p_i^J are the values of the displacements and tractions respectively in the direction "i" at point "J",

$z = 1, 2, 3 \ldots\ldots\ldots\ldots N$ boundary segments.

The following notations are now introduced:

$$\hat{H}_{ji} (J,z) = \int_{\Gamma_j} p_{ji}^{\star} (J,z)\, d\Gamma (J)$$

$$G_{ji} (J,z) = \int_{\Gamma_J} u_{ji}^{\star} (J,z)\, d\Gamma (J)$$

$$u_j(z) = u_j^z$$

$$u_i(J) = u_i^J$$

$$p_i(J) = p_i^J \qquad (2.22)$$

By using these notations, Equation 2.21 can be written in the following matrix form:

$$\begin{bmatrix} [\hat{H}_{ji}(1,1) + \frac{1}{2}] & [\hat{H}_{ji}(1,2)] & & \\ [\hat{H}_{ji}(2,1)] & [\hat{H}_{ji}(2,2) + \frac{1}{2}] & & \\ & & & \\ & & & [\hat{H}_{ji}(N,N) + \frac{1}{2}] \end{bmatrix} \begin{bmatrix} u_i(1) \\ u_i(2) \\ \vdots \\ u_i(N) \end{bmatrix}$$

$$= \begin{bmatrix} G_{ji}(1,1) & G_{ji}(1,2) & & \\ G_{ji}(2,1) & G_{ji}(2,2) & & \\ & & & \\ & & & G_{ji}(N,N) \end{bmatrix} \begin{bmatrix} p_i(1) \\ p_i(2) \\ \vdots \\ p_i(N) \end{bmatrix} \qquad 2.23$$

It should be noted that the submatrices in Equation 2.23 are defined as follows:

$$[\hat{H}_{ji}(1,1) + \frac{1}{2}] = \begin{bmatrix} H_{11}(1,1) & H_{12}(1,1) \\ H_{21}(1,1) & H_{22}(1,1) \end{bmatrix} + \begin{bmatrix} \frac{1}{2} & 0 \\ 0 & \frac{1}{2} \end{bmatrix}$$

$$G_{ji}(1,1) = \begin{bmatrix} G_{11}(1,1) & G_{12}(1,1) \\ G_{21}(1,1) & G_{22}(1,1) \end{bmatrix}$$

$$u_i\ (1) = \begin{Bmatrix} u_1\ (1) \\ u_2\ (1) \end{Bmatrix}$$

and

$$p_i\ (1) = \begin{Bmatrix} p_1\ (1) \\ p_2\ (1) \end{Bmatrix}$$

Thus Equation 2.23 represents an algebraic system of 2N linear simultaneous equations in 4N tractions and displacements (2N displacements and 2N tractions). Before Equation 2.23 can be solved one must specify half of the total number of components of tractions and displacements; the other half then become the unknowns to be solved.

Therefore in summary, Equation 2.23 represents a set of 2N linear simultaneous equations in 2N unknowns(tractions and displacements).

2.5.1.1 Solution Technique

Equation 2.23 can be put in the following form:

$$\{\tfrac{1}{2}\,[I] + [\hat{H}]\}\{u\} = [G]\{p\}. \qquad \text{or}$$

$$[H]\{u\} = [G]\{p\} \qquad \text{where } [H] = \tfrac{1}{2}\,[I] + [\hat{H}]$$

and [I] is the identity matrix. By denoting the known surface tractions and displacements as $\{p^B\}$ and $\{u^B\}$, respectively, and the unknown surface tractions and displacement as $\{p^A\}$ and $\{u^A\}$, respectively, the above equation can be represented as:

$$[H^A\ H^B] \begin{Bmatrix} u^A \\ u^B \end{Bmatrix} = [G^B\ G^A] \begin{Bmatrix} p^B \\ p^A \end{Bmatrix}$$

A rearrangement of the terms gives

$$[H^A - G^A] \begin{Bmatrix} u^A \\ p^A \end{Bmatrix} = [G^B - H^B] \begin{Bmatrix} p^B \\ u^B \end{Bmatrix}$$

Thus all the unknowns having been transferred to the left hand side and one can write:

$$[B]\ \{X\} = \{F\} \tag{2.24}$$

where $\{X\}$ is the vector of unknown u_s^A and p_s^A .

Once the values of u_s and p_s on the boundary are known one can calculate the value of displacements and stresses at any interior point by using Equation 2.16 as follows:

$$u_\ell^P = \int_\Gamma p_k\ u_{\ell k}^*\ d\Gamma + \int_\Omega b_k\ u_{\ell k}^*\ d\Omega - \int_\Gamma u_k\ p_{\ell k}^*\ d\Gamma \tag{2.25}$$

and in the absence of body forces as

$$u_\ell^P = \sum_{J=1}^{N} p_k \int_{\Gamma_J} u_{\ell k}^*\ d\Gamma - u_k \int_{\Gamma_J} p_{\ell k}^*\ d\Gamma \tag{2.26}$$

where u_ℓ^P is the displacement in the direction of 'ℓ' at the internal point (P).

According to Hooke's Law, the stress tensor σ_{ij} at any interior point (P) is given in terms of displacement by:

$$\sigma_{ij} = \frac{2G\nu}{1-2\nu}\ \Delta_{ij} \frac{\partial u_\ell}{\partial x_\ell} + G\ \left(\frac{\partial u_i}{\partial x_j} + \frac{\partial u_j}{\partial x_i}\right) \tag{2.27}$$

Using expression 2.25 for u_ℓ and carrying out the indicated differentiation one obtains,

$$\sigma^{P}_{ij} = \int_{\Gamma} \{ \frac{2G\nu}{1-2\nu} \Delta_{ij} \frac{\partial u^{*}_{\ell k}}{\partial x_{\ell}} + G \left(\frac{\partial u^{*}_{ik}}{\partial x_j} + \frac{\partial u^{*}_{jk}}{\partial x_i}\right) \} p_k \, d\Gamma$$

$$+ \int_{\Omega} \{ \frac{2G\nu}{1-2\nu} \Delta_{ij} \frac{\partial u^{*}_{\ell k}}{\partial x_{\ell}} + G \left(\frac{\partial u^{*}_{ik}}{\partial x_j} + \frac{\partial u^{*}_{jk}}{\partial x_i}\right) \} b_k \, d\Omega$$

$$- \int_{\Gamma} \{ \frac{2G\nu}{1-2\nu} \Delta_{ij} \frac{\partial p^{*}_{\ell k}}{\partial x_{\ell}} + G \left(\frac{\partial p^{*}_{ik}}{\partial x_j} + \frac{\partial p^{*}_{jk}}{\partial x_i}\right) \} u_k \, d\Gamma \qquad (2.28)$$

Now if the following definitions are used

$$D_{kij} = \frac{2G\nu}{1-2\nu} \Delta_{ij} \frac{\partial u^{*}_{\ell k}}{\partial x_{\ell}} + G \frac{\partial u^{*}_{ik}}{\partial x_j} + G \frac{\partial u^{*}_{jk}}{\partial x_i}$$

$$S_{kij} = \frac{2G\nu}{1-2\nu} \Delta_{ij} \frac{\partial p^{*}_{\ell k}}{\partial x_{\ell}} + G \frac{\partial p^{*}_{ik}}{\partial x_j} + G \frac{\partial p^{*}_{jk}}{\partial x_i}$$

Equation 2.27 can be expressed as

$$\sigma_{ij} = \int_{\Gamma} D_{kij} p_k \, d\Gamma - \int_{\Gamma} S_{kij} u_k \, d\Gamma + \int_{\Omega} D_{kij} b_k \, d\Omega \qquad (2.29)$$

When the body forces are absent Equation 2.29 reduces to

$$\sigma_{ij} = \int_{\Gamma} D_{kij} p_k \, d\Gamma - \int_{\Gamma} S_{kij} u_k \, d\Gamma \qquad (2.30)$$

For a two dimensional case it can be proved that

$$D_{kij} = \frac{1}{4\pi(1-\nu)r} \{(1-2\nu) [\Delta_{ki} \frac{\partial r}{\partial x_j} + \Delta_{kj} \frac{\partial r}{\partial x_i} - \Delta_{ij} \frac{\partial r}{\partial x_k}]$$

$$+ 2 \frac{\partial r}{\partial x_i} \cdot \frac{\partial r}{\partial x_j} \cdot \frac{\partial r}{\partial x_k} \} \qquad (2.31)$$

$$S_{kij} = \frac{2G}{4\pi(1-\nu)r^2} \{ 2 \frac{\partial r}{\partial n} [(1-2\nu) \Delta_{ij} \frac{\partial r}{\partial x_k} + \nu(\Delta_{ik} \frac{\partial r}{\partial x_j}$$

$$+ \Delta_{jk} \frac{\partial r}{\partial x_i}) - 4 \frac{\partial r}{\partial x_i} \cdot \frac{\partial r}{\partial x_j} \cdot \frac{\partial r}{\partial x_k}] + 2 \nu(n_i \frac{\partial n}{\partial x_j} \cdot \frac{\partial r}{\partial x_k}$$

$$+ n_j \frac{\partial r}{\partial x_i} \cdot \frac{\partial r}{\partial x_k}) + (1-2\nu) (2n_k \frac{\partial r}{\partial x_i} \frac{\partial r}{\partial x_j} + n_j \Delta_{ik} + n_i \Delta_{jk})$$

$$- (1-4\nu) n_k \Delta_{ij} \} \qquad (2.32)$$

where the derivatives are taken on the boundary (Figure 2.4).

2.5.1.2 Body Forces

If body forces such as gravity or centrifugal forces are present Equation 2.20 becomes

$$\frac{1}{2} u_j^z + \sum_{J=1}^{N} u_i^J \int_{\Gamma_J} p_{ji}^* \, d\Gamma = \sum_{J=1}^{N} p_i^J \int_{\Gamma_J} u_{ji}^* \, d\Gamma + \int_{\Omega} u_{ji}^* \, b_i \, d\Omega$$

$$j=1,2 \qquad (2.33)$$

where u_i^J and p_i^J are the nodal displacement and traction in direction i in the element 'J'. To carry out the integral over the domain it is convenient to define internal cells. These cells are used only for the numerical integration of the body force terms and should not be confused with finite elements.

If there are m of these cells (Figure 2.7) than by using Gaussian Quadrature one can write

$$\int_{\Omega} u^{*}_{ji}\, b_i \, d\Omega = \sum_{s=1}^{m} \left\{ \sum_{p=1}^{\ell} (u^{*}_{ji} b_i)_p \, w_p \right\} A_s = b^z_j \tag{2.34}$$

where w_p are the weighting coefficients for the numerical integration and A_s is the area of the element under consideration. By using the same short notation as in Equation 2.22, Equation 2.33 becomes

$$\frac{1}{2} . u^z_j + \sum_{J=1}^{N} H_{ji} \cdot u^J_i = \sum_{J=1}^{N} G_{ji} \cdot p^J_i + b^z_j \tag{2.35}$$

This equation relates the value of u at mid-node 'z' with the values of u's and p's at all the nodes on the boundary, including 'z'. The whole set of equations for the n boundary nodes can be expressed in matrix form as

$$Hu = GP + B \tag{2.36}$$

Reordering the equations in the same way as explained at the beginning of section 2.5.1.1, i.e. with the unknowns transferred to the left hand side one obtains

$$Ax = F + B \tag{2.37}$$

where x is the vector of unknowns.

2.5.1.3 Numerical Solution of the Integral Equation

General analytic solutions to the integral Equations 2.16 are not available and it is therefore necessary to solve the equations numerically. The integral equations are reduced to algebraic equations by discretizing the boundary data. For the constant element method it is assumed that on each element of the boundary the traction and displacement are constant. Also each boundary element is denoted by its centroidal point, z or J, depending on whether the point is fixed or variable with respect to the integration.

When the boundary data is discretized in this way, the descretized form is given by Equation 2.21. When numerical integration is carried out by a 4 point Gaussian Quadrature [3], Equation 2.21 becomes:

$$\frac{1}{2} u_i^z + \sum_{J=1}^{N} \left\{ \sum_{k=1}^{4} w_k \, (p_{ji}^*)_k \right\} u_i^J = \sum_{J=1}^{N} \left\{ \sum_{k=1}^{4} w_k \, (u_{ji}^*)_k \right\} p_i^J$$

where w_k = weight assigned to an integration point, and

$(p^*)_k$, $(u^*)_k$ are the values of the functions at the integration point

When 'z' is concident with 'J' the following results apply,

$$G_{ji} = \int_\Gamma u_{ji}^* \, d\Gamma \qquad i = 1,2 \quad j = 1,2$$

The four elements of G can be arranged in the matrix form

$$\begin{bmatrix} G_{11} & G_{12} \\ G_{21} & G_{22} \end{bmatrix}$$

With the definitions shown in Figure 2.8a and 2.8b the element of the G matrix are given by

$$G_{11} = \frac{R}{4\pi G(1-\nu)} \left[(3-4\nu)(1-\ln R) + \frac{r_1^2}{4R^2} \right]$$

$$G_{12} = G_{21} = \frac{r_1 r_2}{4R} \cdot \frac{1}{4\pi G(1-\nu)}$$

$$G_{22} = \frac{R}{4\pi G(1-\nu)} \left[(3-4\nu)(1-\ln R) + \frac{r_2^2}{4R^2} \right] \tag{2.38}$$

Detailed derivation is given in Appendix B.

The matrix H_{ji} is given by

$$H_{ji} = \begin{bmatrix} 0.5 & 0 \\ 0 & 0.5 \end{bmatrix}$$

2.5.2 Linear Boundary Element

In many situations a more accurate solution could be expected if (rather than remaining constant) displacements and tractions were assumed to vary linearly on a boundary element. The advantage of this approach lies in the ability to model non-uniform boundary conditions more accurately.

In linear elements, values of traction and displacement are assigned to nodes located at the intersection of the boundary segments rather than to their center points. Continuity of displacement is assured since two adjacent elements share one common node. One difficulty becomes immediately apparent. Since the nodes now lie at intersections between elements, the possibility exists for nodes to occur at corners rather than on flat portions of the boundary. This means that the constant in Equation 2.21 may be different from $\frac{1}{2}$.

Suppose the internal point (P) approaches a corner point of included angle α as illustrated schematically in Figure 2.9a. The individual terms of Equation 2.18 are then given by:

$$\lim_{P\to z} u_j^P = u_j^z \qquad j=1,2$$

$$\lim_{P\to z} \int_\Gamma u_i \cdot p_{ji}^* \, d\Gamma = - C_{ji} \, u_i^z + \lim_{s^*\to 0} \int_{\Gamma - s^*} u_i \, p_{ji}^* \, d\Gamma \qquad j=1,2$$

$$\lim_{P\to z} \int_\Gamma p_i \cdot u_{ji}^* \, d\Gamma = \lim_{s^*\to 0} \int_{\Gamma - s^*} p_i \, u_{ji}^* \, d\Gamma \qquad j = 1,2 \tag{2.39}$$

The jump term is given in terms of the tensor C_{ji} which is defined as follows:

$$C_{11} = [1 - \frac{\alpha}{2\pi} - \frac{\cos(2\gamma)\sin(\alpha)}{4\pi(1-\nu)}]$$

$$C_{12} = C_{21} = - [\frac{\sin(2\gamma)\sin(\alpha)}{4\pi(1-\nu)} \qquad (2.40)$$

$$C_{22} = [1 - \frac{\alpha}{2\pi} + \frac{\cos(2\gamma)\sin(\alpha)}{4\pi(1-\nu)}]$$

where α is the included angle of the corner and γ is the angle between the bisector of α and the x_1 coordinate axis as shown in Figure 2.9.

Detailed derivation of Equation 2.40 is given in Appendix C. If the boundary is flat in the vicinity of a node C_{ij} reduces to a diagonal tensor with values of $\frac{1}{2}$ as in the case of a constant element and $-C_{ji}U_i^z$ becomes $-\frac{1}{2}u_j$. Substitution of Equation 2.39 into Equation 2.19 yields the boundary constraint equation for linear elements:

$$(\Delta_{ji} - C_{ji})\, u_i^z + \int_\Gamma u_i\, p_{ji}^*\, d\Gamma = \int_\Gamma p_i\, u_{ji}^*\, d\Gamma \qquad j=1,2 \qquad (2.41)$$

The integral in the above can be broken down into sum of the integral over each element (J):

$$(\Delta_{ji} - C_{ji})\, u_i^z + \sum_{J=1}^{Nseg.} \int_{\Gamma_J} u_i^J\, p_{ji}^*\, (J,z)\, d\Gamma(J) = \sum_{J=1}^{N} \int_{\Gamma_J} p_i^J\, u_{ji}^*\, (J,z)\, d\Gamma(J)$$

$$j=1,2 \qquad (2.42)$$

where Γ_J refers to the length of element 'J'. It will be noted that u_i^J and p_i^J terms have not been factored out of the integrals as they were in the

case of Equation 2.21 for constant elements. Using the linear representation of boundary displacement and traction given in Figure 2.10, Equation 2.42 can be rewritten in the following form:

$$(\Delta_{ji} - C_{ji})\, u_i^z + \sum_{J=1}^{Nseg.} \{[u_i(B) - u_i(A)] \int_{\Gamma_J} p^*_{ji} \phi\, (J)\, d\Gamma\, (J)$$

$$+ u_i(A) \int_{\Gamma_J} p^*_{ji}\, (J,z)\, d\Gamma\, (J)\} = \sum_{J=1}^{N} \{[p_i(B) - p_i(A)] \int_{\Gamma_J} u^*_{ji}\, (J,z)\, \phi\, (J)\, d\Gamma\, (J)$$

$$+ p_i(A) \int_{\Gamma} u^*_{ji}\, (J,z)\, d\Gamma\, (J)\} \qquad j=1,2 \qquad (2.43)$$

where ϕ has been defined in Figure 2.10.

Since the reference is to values of displacement and traction at the nodes, it is convenient to eliminate reference to segment 'J' before putting Equation 2.43 in matrix form.

Referring to Figure 2.11, Equation 2.43 can be expanded and expressed in the following form:

$$(\Delta_{ji} - C_{ji})\, u_i^z + \{[(u_i(B) - u_i(A)) \int_{\Gamma_{BA}} p^*_{ji} \cdot \phi\, d\Gamma + u_i(A) \int_{\Gamma_{BA}} p^*_{ji}\, d\Gamma$$

$$+ [(u_i(M) - u_i(B)) \int_{\Gamma_{MB}} p^*_{ji}\, \phi\, d\Gamma + u_i(B) \int_{\Gamma_{MB}} p^*_{ji} \cdot \phi\, d\Gamma]$$

$$+ [(u_i(F) - u_i(M)) \int_{\Gamma_{MF}} p^*_{ji}\, \phi\, d\Gamma + u_i(m) \int_{\Gamma_{MF}} p^*_{ji}\, d\Gamma\,]$$

$$+ \ldots\} = \{[(p_i(B) - p_i(A)) \int_{\Gamma_{BA}} u^*_{ji}\, \phi\, d\Gamma + p_i(A) \int_{\Gamma_{BA}} u^*_{ji}\, d\Gamma] + [(p_i(M) - p_i(B))$$

$$\int_{\Gamma_{MB}} u^*_{ji}\ \phi\ d\Gamma + p_i(b) - \int_{\Gamma_{MB}} u^*_{ji}\ d\Gamma] + [(p_i(F) - p_i(M))$$

$$\int_{\Gamma_{MF}} u^*_{ji}\ \phi\ d\Gamma + p_i(M) \int_{\Gamma_{MF}} u^*_{ji}\ d\Gamma\ ]$$

$$+ \ldots\} \qquad j=1,2$$

which reduces to

$$(\Delta_{ji} - C_{ji})\ u^z_i + \sum_{M=1}^{NNode} u_i(M)\ \{\int_{\Gamma_{MB}} p^*_{ji}\ (z,MB)\ \phi\ d\Gamma - \int_{\Gamma_{MF}} p^*_{ji}\ (z,MF)\ \phi\ d\Gamma$$

$$+ \int_{\Gamma_{MF}} p^*_{ji}\ (z,MF) d\Gamma\} = \sum_{M=1}^{NNode} p_i(M)\{\int_{\Gamma_{MB}} u^*_{ji}\ (z,MB)\ \phi\ d\Gamma - \int_{\Gamma_{MF}} u^*_{ji}\ (z,MF)\phi\ d\Gamma$$

$$+ \int_{\Gamma_{MF}} u^*_{ji}\ (z,MF)\ d\Gamma \qquad j=1,2$$

or to

$$(\Delta_{ji} - C_{ji})\ u^z_i + \sum_{M=1}^{NNode} u_i(M)\ \{\int_{\Gamma_{MB}} p^*_{ji}\ (z,MB)\phi_2\ d\Gamma + \int_{\Gamma_{MF}} p^*_{ji}\ (z,MF)\phi_1\ d\Gamma$$

$$= \sum_{M=1}^{NNode} p_i(M)\ \{\int_{\Gamma_{MB}} u^*_{ji}\ (z,MB)\phi_2\ d\Gamma + \int_{\Gamma_{MF}} u^*_{ji}\ (z,MF)\phi_1\ d\Gamma \qquad 2.44$$

where NNode is the number of nodes

$\phi_2 = \frac{1}{2}\ (1+\xi)$

$\phi_1 = \frac{1}{2}\ (1-\xi)$

and $\xi = 2x/\ell$ as shown in Figure 2.10.

The following notations are now introduced:

$$H^B_{ji}(m,n) = \int_{\Gamma_{MB}} p^*_{ji}\ (z,MB)\ \phi_2\ d\Gamma$$

$$H^F_{ji}\ (m,n) = \int_{\Gamma_{MF}} p^*_{ji}\ (z,MF)\ \phi_1\ d\Gamma$$

$$G^B_{ji}\ (m,n) = \int_{\Gamma_{MB}} u^*_{ji}\ (z,MB)\ \phi_2\ d\Gamma$$

$$G^F_{ji}\ (m,n) = \int_{\Gamma_{MF}} u^*_{ji}\ (z,MF)\ \phi_1\ d\Gamma \qquad (2.45)$$

where superscripts F and B refer to the element preceeding and following node M.

If there are N nodes, these will N sets of the equations of the type 2.44. Each set consists of two equations corresponding to j=1 and 2. These equations can be expressed in matrix form as follows:

$$[A]\{u\} = [B]\{p\} \tag{2.46}$$

where matrix A is formed of submatrices of the type,

$$\hat{A}_{ji}\ (m,n) = \begin{bmatrix} A_{11}\ (m,n) & A_{12}\ (m,n) \\ A_{21}\ (m,n) & A_{22}\ (m,n) \end{bmatrix}$$

where

$$A_{ji}\ (m,n) = \Delta_{mn}\ [\Delta_{ji} - C_{ji}] + H^{B}_{ji}\ (m,n) + H^{F}_{ji}\ (m,n)$$

Matrix B contains submatrices $\hat{B}_{ji}$ given by

$$\hat{B}_{ji}\ (m,n) = \begin{bmatrix} B_{11}\ (m,n) & B_{12}\ (m,n) \\ B_{21}\ (m,n) & B_{22}\ (m,n) \end{bmatrix}$$

where

$$B_{ji}\ (m,n) = G^{B}_{ji}\ (m,n) + G^{F}_{ji}\ (m,n)$$

Vectors u and p consist of subvectors given by

$$u_i\ (m) = \begin{Bmatrix} u_1\ (m) \\ u_2\ (m) \end{Bmatrix}$$

$$p_i\ (m) = \begin{Bmatrix} p_1\ (m) \\ p_2\ (m) \end{Bmatrix}$$

Equation 2.46 represents a set of (2xNNod) Linear simultaneous equations in (2xNNod)unknowns which can be solved to yield the unknown displacements and tractions at the node.

Step changes in traction boundary condition can be handled by simply placing two nodes very close to each other and assigning different traction values to each.

Once Equation 2.46 is solved for the unknown boundary traction and displacement by a solution technique similar to that used for constant elements, the results can be used to evaluate the displacement at any internal point 'P' using

$$u_j^P = - \sum_{M=1}^{NNode} u_i\,(M)\,\Big[\int_{\Gamma_{MB}} p^*_{ji}\,(P,MB)\,\phi_2\,d\Gamma\,(MB)$$

$$+ \int_{\Gamma_{MF}} p^*_{ji}\,(P,MF)\,\phi_1\,d\Gamma\,(MF)\Big] + \sum_{M=1}^{NNode} p_i\,(M)\,\Big[\int_{\Gamma_{MB}} u^*_{ji}\,(P,MB)\,\phi_2\,d\Gamma\,(MB)$$

$$+ \int_{\Gamma_{MF}} u^*_{ji}\,(P,MF)\,\phi_1\,d\Gamma\,(MF) \qquad (2.48)$$

Displacement gradient at any internal point 'P' can be evaluated by differentiating Equation 2.48. These displacement gradients can then be used to compute the stresses at the internal point using Equation 2.30.

2.5.2.1 Numerical Solution of the Integral Equation

As stated earlier, in the linear element method it is assumed that on each element traction and displacement vary linearly. The reference values of tractions and displacements are assigned to nodes located at the intersection of the boundary elements and the summation is therefore carried out over the nodes rather than over the elements.

The integrals in Equation 2.44 can be evaluated by using 4 point Gaussian Quadrature formulas as follows:

$$C^z u^z + \sum_{M=1}^{NNode} u(M) \left\{ \sum_{k=1}^{4} w_k \left((p^* . \phi_2)_B + (p^* . \phi_1)_F \right)_K \right\}$$

$$= \sum_{M=1}^{NNode} p(M) \left\{ \sum_{k=1}^{4} w_k \left((u^* . \phi_2) + (u^* . \phi_1) \right)_K \right\} \qquad (2.49)$$

where F and B refer to the element in the front and back of node M. When z coincides with M, an analytical method rather than numerical integration is used for the evaluation of the integrals in Equation 2.44. The relevant results are as given below:

$$G_{ji} = \int_{\Gamma_B} u^*_{ji} \cdot \phi_2 \, d\Gamma + \int_{\Gamma_F} u^*_{ji} \, \phi_1 \, d\Gamma = \hat{G}^B_{ji} + \hat{G}^F_{ji}$$

The elements of G can be arranged in a matrix form as below:

$$\hat{G}^F_{ji} = \begin{bmatrix} G^F_{11} & G^F_{12} \\ G^F_{21} & G^F_{22} \end{bmatrix} \quad \text{and} \quad \hat{G}^B_{ji} = \begin{bmatrix} G^B_{11} & G^B_{12} \\ G^B_{21} & G^B_{22} \end{bmatrix}$$

where

$$G^F_{11} = \frac{\ell}{8\pi G(1-\nu)} \left[(3-4\nu) \left\{ (1-\ln(\ell)) - \frac{1}{4} (1-2 \ln(\ell) \right\} + \frac{r_1^2}{2\ell^2} \right]$$

$$G^F_{12} = \frac{r_2 \cdot r_1}{16\pi G(1-\nu)\ell}$$

$$G^F_{21} = G^F_{12}$$

$$G^F_{22} = \frac{\ell}{8\pi G(1-\nu)} \left[(3-4\nu) \left(1-\ln(\ell) \right) - \frac{1}{4} \left(1-2\ln(\ell) \right\} + \frac{r_2^2}{2\ell^2} \right]$$

$$G_{12}^{B} = \frac{r_2 \cdot r_1}{16\pi G(1-\nu)\ell} \tag{2.50}$$

$$G_{21}^{B} = G_{12}^{B}$$

$$G_{22}^{B} = \frac{\ell}{8\pi G(1-\nu)} \left[(3-4\nu) \left\{\frac{1}{4} (1-2\ln(\ell))\right\} + \frac{r_2^2}{2\ell^2}\right.$$

where

ℓ = length of the element,

r_1, r_2 = the projection of ℓ on x_1 and x_2 respectively (Figure 2.11).

Detailed derivation of Equation 2.50 is given in Appendix D.

In a similar manner the relevant expressions for $\hat{H}_{ji}$ are

$$\hat{H}_{ji} = C^z = (\Delta_{ji} - C_{ji}) = \begin{bmatrix} 1 & 0 \\ 0 & 1 \end{bmatrix} - \begin{bmatrix} C_{11} & C_{12} \\ C_{21} & C_{22} \end{bmatrix}$$

$$= \begin{bmatrix} 1-C_{11} & -C_{12} \\ -C_{21} & 1-C_{22} \end{bmatrix} \tag{2.51}$$

where C_{11}, C_{12}, C_{21}, C_{22} are as in Equation 2.40.

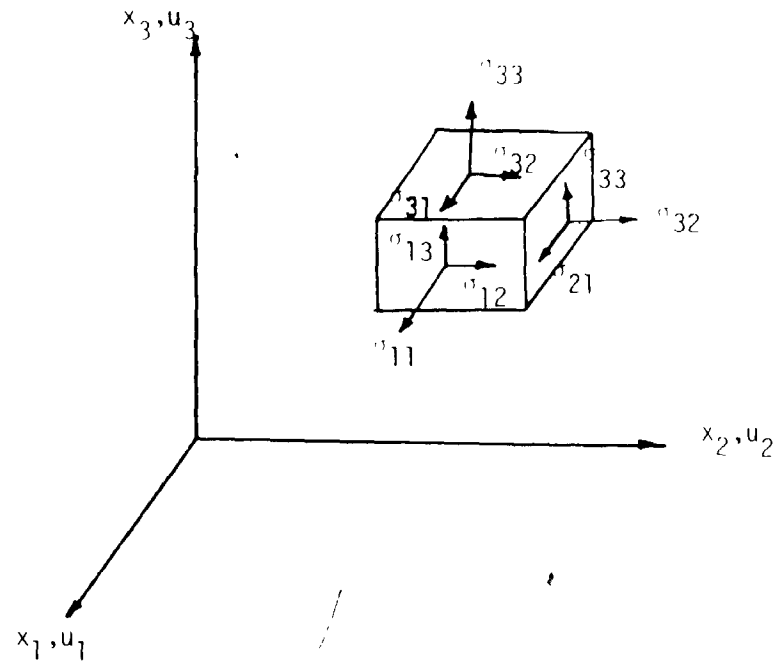

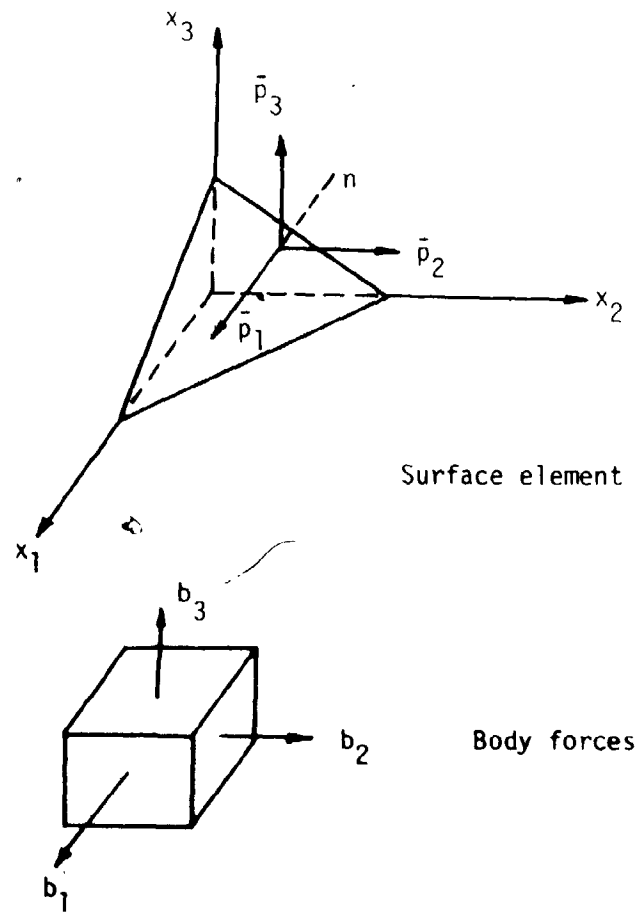

Figure 2.1 Notations for Force, Stress and Displacement

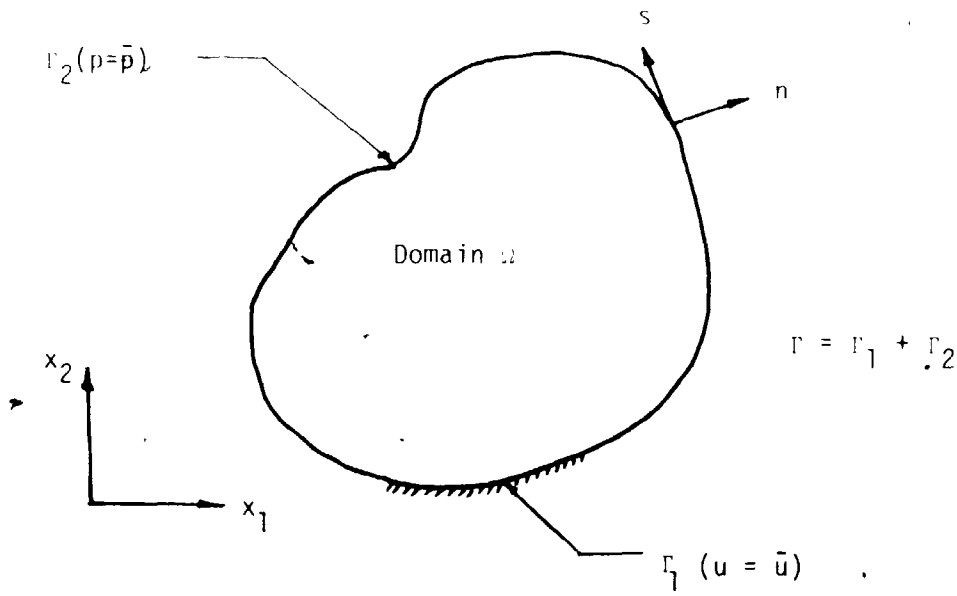

Figure 2.2 Definitions of the Domain and the Boundary

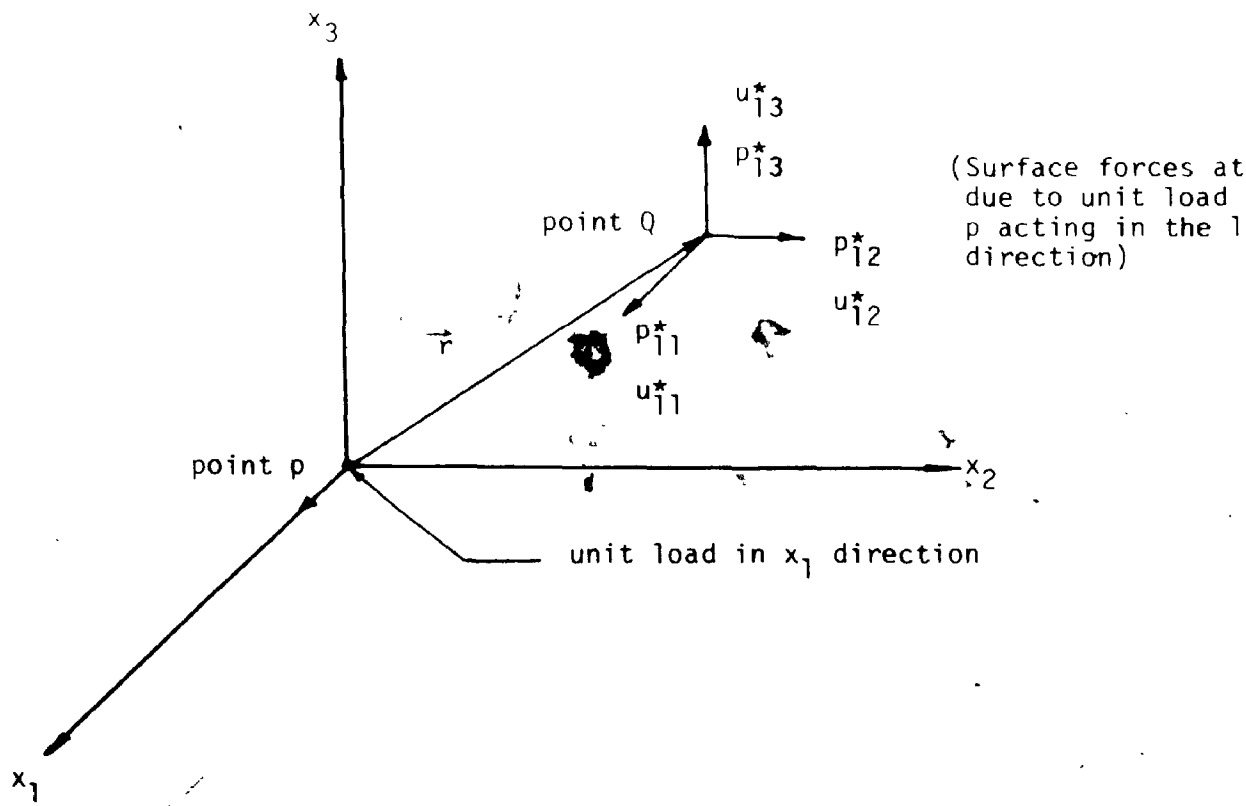

Figure 2.3 Fundamental Solution for the Three Dimensional Case (Kelvin Solution)

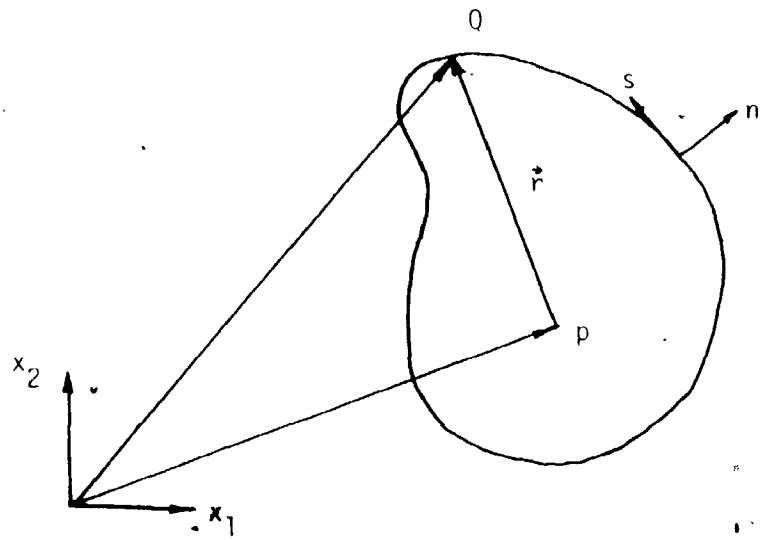

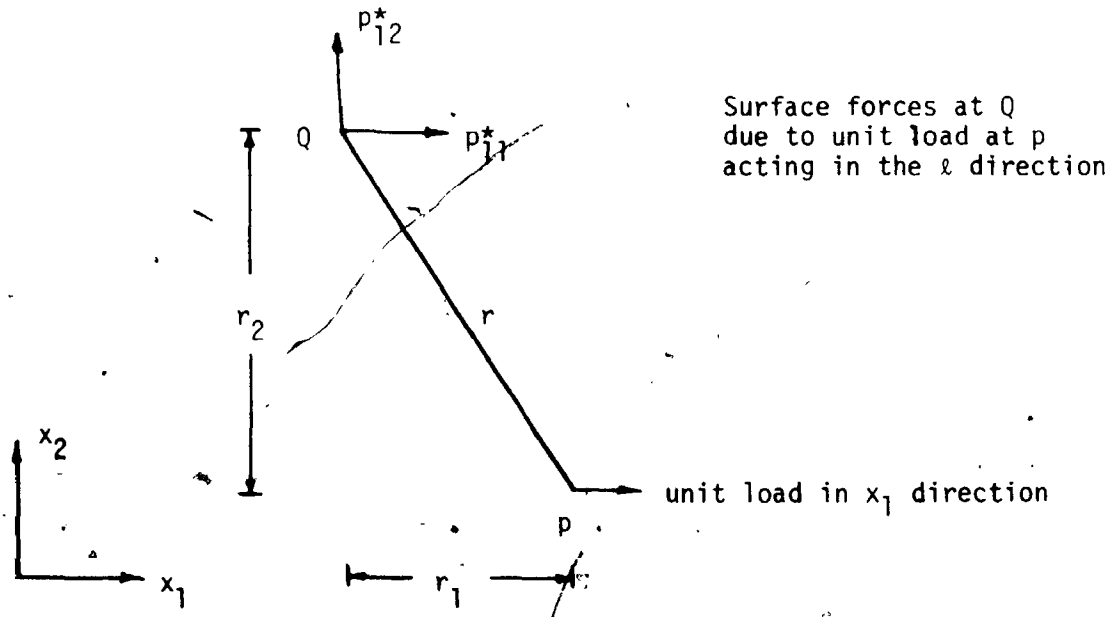

$$r^2 = r_1^2 + r_2^2 \qquad \therefore \frac{\partial r}{\partial x_1} = \frac{r_1}{r}$$

Figure 2.4 Geometrical Definitions for the Points p and Q

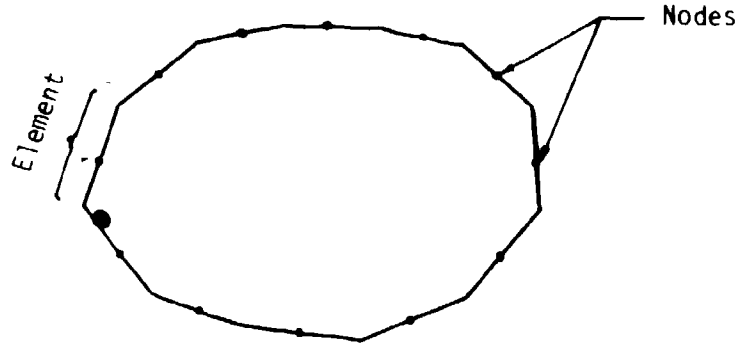

(a) Constant Elements

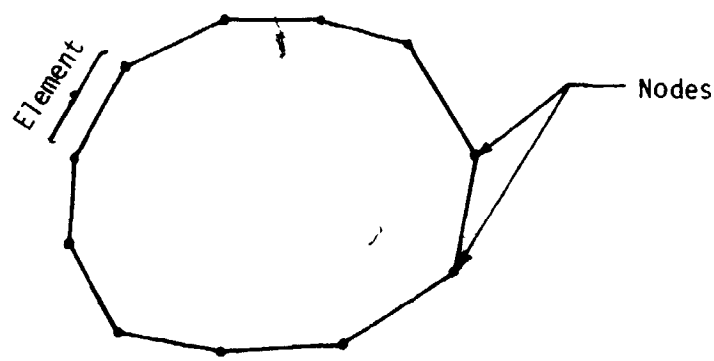

(b) Linear Elements

Figure 2.5 . Two Dimensional Body Divided into Boundary Elements

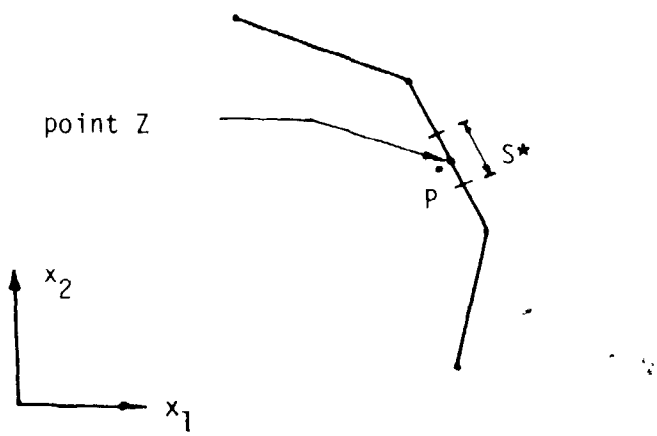

Figure 2.6a Point (P) Approaching A Flat Boundary

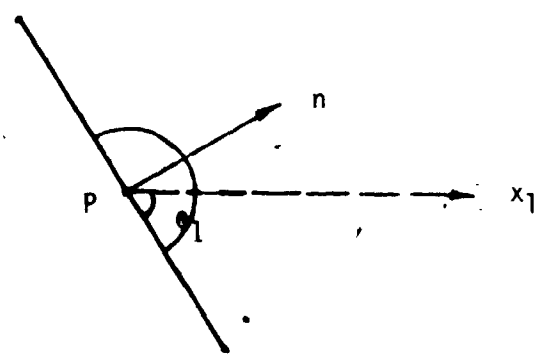

Figure 2.6b Representation of Boundary Surface S* by a Semi-Circle for the Purposes of Integration

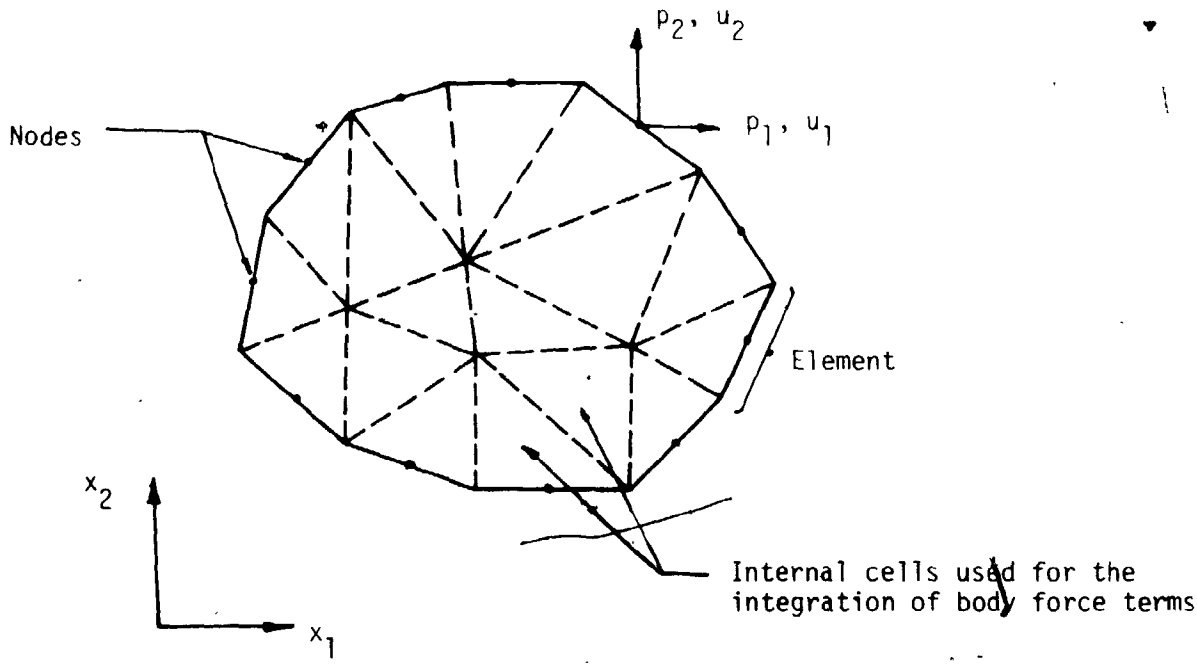

Figure 2.7 Two-Dimensional Body Divided into Boundary Elements and Internal Cells

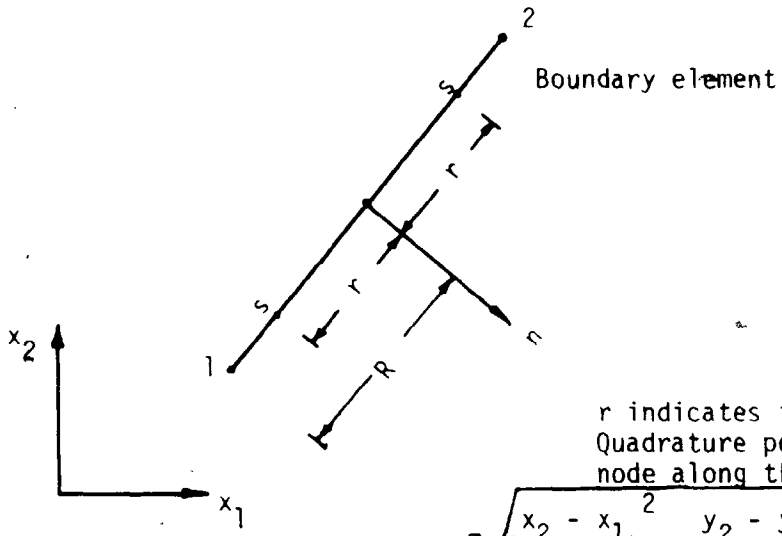

r indicates the distance of Gaussian Quadrature points from the mid-side node along the element.

$$R = \sqrt{\left(\frac{x_2 - x_1}{2}\right)^2 + \left(\frac{y_2 - y_1}{2}\right)^2}$$

Figure 2.8a Element Definition

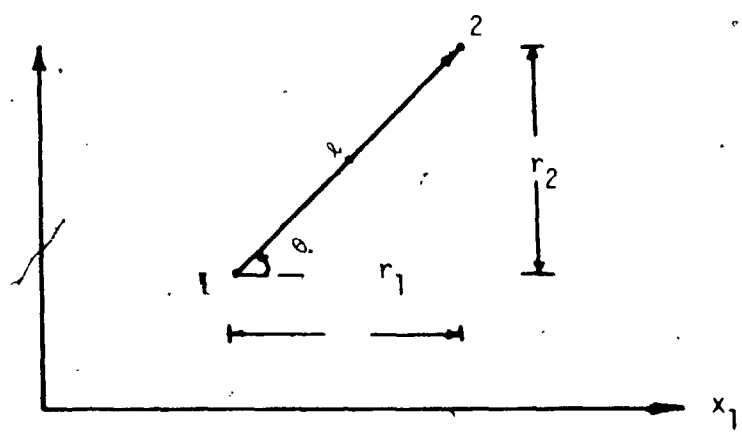

$$r_1 = x_2 - x_1 \quad , \quad r_2 = y_2 - y_1$$

Figure 2.8b Geometrical Definitions for an Element and its Terminal Points

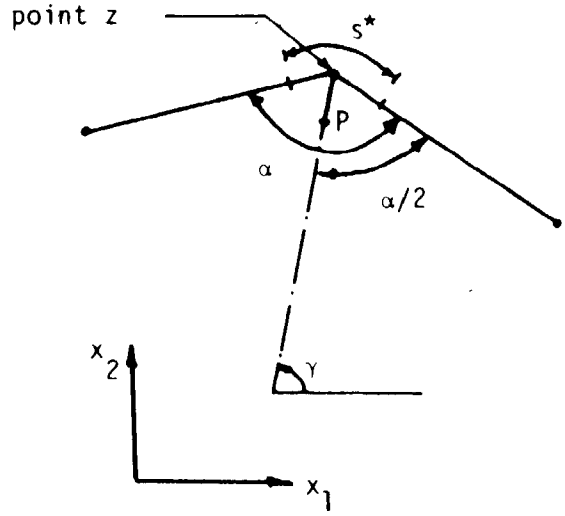

Figure 2.9a Procedure for P Approaching Boundary Corner of Included Angle α

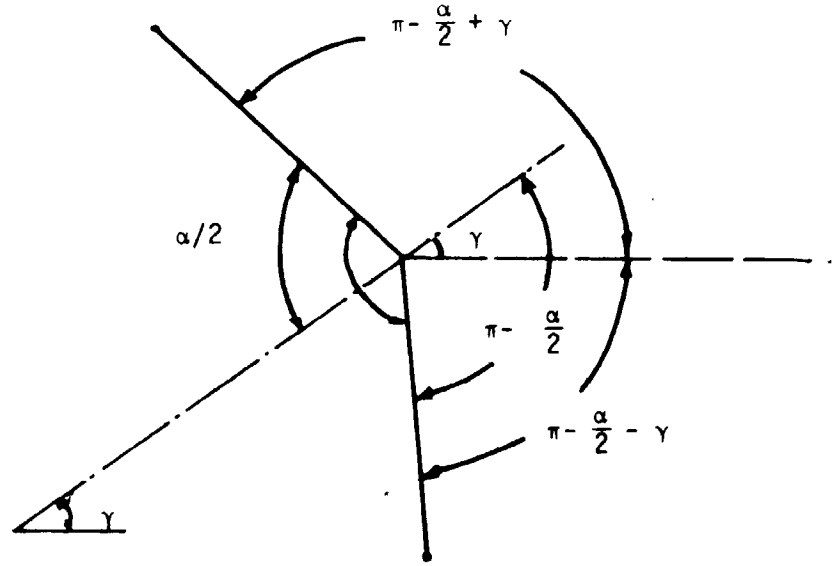

Figure 2.9b Boundary Surface Γ_s^* Assumed Part of Circle for Integration Purposes

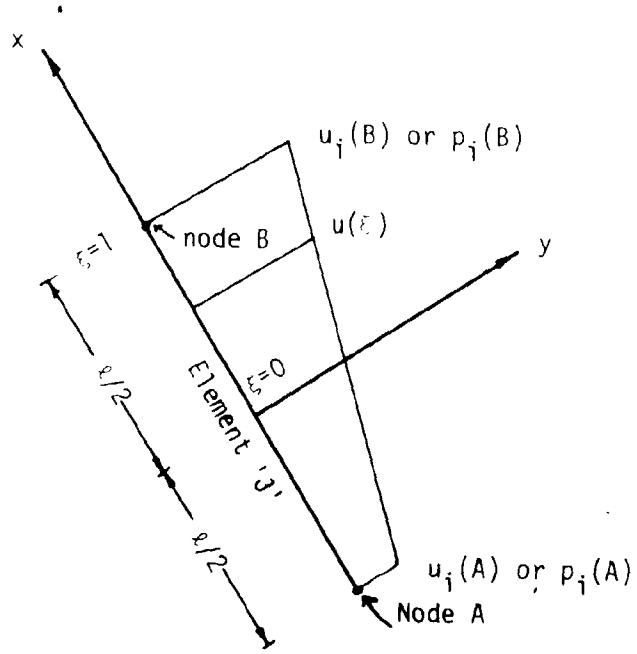

$$u_i(\xi) = u_i(A) + \frac{(u_i(B) - u_i(A))\ (1+2x/\ell)}{2} = u_i(A) + \frac{(u_i(B) - u_i(A))\ (1+\xi)}{2}$$

$$= u_i(A) + (u_i(B) - u_i(A))\phi$$

$$P_i(\xi) = P_i(A) + (P_i(B) - P_i(A))\phi$$

where $\xi = \frac{2x}{\ell}$, $\phi = \frac{1}{2}(1+\xi)$

Figure 2.10 Linear Boundary Element

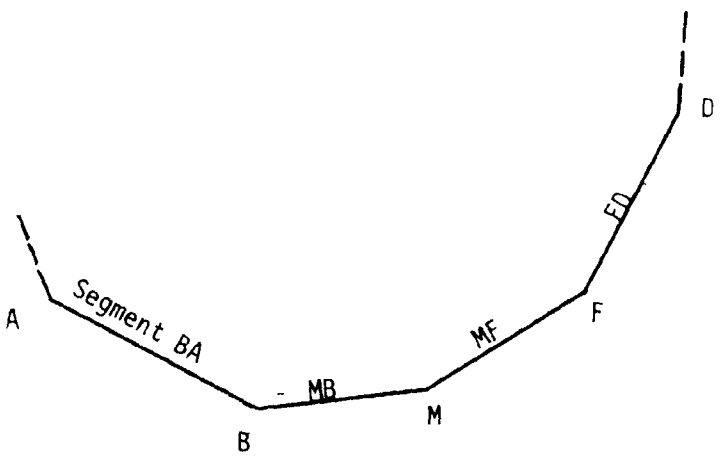

Figure 2.11 A Typical Boundary Modelled by Linear Boundary Element

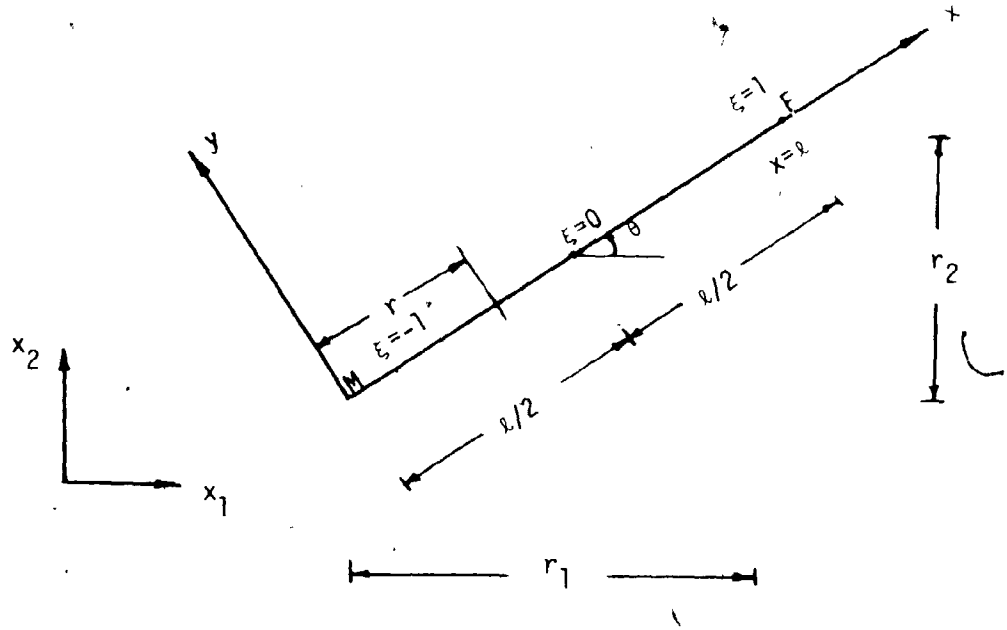

Figure 2.12 Geometrical Definition for the Points M and F

CHAPTER 3

APPLICATION OF BOUNDARY ELEMENT METHOD TO CERTAIN ELASTICITY PROBLEMS

In order to demonstrate the range and the accuracy of the boundary element technique, two problems are solved using both the constant element method discussed in section 2.5.1 and the linear element method discussed in section 2.5.2. The problems solved belong to the following classes:

1. Finite domain problems such as
   a) Disc under internal pressure
   b) Bodies with more than one surface
2. Infinite medium problems.

The results of these solutions are compared with the available closed form solution[28] and those obtained by the finite element method.

3.1 Finite Domain Problems

3.1.1 Disc Under Internal Pressure

The example of a thin disc under the action of an internal pressure, has been selected to show the versatility of the method, and to give an indication of the accuracy obtainable. In order that an indication of the accuracy can be had, the results obtained by using constant and linear elements are compared with the exact and finite elements solutions.

For the thin disc shown in Figure 3.1, because of symmetry, one can use a 90° segment in the analysis. The finite element mesh covering the segement is shown in Figure 3.2, the boundary element discretization using constant elements is shown in Figure 3.3 and that using linear elements is shown in Figure 3.4.

In the case of linear boundary elements, problems appear at the corner points. To each corner node can be assigned two values of traction depending on the side under consideration. A simple way to resolve this ambiguity is to assume that there are two points very near each other but belonging to different sides as shown in Figure 3.4.

The finite element mesh shown in Figure 3.2 consists of 52 nodes and 76 elements, while the boundary element discretization has 26 constant elements and 30 linear elements.

To avoid rigid body motion a series of displacement components must be given specified values. These values are determined from the nature of the problem. Because of symmetry, only radial motion are permitted for the nodes on the x_1 and x_2 axes. Normal displacement of nodes on the x_1 axis and x_2 axis should therefore be constrained as shown in Figure 3.2, 3.3 and 3.4.

The results for radial and hoop stresses are computed at 4 internal points using the boundary element methods and are presented in Table 3.1 and in Figure 3.5. For the sake of comparison the results obtained from both the classical and the finite element solutions are also shown.

The agreement of results between the boundary element solution and classical solution is quite satisfactory. The boundary element results are better than the finite element results. In fact when the stresses at a specific point need to be calculated, the boundary element method will in general yield more accurate results than the finite element method. To obtain comparable accuracy, a larger number of finite elements will have to be used.

A comparison of the data input and run time required for the three methods is presented in Table 3.2. One can notice that the volume of data required by the finite element method is significantly larger than that required by any of the boundary element programs. Also the number of equations to be solved in any one of the boundary element methods is smaller than those in the finite element method.

In spite of this, however, the run time requested with the boundary methods is larger than that required by the finite element method. This is to a large extent due to the fact that while the finite element equations are symmetric and banded with a small bandwidth, the boundary equations are fully populated and asymmetric. It should be noted that for obtaining comparable accuracy in the stress at a point, a larger number of finite elements will have to be used and the run time with the increased number of finite elements will probabily be similar to that required for the boundary method.

Further, in this particular problem the linear element results are no more accurate than the constant element results and the former does not therefore offer any advantage.

3.1.2 Bodies With More Than One Surface

The boundary element method can be used to study problems with more than one surface, such as the case of a body with holes illustrated in Figure 3.6. The body shown in Figure 3.6 has two types of boundaries: internal and external.

In order to define an external or internal boundary one needs to identify the direction of the normal. This can be done for two dimensional problems by adopting the following rule.

1. For external surfaces the numbering scheme used is such that the element numbers increase in the counter clockwise direction.
2. For internal surfaces the element numbers increase in a clockwise direction.

Example:

As an example the disc shown in Figure 3.1, is solved by the boundary element method, this time not taking advantage of the symmetry so that the problem results are that of a body with two surfaces. The results obtained by using constant and linear elements are compared with the exact solutions.

The boundary element discretization using constant elements is shown in Figure 3.7a and that using linear elements is shown in Figure 3.7b. The external boundary has been divided into 24 elements, numbered in the counter clockwise direction; the internal surface has also been divided into 24 elements, numbered in the clockwise direction.

Stress and displacements are computed at 12 internal points. To avoid ridig body motion a series of displacement components are prescribed as equal to zero. These are respectively the displacements in the x_1 direction at nodes 7, 43, 31 and 19, and the displacements in the x_2 direction at nodes 1, 25, 37 and 13.

The results for radial and hoop stresses are presented in Table 3.3 and in Figure 3.8. For the sake of comparison the results obtained from classical solutions are also shown. The agreement of results between the boundary element solution and classical solution is acceptable.

It should however be pointed out that boundary element stresses very close to the boundary are in significant error and the errors occur for all internal points that are situated at a distance from the boundary less than half an element length as shown in Table 3.3. It should be noted that the same situation exists in the finite element solution. In that case the stresses calculated near the boundary are in fact average over the area of finite element adjacent to the boundary. To get accurate estimates of the edge stresses, the size of finite element must be reduced.

3.2 Infinite Medium Problem

When using the boundary element method, the boundaries at infinity can be modelled conveniently without the need of truncating the domain at some arbitrary distance from the region of interest. As an example the problem of a circular cavity under internal pressure in an infinite medium as shown in Figure 3.9 is solved by constant and linear boundary element methods.

The boundary is divided into 24 constant elements and an equal number of nodes as shown in Figure 3.10a. For the linear element solution too the boundary is divided into 24 linear elements and 24 nodes as shown in Figure 3.10b.

To avoid rigid body motion the displacements in the x_1 direction at nodes 12 and 24 and the displacements in the x_2 direction at nodes 6 and 18 are specified as zero.

Stresses and displacements are computed at 10 internal points. The results for radial stresses are presented in Table 3.4 and in Figure 3.11. It can be seen from the results that the displacements and stresses decay with increasing distance from the cavity. The radial and hoop stresses at the internal points have the same absolute value but different signs which is correct.

For the sake of comparison the results obtained from classical solution [28] are also shown in Figure 3.11 and Table 3.4. The agreement of results is satisfactory. Again, there is no significant difference between the results obtained from the constant and linear boundary elements respectively.

3.3 Comments

1. For the problems solved here the results obtained using the constant element and the linear element compare well with the exact solutions. The results obtained by using constant elements are however as accurate as those obtained by the linear element method. The latter method does not seem to offer any advantage.

2. In the case of boundary element method, errors due to discretization are usually confined to the boundaries, for the finite element method the entire domain needs to be discretized and hence discretization errors are present, in each element of the domain.

3. In general since only the boundaries are discretized a much smaller system of equations is developed than when the finite element method is used.

4. Values of the solution variables need only be obtained where required at specified internal points where as in finite element the variables are calculated at every node.

5. An advantage of the boundary element method is that the boundary at infinity can be modelled without truncating the domain at some arbitrary distance from the region of interest.

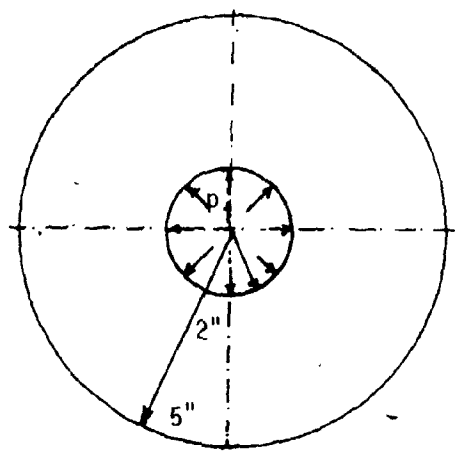

P_i = 1000 psi

E = 30 x 10^6 psi

ν = 0.3

Figure 3.1 Thin Disc with Internal Pressure

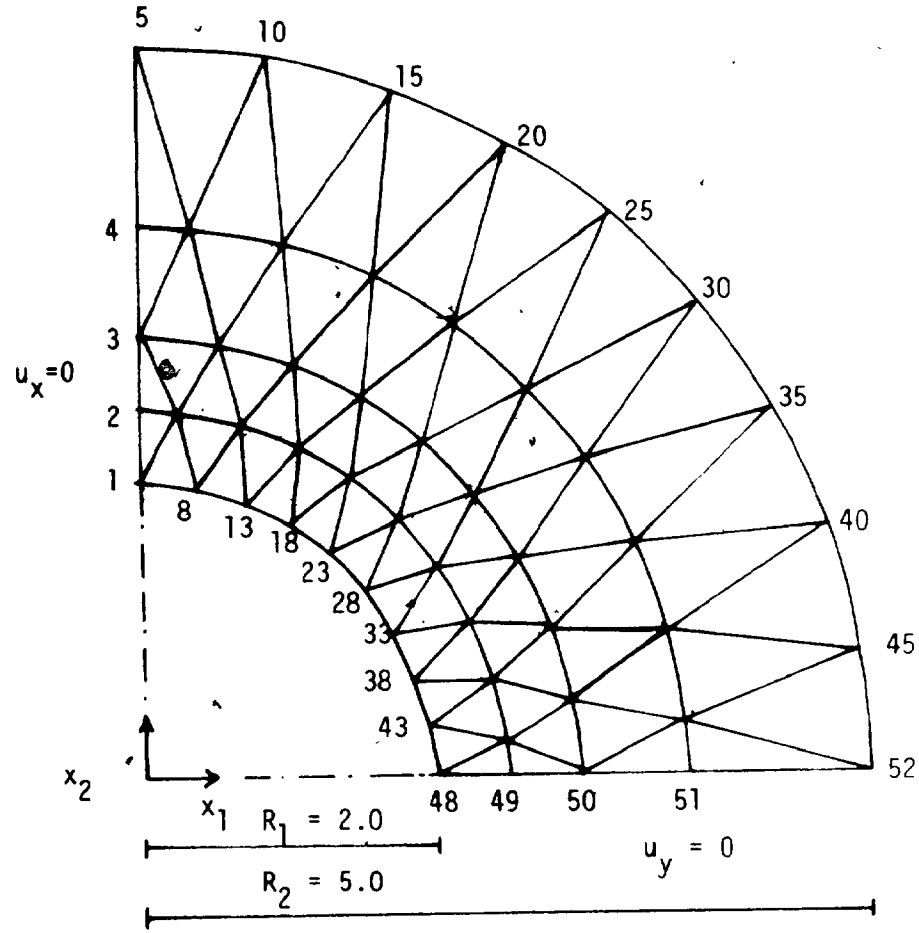

Figure 3.2 Finite Element Mesh

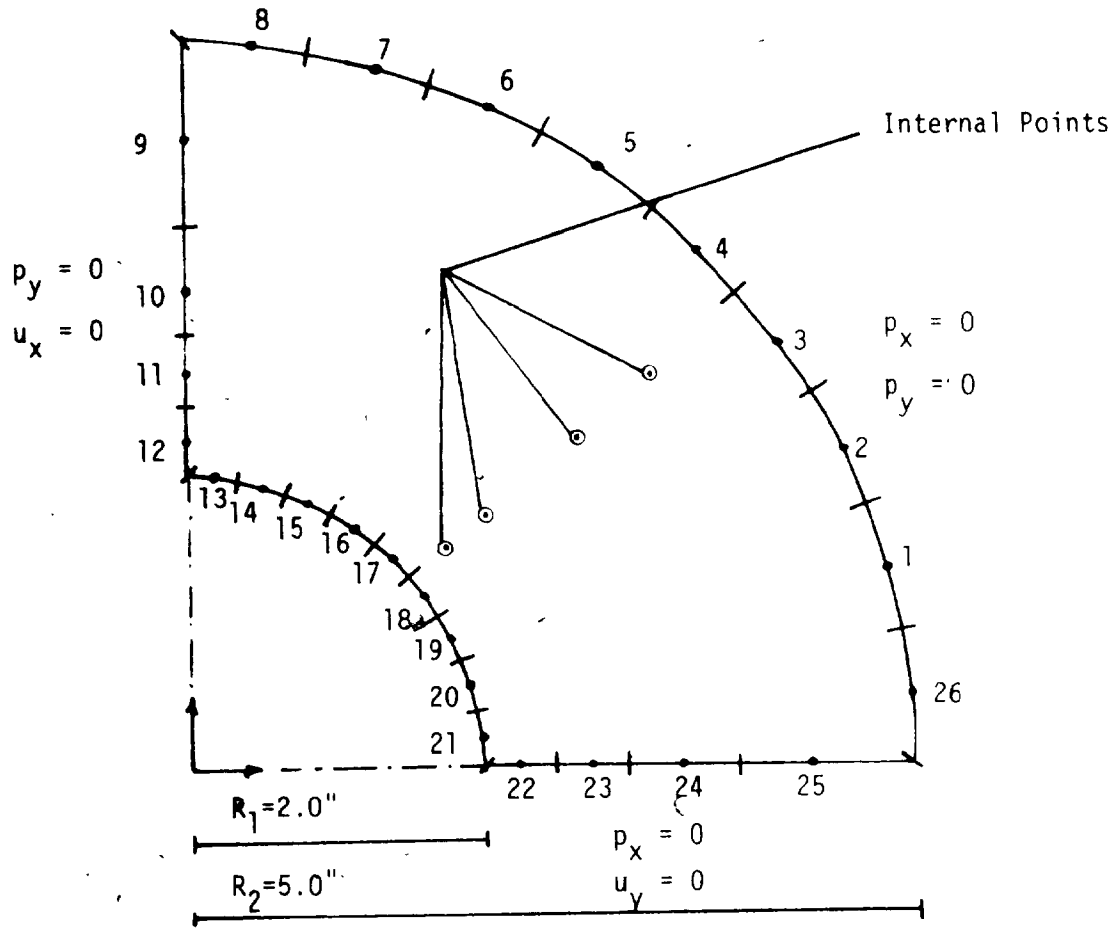

Figure 3.3 Constant Boundary Element Discretization

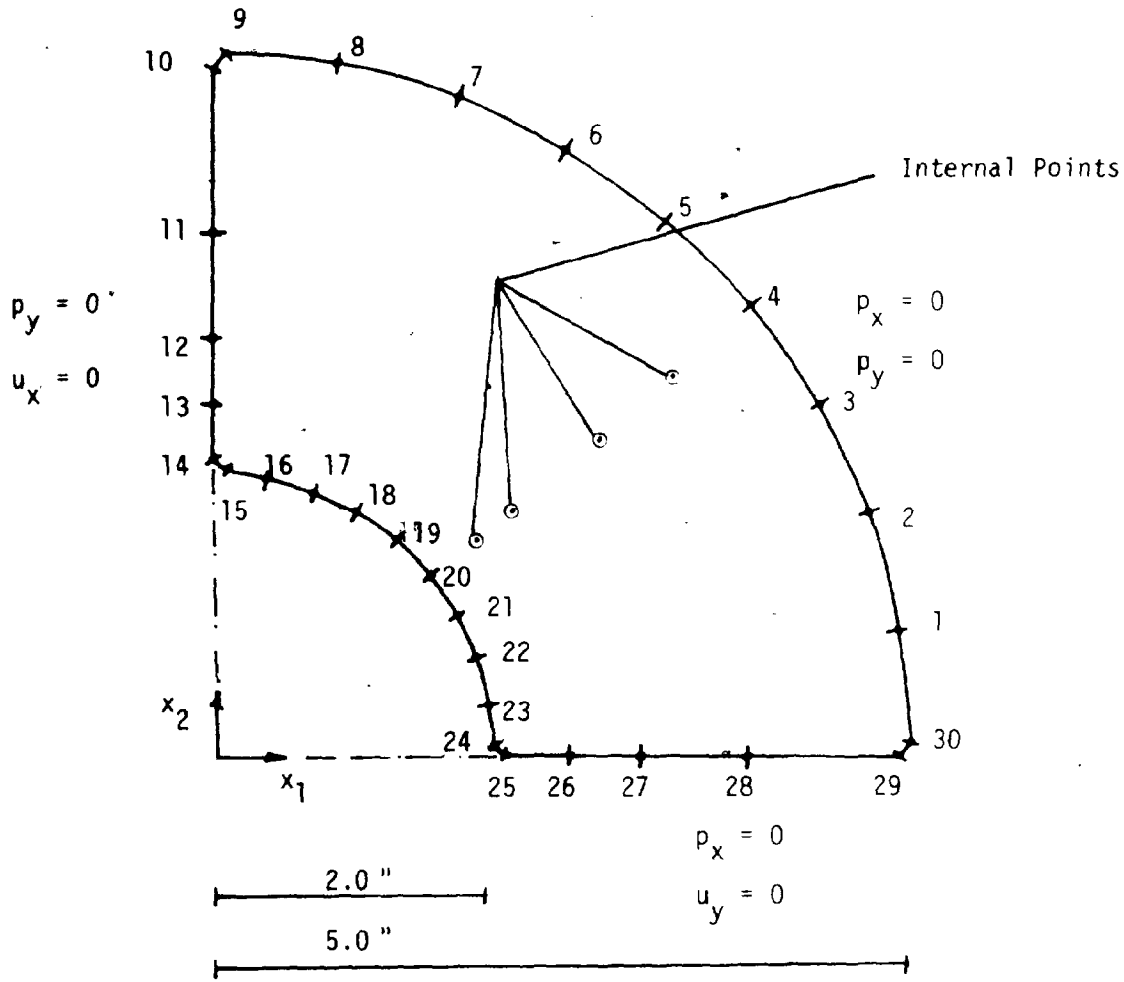

Figure 3.4 Linear Boundary Element Discretization

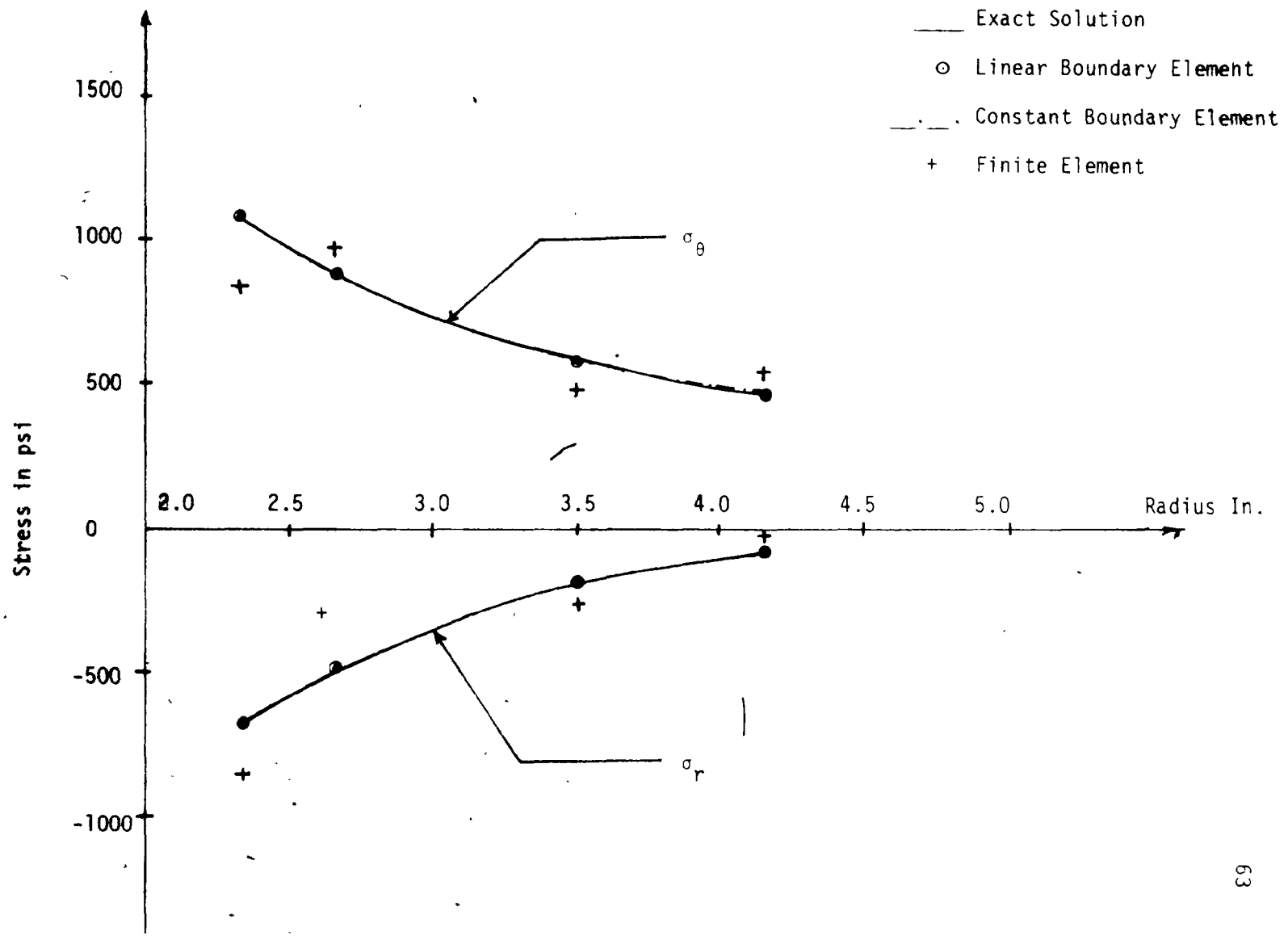

Figure 3.5 Comparison of Exact Solution with Finite Element and Boundary Element Solution

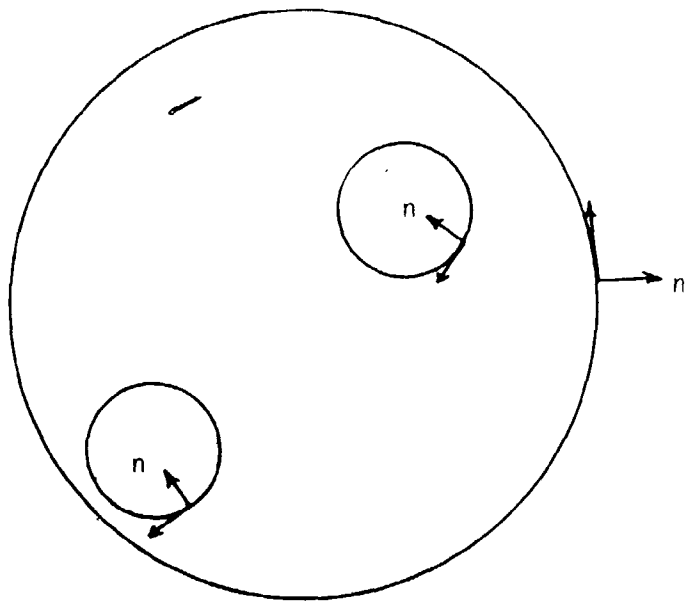

Figure 3.6 Body with Holes

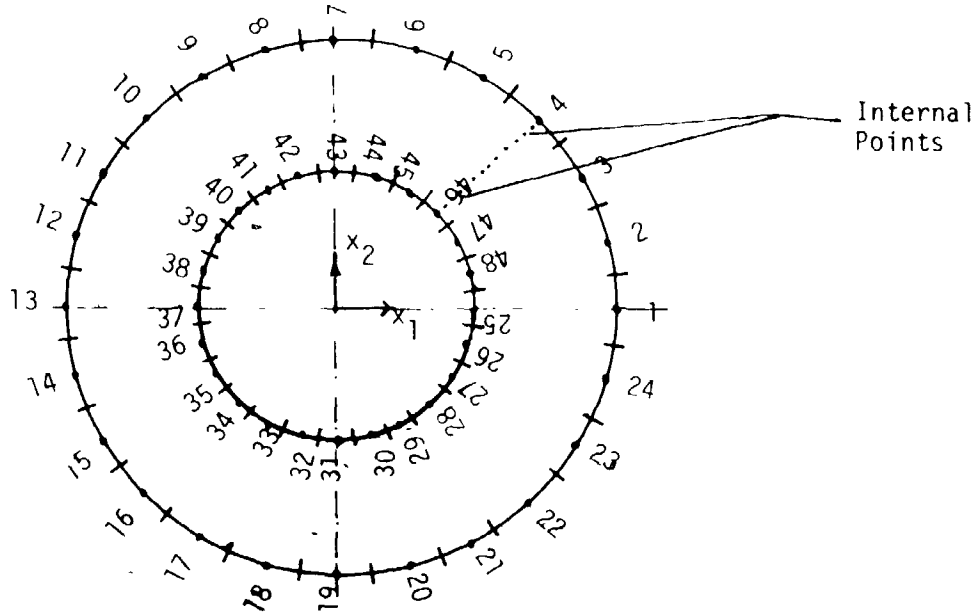

(a) Constant Element

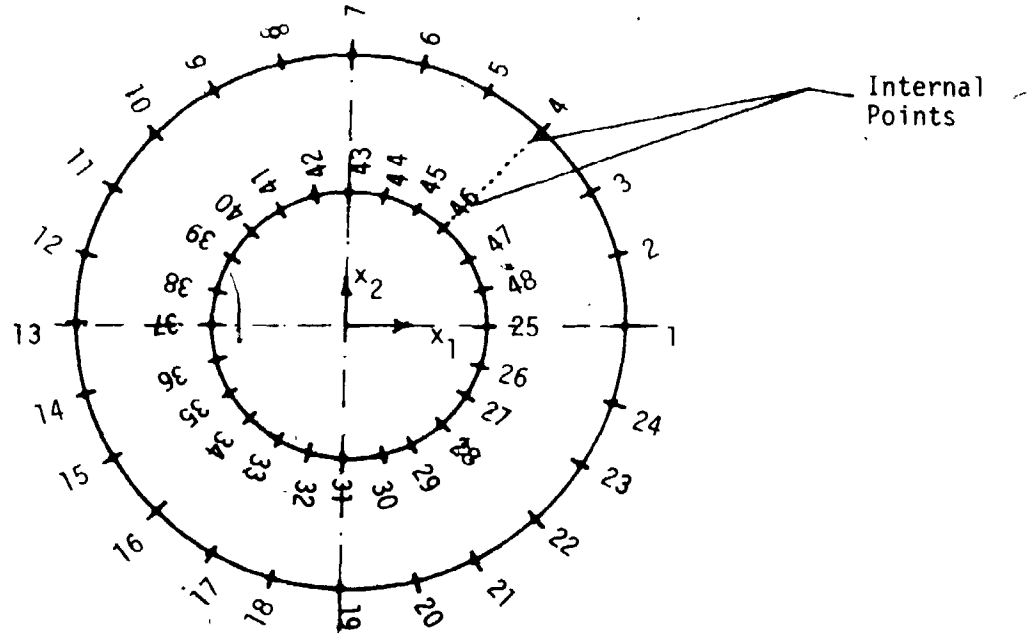

(b) Linear Element

Figure 3.7 Boundary Element Discretization

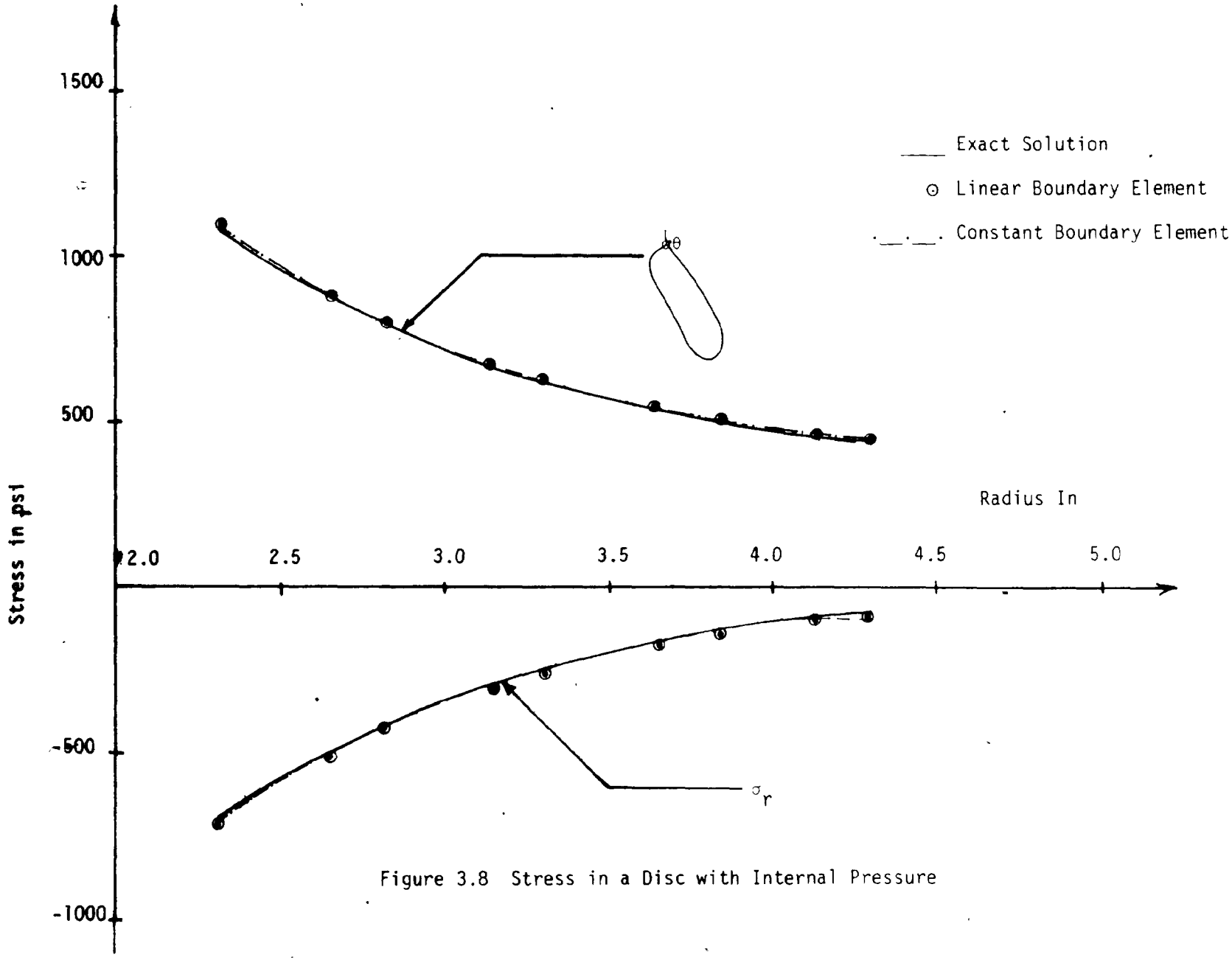

Figure 3.8 Stress in a Disc with Internal Pressure

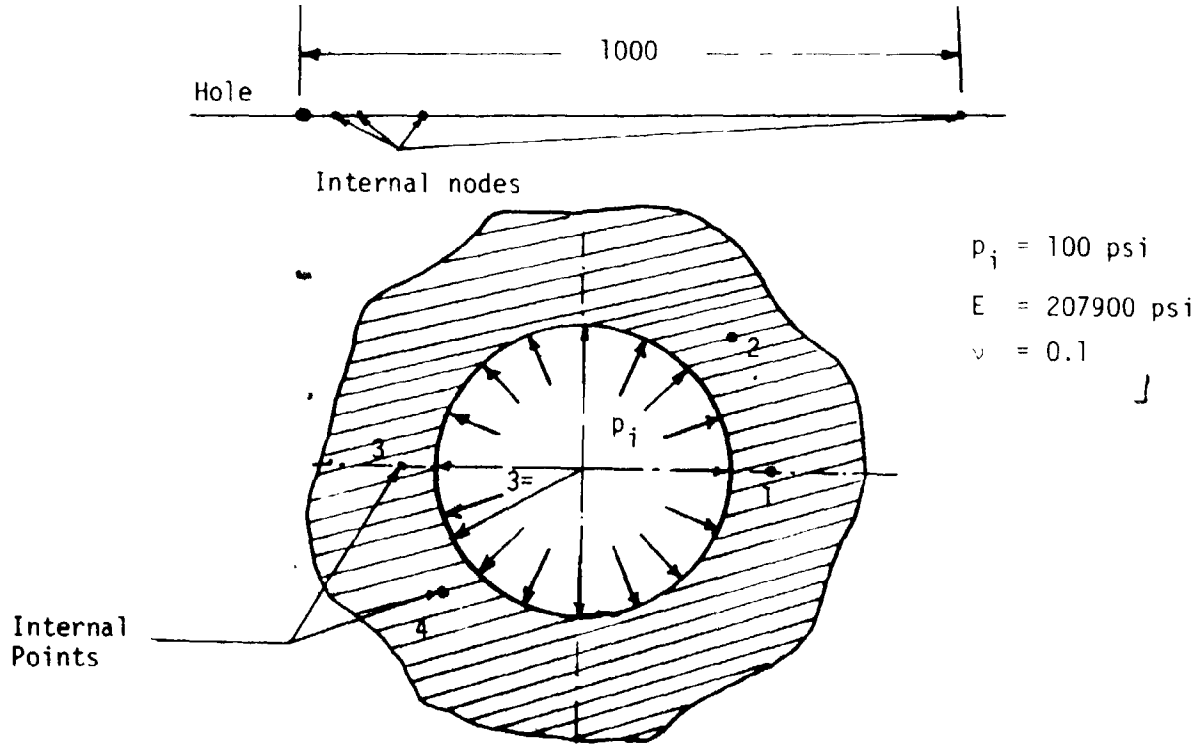

Figure 3.9 Circular Cavity Under Internal Pressure

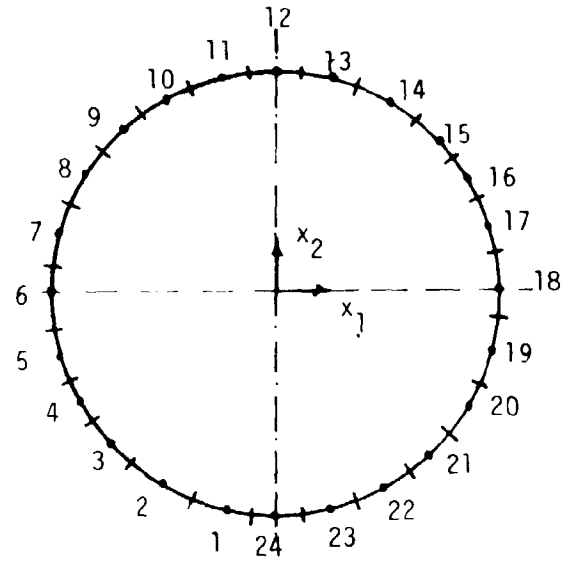

(a) Constant Element Discretization

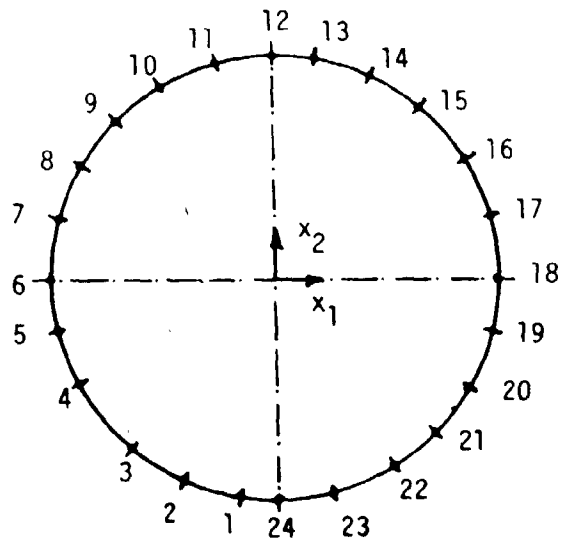

(b) Linear Element Discretization

Figure 3.10 Boundary Element Discretization for Circular Cavity

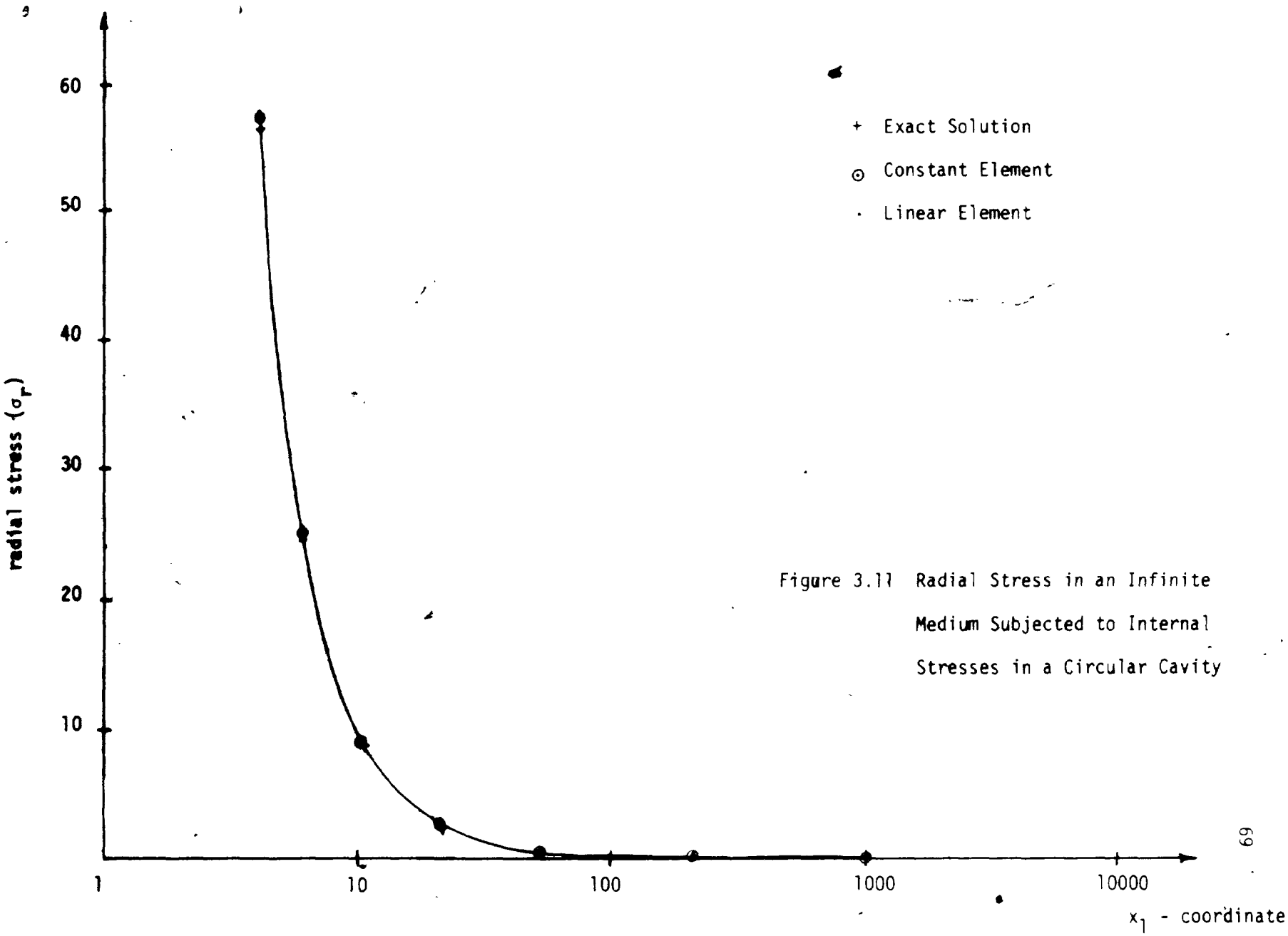

Figure 3.11 Radial Stress in an Infinite Medium Subjected to Internal Stresses in a Circular Cavity

TABLE 3.1

Comparison of Radial and Hoop Stresses in a Disc Segment Obtained by the Classical and the Numerical Methods

Function	Radius	Exact Solution	Finite Element	Boundary Elements Linear	Boundary Elements Constant
Radial Stress (σ_r) lb/in^2	2.33	- 686.66	- 845.0	- 685.67	- 676.6
	2.66	- 482.52	- 336.0	- 471.0	- 487.9
	3.49	- 200.5	- 271.0	- 190.5	- 204.3
	4.156	- 85.22	- 395.0	- 80.0	- 97.5
Hoop Stress (σ_θ) lb/in^2	2.33	1067.6	827.0	1100.0	1067.0
	2.66	863.47	979.0	896.0	870.5
	3.49	581.43	471.0	566.7	588.3
	4.156	466.17	551.0	425.0	483.1

TABLE 3.2

Comparison of Data Input and Run Time Required

Analysis	Number of Degrees of Freedom	Program Length	Number of Cards of Data	Run Time (minute)
Finite Elements	104	16 K	166	0.19
Constant Boundary Element	52	14.8 K	56	0.34
Linear Boundary Element	60	20.6 K	65	0.53

TABLE 3.3

Comparison of Radial and Hoop Stresses

in a Disc Obtained by Classical and Numerical Methods

Radius (in)	Exact Solution		Linear Boundary Element		Constant Boundary Element	
	σ_θ lb/in^2	σ_r lb/in^2	σ_θ lb/in^2	σ_r lb/in^2	σ_θ lb/in^2	σ_r lb/in^2
2.15	1219	-838	1538	-1269	1004	- 650
2.31	1078	-697	1108	- 726	1096	- 725
2.65	870	-489	904.3	- 514	873	- 503
2.81	793	-412	814	- 434	794	- 423
3.14	672	-291	689	- 309	671	- 300
3.3	625	-244	641	- 261	625	- 253
3.64	549	-169	562	- 182	549	- 177
3.8	520	-139	530	- 150	520	- 149
4.13	468	- 87	479	- 99	477	- 110
4.3	447	- 66	463	- 85	471	- 115
4.63	412	- 31	302	85	527	- 207
4.8	397	- 16	612	307	-2332	-1577

TABLE 3.4

Radial Stresses[+] in an Infinite Medium Subjected to Internal Stresses in a Circular Cavity

Point	x_1 - Coordinate	x_2 - Coordinate	Boundary Element Method: Constant Element	Boundary Element Method: Linear Element	Exact Solution
1	4.0	0.0	-57.23	-57.78	-56.25
2	2.83	2.83	-57.23	-57.78	-56.25
3	-4.0	0.0	-57.23	-57.78	-56.25
4	-2.83	-2.83	-57.23	-57.78	-56.25
5	6.0	0.0	-25.29	-25.67	-25.0
6	10.0	0.0	- 9.1	- 9.2	- 9.0
7	20.0	0.0	- 2.27	- 2.3	- 2.25
8	50.0	0.0	- 0.36	- 0.37	- 0.36
9	200.0	0.0	- .02276	- 0.023	- 0.0225
10	1000.0	0.0	- .00091	- 0.00092	- 0.0009

[+] The hoop stresses have the same value but are opposite in sign.

Exact Solution: $\sigma_r = -p_1 \frac{r_1^2}{r^2}$ $\sigma_\theta = p_1 \frac{r_1^2}{r^2}$

CHAPTER 4

COMBINATION OF BOUNDARY AND FINITE ELEMENTS IN ELASTOSTATICS

4.1 Introduction

The possibility of combining the finite and the boundary element methods in the solution of elasticity problems has been investigated by many researchers (Osias [21], Mei [18], Brebbia [4]). The advantage of a combined method is that the infinite domains can be efficiently represented by the boundary method while the finite part of the domain is best represented by the finite element particularly if it contains nonhomogeneous material. Example of situations are shown in Figure 4.1, where the soil region is treated as an infinite or semi-infinite space and the structure is represented by a finite element model.

The mathematical formulation of the combination between boundary and finite elements is developed in this chapter. Two alternative approaches to the combination are possible. The first method converts the boundary element region into an equivalent finite element region and the second treats the finite element region as an equivalent boundary element region. The first approach offers the additional advantage that it can easily be incorporated into existing finite element codes.

4.2 The Relationship Between Finite and Boundary Elements

This section develops the mathematical formulation of a combined finite element boundary element method using the two alternative approaches. The first approach transforms the boundary elements region to an equivalent finite element region and the second approach transforms the finite element region to an equivalent boundary elements region.

4.2.1 Equivalent Finite Element Approach

Figure 4.2 shows two regions Ω^1 and Ω^2 joined by an interface Γ^I, where Ω^1 represents boundary element region and Ω^2 represents the finite element region. The equivalent stiffness matrix for boundary elements region is calculated and is combined with the stiffness matrix of finite elements region to get a global equivalent stiffness matrix and the overall system is then solved as a stiffness problem.

The first step in this approach is to convert the tractions on the boundary to forces at nodes. If $q(\xi)$ is the applied force per unit length of the element as shown in Figure 4.3a. The equivalent nodal forces are calculated by the principal of virtual work,

$$[v^*]^T \cdot \{F^e\} = \int_0^L [v^*(\xi)]^T \cdot \{q(\xi)\}\, d\xi \qquad 4.1$$

where

v^* is a raw vector containing the nodal virtual displacements,

F^e is a column vector containing the nodal forces,

$v^*(\xi)$ is a raw vector containing the virtual displacement values along the length of the element

$q(\xi)$ is a column vector containing the traction values along the length of the element

For the two dimensional case, vectors v^* and F^e will have four elements each and vectors $v^*(\xi)$ and $q(\xi)$ will have two elements each.

Now let $q(\xi)$ be denoted in terms of the nodal tractions (force per unit length) q_1 and q_2 by using linear interpolation function (see Figure 4.3c).

$$\begin{Bmatrix} q_x(\xi) \\ q_y(\xi) \end{Bmatrix} = \begin{bmatrix} 1-\xi/L & 0 & \xi/L & 0 \\ 0 & 1-\xi/L & 0 & \xi/L \end{bmatrix} \begin{bmatrix} q_{1x} \\ q_{1y} \\ q_{2x} \\ q_{2y} \end{bmatrix} \tag{4.2}$$

$$= \begin{bmatrix} \phi_1 & 0 & \phi_2 & 0 \\ 0 & \phi_1 & 0 & \phi_2 \end{bmatrix} \begin{bmatrix} q_{1x} \\ q_{1y} \\ q_{2x} \\ q_{1y} \end{bmatrix}$$

If the same interpolation functions are used for the displacements

$$\begin{Bmatrix} v_x^*(\xi) \\ v_y^*(\xi) \end{Bmatrix} = \begin{bmatrix} \phi_1 & 0 & \phi_2 & 0 \\ 0 & \phi_1 & 0 & \phi_2 \end{bmatrix} \begin{bmatrix} v_{1x}^* \\ v_{1y}^* \\ v_{2x}^* \\ v_{2y}^* \end{bmatrix}, \tag{4.3}$$

On substituting Equations 4.2 and 4.3 into Equation 4.1

$$[v^*]^T\{F^e\} = [v^*]^T \int_0^L \begin{bmatrix} \phi_1 & 0 \\ 0 & \phi_1 \\ \phi_2 & 0 \\ 0 & \phi_2 \end{bmatrix} \begin{bmatrix} \phi_1 & 0 & \phi_2 & 0 \\ 0 & \phi_1 & 0 & \phi_2 \end{bmatrix} d\xi \begin{bmatrix} q_{1x} \\ q_{1y} \\ q_{2x} \\ q_{2y} \end{bmatrix}$$

or $\{F^e\} = [Q^e]\ \{P^e\}$

where $[Q^e]$ is a transformation matrix given by

$$[Q^e] = \int_0^L \begin{bmatrix} \phi_1^2 & 0 & \phi_1\phi_2 & 0 \\ 0 & \phi_1^2 & 0 & \phi_1\phi_2 \\ \phi_1\phi_2 & 0 & \phi_2^2 & 0 \\ 0 & \phi_1\phi_2 & 0 & \phi_2^2 \end{bmatrix} d\xi$$

$$= L \begin{bmatrix} 1/3 & 0 & 1/6 & 0 \\ 0 & 1/3 & 0 & 1/6 \\ 1/6 & 0 & 1/3 & 0 \\ 0 & 1/6 & 0 & 1/3 \end{bmatrix} \tag{4.4}$$

For the constant element shown in Figure 4.3d, [Q] will be given by

$$[Q^e] = L \begin{bmatrix} 1 & 0 \\ 0 & 1 \end{bmatrix} \tag{4.5}$$

Equation 4.4 and 4.5 are the transformation matrices for linear and constant elements, respectively. The assembly of the element transformation matrices will give a global transformation matrix so that,

$$[Q] = \Sigma Q^e \tag{4.6}$$

The equation of boundary element as defined in Equation 2.23 is

$$[H]\{v\} = [G]\{q\} \tag{4.7}$$

The above equation can be expressed in the form

$$[G]^{-1} [H]\{v\} = \{q\} \tag{4.8}$$

premultiplication of the two sides of Equation 4.8 by the matrix Q described in Equation 4.6 gives

$$[Q] [G]^{-1} [H]\{v\} = [Q]\{q\} \tag{4.9}$$

Defining

$$\begin{aligned} [\bar{k}] &= [Q][G]^{-1} [H] \\ \{F\} &= [Q]\{q\} \end{aligned} \tag{4.10}$$

Equation 4.9 takes the following finite element form:

$$[\bar{k}]\{v\} = \{F\} \tag{4.11}$$

The matrix $\bar{k}$ is a finite element type matrix and should be symmetric from basic principles. In practice matrix $\bar{k}$ is not symmetric due to

the approximation involved in the discretization process and the choice of the assumed solution. The simplest way of making $\bar{k}$ symmetric is by using the method of least squares [5] to minimize the error associated with $\bar{k}_{ij} \neq \bar{k}_{ji}$.

The error can be expressed as the difference between $\bar{k}_{ij}$ and $\bar{k}_{ji}$ and the unknown coefficient k_{ij}, which is symmetric, i.e.:

$$\varepsilon_{ij} = \frac{1}{2} \{(k_{ij} - \bar{k}_{ij}) + (k_{ij} - \bar{k}_{ji})\} \tag{4.12}$$

The square of this error is now minimized giving

$$\frac{\partial}{\partial k_{ij}} (\varepsilon_{ij}^2) = 2k_{ij} - \bar{k}_{ji} - \bar{k}_{ij} = 0 \tag{4.13}$$

Hence the new symmetric coefficients are,

$$k_{ij} = \frac{1}{2} (\bar{k}_{ij} + \bar{k}_{ji}) \tag{4.14}$$

and the corresponding matrix k which is now symmetric is

$$k = \frac{1}{2} (\bar{k} + \bar{k},T) \tag{4.15}$$

Hence Equation 4.11 now becomes,

$$[k]\{v\} = \{F\} \tag{4.16}$$

where k is the equivalent stiffness matrix of the boundary element region.

To formulate global stiffness matrix for the combined region shown in Figure 4.2 define the following vector functions

$\underset{\sim}{q}_B$ - Tractions on external surface of region 1

$\underset{\sim}{q}_I$ - Tractions on interface Γ^I (considering it belongs to region 1).

$\underset{\sim}{v}_B$ - Displacement on external surface of region 1.

$\underset{\sim}{v}_I$ - Displacements on interface Γ^I (considering it belongs to region 1)

f_F - Tractions on external surface of region 2

f_I - Tractions on interface Γ^I (considering it belongs to region 2)

u_F - Displacements on external surface of region 2

u_I - Displacements on interface Γ^I (considering that it belongs to region 2)

The equation corresponding to region 1 Equation 4.16 are now represented in a partitioned form as follows

$$\begin{bmatrix} \underset{\sim}{k}^{BB} & \underset{\sim}{k}^{BI} \\ \underset{\sim}{k}^{IB} & \underset{\sim}{k}^{II} \end{bmatrix} \begin{Bmatrix} \underset{\sim}{v}_B \\ \underset{\sim}{v}_I \end{Bmatrix} = \begin{Bmatrix} \underset{\sim}{F}_B \\ \underset{\sim}{F}_I^B \end{Bmatrix} \tag{4.17}$$

where

$$\begin{Bmatrix} \underset{\sim}{F}_B \\ \underset{\sim}{F}_I^B \end{Bmatrix} = \begin{bmatrix} \underset{\sim}{Q}^{BB} & \underset{\sim}{Q}^{BI} \\ \underset{\sim}{Q}^{IB} & \underset{\sim}{Q}^{II} \end{bmatrix} \begin{Bmatrix} \underset{\sim}{q}_B \\ \underset{\sim}{q}_I \end{Bmatrix}$$

For finite element region (region 2) the equations of stiffness can be written as

$$\begin{bmatrix} k^{FF} & k^{FI} \\ k^{IF} & k^{II} \end{bmatrix} \begin{Bmatrix} u_F \\ u_I \end{Bmatrix} = \begin{Bmatrix} F_F \\ F_I^F \end{Bmatrix} \tag{4.18}$$

Now let p_I, u_I indicate the net tractions and displacements at the interface Γ^I, then the following conditions apply,

i) Compatibility $\underset{\sim}{v}_I = u_I$

ii) Equilibrium $\underset{\sim}{q}_I + f_I = p_I$ or $\underset{\sim}{F}_I^B + F_I^F = F_I$ (4.19)

Hence Equations 4.17 and 4.18 can be written as,

$$\begin{bmatrix} \underset{\sim}{k}^{BB} & \underset{\sim}{k}^{BI} & 0 \\ \underset{\sim}{k}^{IB} & (\underset{\sim}{k}^{II}+k^{II}) & k^{FI} \\ 0 & k^{IF} & k^{FF} \end{bmatrix} \begin{Bmatrix} \underset{\sim}{v}_B \\ u_I \\ \underset{\sim}{u}_F \end{Bmatrix} = \begin{Bmatrix} \underset{\sim}{F}_B \\ \underset{\sim}{F}_I^B + F_I^F \\ F_F \end{Bmatrix} \tag{4.20}$$

where

$\underset{\sim}{F}_B$ is the nodal force vector on external surface of boundary element region

F_F is the nodal force vector on external surface of finite element region

$\underset{\sim}{F}_I^B$ is the force vector on interface Γ^I (considering it belongs to boundary element region)

F_I^F is the force vector on interface Γ^I (considering it belongs to finite element region)

F_I indicates the net forces at the interface Γ^I

Equation 4.20 are the final shiftness equations for the entire region.

4.2.2 Equivalent Boundary Element Approach

In this approach the stiffness equations for the finite element region are converted into equivalent boundary element equations.

The first step is again to express the forces at finite element boundary nodes in terms of tractions on the boundary. Following a procedure similar to that described in section 4.2.1, the displacement and tractions vectors along a boundary are expressed in terms of their nodal values as:

$$u^*(x) = \phi\, u^*$$
$$p\,(x) = \psi\, p \tag{4.21}$$

where u^* and p are the nodal virtual displacements and nodal tractions respectively. By the principle of virtual work

$$[u^*]^T \,.\, \{F\} = \int_\Gamma [u^*(x)]^T \,.\, \{p(x)\}\, dx$$

$$= [u^*]^T \int_\Gamma [\phi]^T\, [\psi]\, \{p\}\, dx$$

$$\{F\} = \int_\Gamma [\phi]^T\, [\psi]\, dx\, \{p\}$$

$$\{F\} = [M]\, \{p\} \tag{4.22}$$

where

[M], is a transformation matrix given by

$$[M] = \int_\Gamma [\phi]^T \,.\, [\psi]\, dx \tag{4.23}$$

The standard finite element equation can be written as,

$[k]\{u\} = \{F\}$ or as,

$$[k]\{u\} = [M]\{p\} \tag{4.24}$$

which is of a form similar to that of the boundary element Equation 4.7.

Referring to Figure 4.2, the boundary element equations for region 1 are

$$[H]\{v\} = [G]\{q\}$$

where $\{v\}$ is a vector of displacements and $\{q\}$ is a vector of tractions. The above equations are now written in a partitioned form so that

$$[H_B \; H_I] \begin{Bmatrix} \underset{\sim}{v}_B \\ \underset{\sim}{v}_I \end{Bmatrix} = [G_B \; G_I] \begin{Bmatrix} \underset{\sim}{q}_B \\ \underset{\sim}{q}_I \end{Bmatrix} \tag{4.25}$$

where

$\underset{\sim}{v}_B$, $\underset{\sim}{v}_I$, $\underset{\sim}{q}_B$ and $\underset{\sim}{q}_I$ are as defined in section 4.2.1

In a similar manner, the finite element Equation 4.24 can be written for region 2 as,

$$[k_F \; k_I] \begin{Bmatrix} u_F \\ u_I \end{Bmatrix} = [M_1 \; M_2] \begin{Bmatrix} f_F \\ f_I \end{Bmatrix} \tag{4.26}$$

where the u_F, u_I, f_F and f_I are as defined in section 4.2.1.

Taking into consideration the conditions of equilibrium and compatibility on the interface (Equation 4.19), one can write Equation 4.25 as follows:

$$H_B \cdot \underset{\sim}{V}_B + H_I \cdot \underset{\sim}{V}_I = G_B \cdot \underset{\sim}{q}_B + G_I \, (p_I - f_I) \qquad \text{or}$$

$$H_B \cdot \underset{\sim}{V}_B + H_I \cdot \underset{\sim}{V}_I + G_I\, f_I = G_B\, \underset{\sim}{q}_B + G_I\, p_I \tag{4.27}$$

The finite element equation are,

$$k_F\, u_F + k_I\, u_I = M_1\, f_F + M_2\, f_I \qquad \text{or}$$

$$k_F\, u_F + k_I\, u_I - M_2\, f_I = M_1\, f_F \tag{4.28}$$

Equations 4.27 and 4.28 can be written as

$$\begin{bmatrix} H_B & H_I & G_I & 0 \\ 0 & k_I & -M_2 & k_F \end{bmatrix} \begin{bmatrix} \underset{\sim}{V}_B \\ u_I \\ f_I \\ u_F \end{bmatrix} = \begin{bmatrix} G_B & G_I & 0 \\ 0 & 0 & M_1 \end{bmatrix} \begin{bmatrix} \underset{\sim}{q}_B \\ p_I \\ f_F \end{bmatrix} \tag{4.29}$$

Equation 4.29 represents in their final form the equations for the equivalent boundary element approach.

4.3 Applications

To examine the validity of using the equivalent finite element approach (section 4.2.1), and the effective stiffness k (Equation 4.15) and the applicability of the least square symmetrization technique, the problem described by Figure 4.4 is solved. The problem represents a uniformly distributed gravity load applied on the boundary of a semi infinite soil region. The boundary of the half space is considered to be a straight line.

To avoid rigid body motion the displacements in the x_1 and x_2 directions at nodes 1 and 45, in the constant element case, and at

2 OF / DE 2

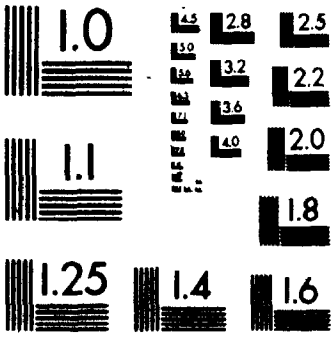

nodes 1 and 46, in the linear element, are specified as zero.

This problem is first solved by using the boundary element method. The H and G matrices are formed, the equations are reordered and then solved to yield the unknown displacement and tractions (Method 1, Tables 4.1 and 4.2).

As an alternative approach, the boundary problem is converted into the equivalent finite element problem. The matrix $k = \frac{1}{2}(\bar{k} + \bar{k}'^{T})$ is formed, where $\bar{k} = Q.G^{-1}.H$. The Q matrix is formed using the procedure described in section 2.4.1. It should be noted this matrix is not the same for the constant element and the linear element case. For the constant element case the formulation is based on the assumption of constant values displacement and traction along an element; in the linear element case both the tractions and displacements vary linearly. The equations of stiffness (Equation 4.16) kv = F are then solved to yield the unknown displacement (Method 2, Tables 4.1 and 4.2). The results obtained are compared with those obtained by Brebbia [4] and are presented in Table 4.1. These results clearly demonstrate the validity of developing an equivalent stiffness matrix from a boundary element formulation and the use of least square technique to symmetrize the stiffness matrix. They also provide a confirmation of the accuracy of computer program used. The problem solved here is thus designed to serve as a benchmark for the testing of programs which are later used in the analysis of beams resting on a half-space.

It should be noted that in the equation kv = F, all values of the vector v are not unknowns. To solve the above equation, without the need for rearranging the matrices, the well-known method of Payne and Irons [2] is used. A brief description of the method is presented below. Let v_i be a known displacement component. Then a ficticious component is put into the force vector in position i. This component is given by

$$F_i = c\, k_{ii}\, v_i$$

where c is a large number say equal to 10^{12}, and k_{ii} is the diagonal element of the stiffness matrix corresponding to v_i.

The stiffness matrix is changed by substituting $c\, k_{ii}$ for k_{ii}. The ith equation is now treated in the same way as the other equations. The above modifications ensure that the equations when solved will give the original known value for v_i by treating in this way each row that contains a known v, the problem is changed to one in which all the F components have numerical values and all the v components are treated as unknowns.

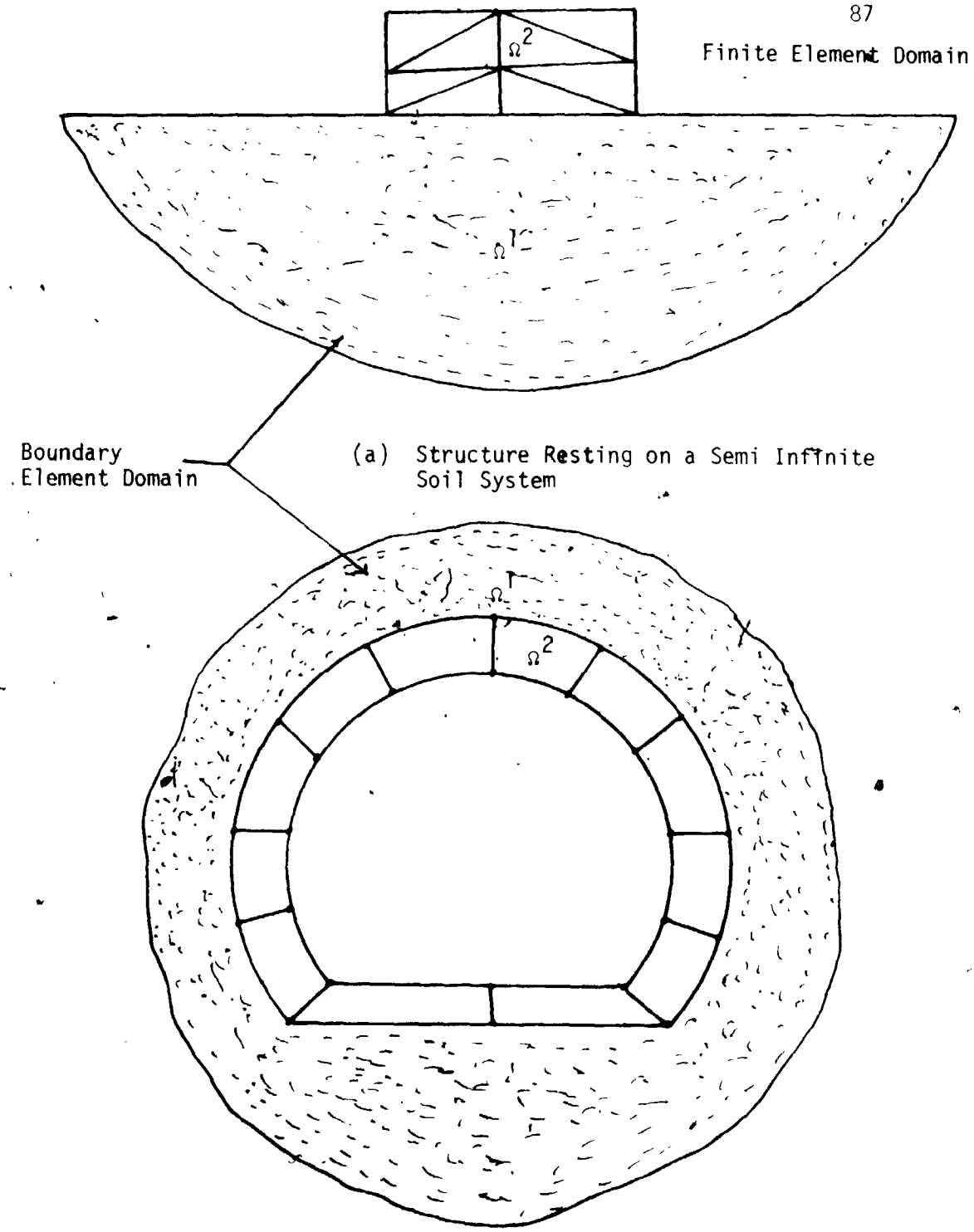

(b) Tunnel in an Infinite Soil Mass

Figure 4.1* Representation of Boundary Elements Domain and Finite Elements Domain

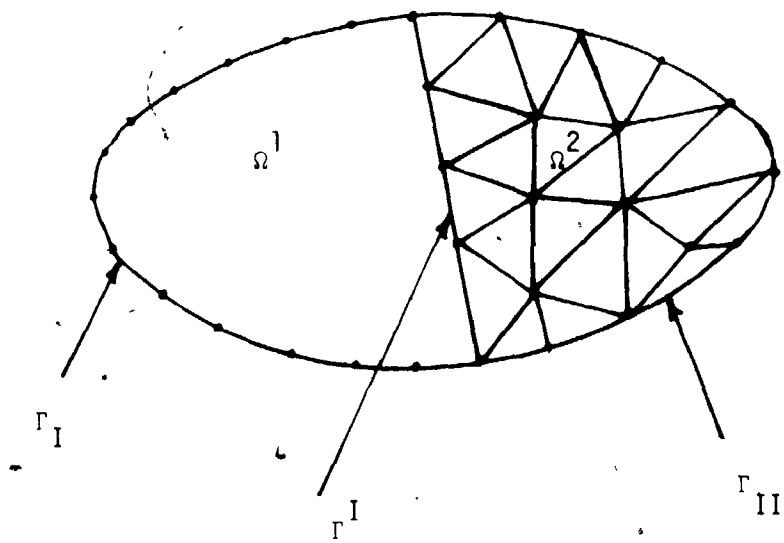

Figure 4.2 Body Divided into Finite Elements and Boundary Elements

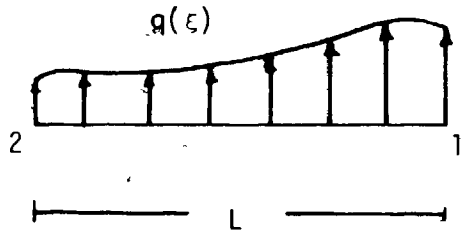

(a) Linear Element

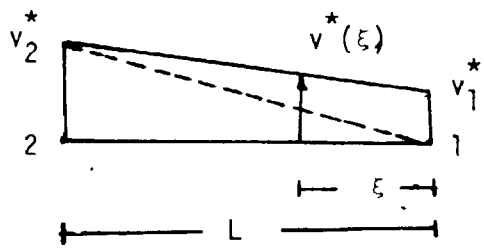

(b) Linear Element Displacements

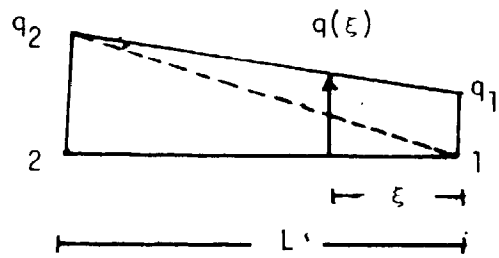

(c) Linear Element Tractions

$$\phi_1 = 1 - \frac{\xi}{L}$$

$$\phi_2 = \frac{\xi}{L}$$

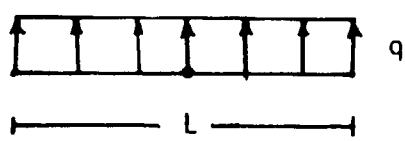

(d) Constant Element

Figure 4.3 Interpolation Functions for Boundary Elements

TABLE 4.1

Comparison of the Results Obtained by Brebbia and Present Work

by Using Constant Boundary Elements

Node	Boundary Element Method (1)				Equivalent k, Method (2)			
	Brebbia Solution		Present Work		Brebbia Solution		Present Work	
	10^{-5} Disp.X (m)	10^{-5} Disp.Y (m)	10^{-5} Disp.X (m)	10^{-5} Disp.Y (m)	10^{-5} Disp.X (m)	10^{-5} Disp.Y (m)	10^{-5} Disp.X (m)	10^{-5} Disp.Y (m)
21	0.61742	11.5865	0.61496	11.5405	0.6144	11.5872	0.61226	11.5412
22	0.31732	11.94694	0.31593	11.8995	0.316	11.948	0.31458	11.9002
23	0	12.0523	0	12.0045	0	12.0528	0	12.0051
24	-0.31732	11.94694	-0.31593	11.8995	-0.316	11.948	-0.31458	11.9002
25	-0.61742	11.5865	-0.61496	11.5405	-0.6144	11.5872	-0.61226	11.5412

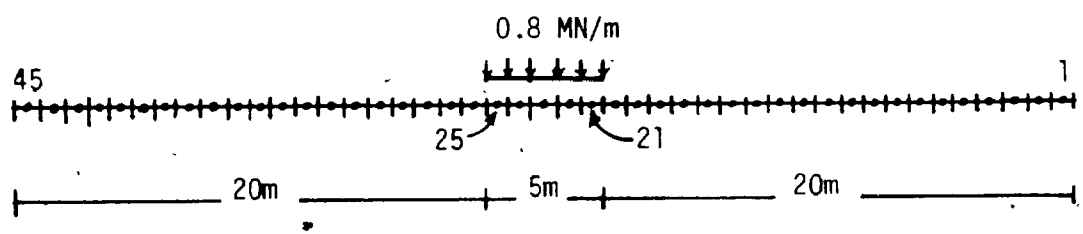

Figure 4.4 Boundary Element Region

TABLE 4.2

Comparison of the Results Obtained from

Boundary Element Method and Equivalent Finite Element Approach,

Using Linear Boundary Elements

Node	Boundary Element Method (1)		Equivalent k, Method (2)	
	Linear Element		Linear Element	
	10^{-5} Displ.X	10^{-5} Displ.Y	10^{-5} Displ.X	10^{-5} Displ.Y
21	0.58541	11.6152	0.5774	11.6178
22	0.2891	12.0195	0.2786	11.9875
23	0	12.1051	0	12.0161
24	0.2891	12.0195	0.2786	11.9875
25	0.58541	11.6152	0.5774	11.6178

CHAPTER 5

COMBINATION OF BOUNDARY AND FINITE ELEMENT FOR THE ANALYSIS OF BEAMS RESTING ON HOMOGENEOUS ELASTIC HALF-SPACE

5.1 Introduction

The analysis of beams resting on an elastic half-space is presented in this chapter. The analysis is based on the following assumptions:

1. The problem is considered as two dimensional
2. Both the beam and supporting soil are assumed to be linearly elastic
3. The friction between the beam and soil is neglected, i.e. only vertical stresses exist at the foundation-soil surface.

Two different methods have been used in the literature for the analysis of beams,

1. Methods based on the "Winkler" solution
2. Methods based on the "Elastic half-space" solution.

The Winkler theory is based on the assumption that the magnitude of subgrade reaction at any point is directly proportional to the foundation deflection at that point. Under this assumption the solution can be obtained by solving a fourth order differential equation for the deflection of the beams (Hetenyi [10], Iyenger [11] or Iwanczewska and Lewandowski [12]).

The elastic half-space solutions are based on the analysis of the problem according to the classical theory of elasticity.

The method used in this chapter is the "Elastic half-space solution". The analysis procedures use two alternative numerical approaches based on a combination of the boundary and finite element discretizations. These are the equivalent finite element approach (section 4.2.1) and the equivalent boundary element approach (section 4.2.2). To compare the relative efficiency of the two alternative approaches, a beam on elastic half-space is solved.

It is demonstrated by a sample solution that the results obtained by the two approaches are almost the same. Thus both approaches are equally accurate in solving the problem. The finite element approach (section 4.2.1) is used for the solution of all other numerical problems reported in this chapter. These include analyses of beams of finite length subjected to concentrated moments, concentrated loads and uniformly distributed loads. More complicated cases of loading can be solved by the superposition of the results obtained from these elementary solutions.

5.2 Relationship Between Soil Parameters and Coefficient of Subgrade Reaction

The semi-infinite soil region in the foundation beam problem is theoretically better represented by an elastic half-space, defined by parameters E_s and ν, rather than by a beam on Winkler's subgrade defined by one parameter k. Furthermore, an exact theoretical interrelationship

does not exist [14] between the above sets of parameters. However, because of its simplicity the Winkler model has often been used and approximate relationships between the coefficient of subgrade reaction (k) and E_s and ν have been proposed.

Using the theory of elasticity, the average settlement S_a of a uniformly loaded flexible or rigid foundation can be expressed [14] in the following form:

$$S_a = p\sqrt{A} \quad \left(\frac{1-\nu^2}{E_s}\right)\omega \tag{5.1}$$

where

- p , average contact stress,
- A , area of the foundation,
- E_s, soil deformation modulus,
- ν , Poissons ratio of soil
- ω , a coefficient dependent on [14] the flexural stiffness and shape of the foundation (refer Table 5.1).

The average coefficient of subgrade reaction k_a can then be defined as:

$$k_a = \frac{p}{s_a} = \frac{E_s}{\sqrt{A}\,(1-\nu^2)\omega} \tag{5.2}$$

For a beam of width B the subgrade reaction per unit of length can be expressed as

$$k = k_a \cdot B \tag{5.3}$$

5.3 Relative Rigidity of the Beam

For the parametric study of beams resting on soil it is useful to define a dimensionless number which will serve as a measure of the ratio of foundation stiffness to the flexural stiffness of the beam. For this purpose it is customary to use a number $\lambda\ell$ defined as follows.

For a beam of constant width B, having modulus of elasticity E_b and moment of inertia I, the term λ is defined as

$$\lambda = \sqrt[4]{\frac{k_a \cdot B}{4EI}} \tag{5.4}$$

where k_a is the coefficient of subgrade reaction. It is seen that λ has the dimension of length^{-1}. The term $\lambda\ell$ is a dimensionless number and is referred to as the relative rigidity, ℓ being the length of the beam.

By using Equation 5.2, one can define the relative rigidity as,

$$\lambda\ell = \left(\frac{\ell^4 \cdot E_s \cdot B}{4EI\sqrt{A}\,(1-\nu^2)\omega}\right)^{\frac{1}{4}} \tag{5.5}$$

It will be noted that the above equation is defined in terms of the soil parameters, and the flexural stiffness and shape of the foundation beam.

From a mathematical point of view, some of the beams may be considered to be infinitely long while others may be considered to have a finite length. From practical considerations, beams are classified [23] into four groups as follows:

1. Short beams $\lambda \ell < 0.8$
2. Medium beams $0.8 < \lambda \ell < 2.25$
3. Moderately long beams $2.25 < \lambda \ell < 5.0$
4. Long beams $\lambda \ell > 5.0$

Short beams are very rigid while medium and long beams are flexible.

5.4 Finite Element Representation of the Beam Element

Referring to Figure 5.1 the vertical displacement of typical beam element, subjected to a vertical load can be approximately represented by a third order polynomial in x given by,

$$y = \alpha_1 + \alpha_2 x + \alpha_3 x^2 + \alpha_4 x^3 \tag{5.6}$$

The corresponding value of the rotation θ is obtained by differentiating the above,

$$\theta = \alpha_2 + 2\alpha_3 x + 3\alpha_4 x^2 \tag{5.7}$$

Now if u_1 and u_2 are the displacements at the two ends of the beam, θ_1 and θ_2 are the two rotations and x_1 and x_2 are the end coordinates, the end displacements and rotations can be expressed by the following matrix equation.

$$\begin{bmatrix} u_1 \\ \theta_1 \\ u_2 \\ \theta_2 \end{bmatrix} = \begin{bmatrix} 1 & x_1 & x_1^2 & x_1^3 \\ 1 & 2x_1 & 2x_1^2 & 3x_1^2 \\ 1 & x_2 & x_2^2 & x_2^3 \\ 0 & 1 & 2x_2 & 3x_2^2 \end{bmatrix} \begin{bmatrix} \alpha_1 \\ \alpha_2 \\ \alpha_3 \\ \alpha_4 \end{bmatrix}$$

or

$$\{v\} = [A]\{\alpha\} \tag{5.8}$$

where $\{v\}$ is a vector of end displacement,

$[A]$ is a matrix that contains functions of the coordinates of the beam ends, and

$\{\alpha\}$ is a vector that contains arbitrary constants, which are as yet unknown.

From Equation 5.8, one can calculate the unknown parameters $[\alpha]$ as follows

$$\{\alpha\} = [A^{-1}]\{v\} \tag{5.9}$$

The bending moment at any section of the beam element is given by

$$M = -EI \frac{d^2y}{dx^2}$$

or

$$M = -EI\ (2\alpha_3 + 6\alpha_4 x) \tag{5.10}$$

In a similar manner the shearing force on the beam element can be expressed as

$$Q = \frac{dM}{dx}$$

$$Q = -EI\ (6\alpha_4) \tag{5.11}$$

Using Equation 5.6 and 5.9, the displacement in the beam element is expressed as follows

$$y = [1 \quad x \quad x^2 \quad x^3]\ \{\alpha\}$$

$$= [N]\{\alpha\} = [N][A^{-1}]\{v\}$$

$$= [\phi_1 \quad \phi_2 \quad \phi_3 \quad \phi_4]\{v\}$$

where $[N] = [1 \quad x \quad x^2 \quad x^3]$ and the terms ϕ_1, ϕ_2, ϕ_3 and ϕ_4 which are functions of x are called shape functions or interpolation functions and

are given by

$$\phi_1(x) = 1-3\left(\frac{x}{L}\right)^2 + 2\left(\frac{x}{L}\right)^3$$

$$\phi_2(x) = x\left(1-\frac{x}{L}\right)^2$$

$$\phi_3(x) = 3\left(\frac{x}{L}\right)^2 - 2\left(\frac{x}{L}\right)^3$$

$$\phi_4(x) = \frac{x^2}{L}\left(\frac{x}{L} - 1\right) \tag{5.12}$$

The internal moment is now expressed as

$$M(x) = EI\,(x)\,\frac{d^2y}{dx^2}$$

$$= EI\,(x)\,[B]\{v\}$$

where [B] is given by

$$[B] = \left[-\frac{6}{L^2} + \frac{12x}{L^3} \quad \frac{6x}{L^2} - \frac{4}{L} \quad \frac{6}{L^2} - \frac{12x}{L^3} \quad \frac{6x}{L^2} - \frac{2}{L}\right]$$

Noting that the curvature is given by $\frac{\partial^2 y}{\partial x^2}$ and change of angle over an element of length dx by $\frac{\partial^2 y}{\partial x^2}\,dx$, the internal work done dut to virtual displacement $\{v^*\}$ at the end nodes is given

$$\int_0^L [v^*]^T\,[B]^T\,EI(x)\,[B]\,\{v\}\,dx = [v^*]^T \int_0^L [B]^T\,EI(x)\,[B]\,dx\,\{v\}$$

If the nodal force vector is {F}, the work done by nodal forces is

$[v^*]\,\{F\}$

Equating the external and internal work

$$[v^*]^T\{F\} = [v^*]^T \int_0^L [B]^T EI(x)\,[B]\,dx\{v\}$$

If this is to be true for arbitrary values of $[v^*]^T$

$$\{F\} = \int_0^L [B]^T EI(x)\,[B]\,dx\,\{v\}$$

which is of the form $\{F\} = [K]\{v\}$, $[K]$ being given by

$$[K] = \int_0^L EI(x)\,[B]^T\,[B]\,dx$$

If EI is constant over the length, this becomes:

$$[K] = EI \begin{bmatrix} \frac{12}{L^3} & \frac{6}{L^2} & -\frac{12}{L^3} & \frac{6}{L^2} \\ \frac{6}{L^2} & \frac{4}{L} & -\frac{6}{L^2} & \frac{2}{L} \\ -\frac{12}{L^3} & -\frac{6}{L^2} & \frac{12}{L^3} & -\frac{6}{L^2} \\ \frac{6}{L^2} & \frac{2}{L} & -\frac{6}{L^2} & \frac{4}{L} \end{bmatrix} \tag{5.13}$$

5.5 Equivalent Finite Element Approach

The following procedure is used in the equivalent finite element approach to the solution of the foundation-beam-soil interaction problem. The beam is divided into a number of finite elements and the global

stiffness matrix for the beam is assembled in the usual manner.

The boundary equations for the soil region are formed next. These are converted into equivalent finite element stiffness equations. The equivalent stiffness matrix for the boundary region (Equation 4.17) is then assembled with the stiffness matrix of the beam to form the overall system of equations (Equation 4.20).

5.6 Computer Program for the Equivalent Finite Element Approach

A computer program which uses the constant elements was developed to analyse a beam resting on elastic half-space. The program is based on the analytical treatment presented in sections 4.2.1 and 5.5. The main steps used in the computer program are as follows:

1) Input half-space data; it will include
   - i) the number of boundary elements
   - ii) the shear modulus of the soil material
   - iii) the Poisson's ratio of the soil;
2) Input beam data which includes
   - i) the Young's modulus of the beam material
   - ii) the total number of finite elements nodes in the beam
   - iii) the number assigned to the first node in the beam
   - iv) the width and height of each element of the beam
3) Form matrices [G] and [H] using numerical integration, Equation 2.23.
4) Compute the inverse of matrix [G].

5) Form transformation matrix [Q], Equation 4.6.

6) Form matrix $[Q][G^{-1}][H]$, Equation 4.10.

7) Form the equivalent stiffness matrix of the boundary element region $[K^B]$ by using the least square symmetrization technique, Equation 4.16.

8) Rearrange matrix $[K^B]$ to form Equation 4.17.

9) Form the global stiffness matrix of the beam $[K^F]$, Equation 4.18.

10) Using matrices $[K^B]$ and $[K^F]$ form the overall stiffness matrix, Equation 4.20.

11) Form vector {F}, Equation 4.20. It can be noted that, the components of vector F are as follows:

    i) Forces at the nodes of the boundary elements

    ii) External forces at the nodes corresponding to the interface boundary

    iii) External forces corresponding to rotation of the beam nodes.

12) Modify matrix [K] and vector {F} by the method of Payne and Irons [2] to take into account the known displacements.

13) Using Gauss elimination method, solve the overall system of equations to obtain the displacement vector {u}.

14) Compute bending moment and shear forces for the beam elements by using Equation 5.10 and 5.11.

Several problems were solved by the equivalent finite element approach using the computer program described in this section and the results are presented later.

5.7 Equivalent Boundary Element Approach

As discussed earlier, the equivalent boundary element approach leads to Equation 4.29. Before these equations can be formed, the transformation matrix [M] (Equation 4.23) for the beam elements must be evaluated. The following procedure is used in the formation of this matrix.

Consider the beam element shown in Figure 5.1a, the interpolation function for beam displacement are given by Equation 5.12. Now let the traction on the beam element be assumed to vary linearly as shown in Figure 5.1b, so that traction p(x) at any point along the length of the beam is given by

$$p(x) = [1-\frac{x}{L} \quad \frac{x}{L}] \begin{bmatrix} p_1 \\ p_2 \end{bmatrix} = [\Psi]\,\{p\}$$

Then using Equation 4.23

$$[M] = \int_0^L [\phi]^T \cdot [\Psi]\, dx$$

$$= \int_0^L \begin{bmatrix} 1-3\,(\frac{x}{L})^2 + 2\,(\frac{x}{L})^3 \\ x\,(1-\frac{x}{L})^2 \\ 3\,(\frac{x}{L})^2 - 2\,(\frac{x}{L})^3 \\ \frac{x^2}{L}\,(\frac{x}{L} - 1) \end{bmatrix} [1-\frac{x}{L} \quad \frac{x}{L}]\, dx$$

Thus for a beam element, [M] is 4 by 2 matrix given by

$$[M] = \begin{bmatrix} \frac{7}{20}L & \frac{3}{20}L \\ \frac{1}{20}L^2 & \frac{1}{30}L^2 \\ \frac{3}{20}L & \frac{7}{20}L \\ -\frac{1}{30}L^2 & -\frac{L^2}{20} \end{bmatrix} \tag{5.14}$$

The M matrices for the beam elements are assembled to form the global M matrix. This is followed by the formulation of Equation 4.26 for the beam and Equation 4.25 for the soil region. All submatrices in Equation 4.29 are now determined. It should be noted that the vector p_I in Equation 4.29 is the vector of external tractions acting at the nodes of the beams.

It will be observed that the matrix M of Equation 5.14 represented the reactions and moments produced at the ends of a fixed-ended beam loaded by a distributed load of linearly varying intensity. A simpler expression for [M] can be obtained by assuming that the distributed load can be represented by statically equivalent concentrated loads at the ends equal to the reactions produced in a simply supported beam. The M matrix derived on this assumption will be

$$M = \begin{bmatrix} L/3 & L/6 \\ 0 & 0 \\ L/6 & L/3 \\ 0 & 0 \end{bmatrix} \tag{5.15}$$

Because this form is compatible with the finite element approach described later, it will be used in this study.

5.8 Computer Program for the Equivalent Boundary Element Approach

A computer program was developed using constant elements for the analysis of a beam on elastic half-space on the basis of the analytical treatment presented in section 4.2.2 and 5.7. The main steps in the computer program are as follows:

1) Input half-space data; it will include
   - i) the number of boundary elements
   - ii) the shear modulus of the soil material
   - iii) the Poisson's ratio of the soil
2) Input beam data which includes
   - i) the Young's modulus of the beam material
   - ii) the total number of finite element nodes in the beam
   - iii) the number assigned to the first node in the beam
   - iv) the width and height of each element of the beam
3) Form matrices [G] and [H] using numerical integration, Equation 2.23.
4) Rearrange matrices [G] and [H] to form Equation 4.25.
5) Form global transformation matrix [M] for the beam, Equation 5.14.
6) Form the global stiffness matrix of the beam, Equation 4.26.
7) Form vector {p}, Equation 4.29. It should be noted, that, the components of vector {p} are as follows:

i) Tractions at the nodes of the boundary elements.

ii) External tractions at the nodes corresponding to the interface boundary.

iii) External tractions corresponding to rotation of the beam nodes. These are taken to be zero.

8) Form the global matrices for the combined beam and soil region, Equation 4.29.

9) Rearrange Equation 4.29 and vectors {u} and {p} so that all unknowns are placed in vector {u} and all knowns in vector {p}. This is done by using a procedure similar to that explained in section 2.5.1.2.

10) Using Gauss elimination method solve the system of equations given by Equation 4.29, to obtain the displacement vector {u}.

11. Compute bending moment, and shear forces for the beam elements by using Equations 5.10 and 5.11.

One problem was solved by the equivalent boundary element approach using the computer program described in this section. The results are presented in a later part of this chapter where they are also compared with those obtained from the equivalent finite element approach and it is shown that, but for small differences, the two approaches give essentially similar results.

5.9 Analytical Results

5.9.1 Comparison Between the Equivalent Finite Element and Boundary Element Approach

In order to compare the results obtained by the two approaches described in the previous sections, a typical problem is investigated and the results are compared. Figure 5.2 shows the problem with its associated dimensions and parameters used in the solution. It can be seen from Table 5.2 and Figures 5.3, 5.4 and 5.5 for displacements, shearing forces and bending moments, respectively, that the two approaches compare quite closely. The maximum difference in the vertical displacement is within 4%. It should be noted that:

a) The equation which defines the transformation matrix M in the equivalent boundary element approach is Equation 5.15.

b) The number of elements of the beam used in the equivalent boundary element approach is one more than that used in the finite element approach. As shown in Figure 5.2, this is necessary for adequate representation of the loading.

5.9.2 Effect of the Finite Representation of Infinite Boundary

In the solution of the beam resting on soil, the semi infinite soil region must be represented by a finite length. It is to be expected that if this length is sufficiently large, the truncation of the infinite medium will not have any significant effect on the results of analysis. To test the convergence of the results, the effect of the extent of soil region discretized by boundary elements is studied by the analysis of beam shown in Figure 5.6. In this figure a is the half length of the beam, and r represents clear distance between the edge of the beam and the assumed boundary of the half-space. Analysis is carried out for the various values of the $\frac{r}{a}$ ratio, and the results are presented in Table 5.3 and in Figure 5.7. It can be seen that when $\frac{r}{a}$ ratio exceeds 25 the variation in the central displacement and central bending moment becomes negligible. It should be noted that since a Kelvin solution is used the tractions along the interface line beyond the position discretized by boundary elements are not zero. These tractions are not however likely to have significant influence on the displacements and stresses in the region of interest.

5.9.3 Effect of Relative Rigidity

To study the effect of relative rigidity on beam displacements, shears and moments a set of beams with relative rigidities equal to 1, 4, 10 and 50, are analysed. Figure 5.8a shows distributed loads spread over a portion of the beam. The calculated displacements are plotted in Figure 5.8b. It is seen that the displacements are almost the same throughout the length of the beam when $\lambda\ell = 1.0$ (rigid beam). It may be of interest to note the variation in the beam displacement as $\lambda\ell$ increases. For $\lambda\ell$ in the range 4 to 50, the displacements are almost the same under the loaded portion, this means that when $\lambda\ell$ exceeds a value 4, the displacements under the loaded portion do not change. Also one can observe that for $\lambda\ell$ in the range 10 to 50, the displacements

throughout the length do not change. This means that when $\lambda\ell$ exceeds a value of 10, the beam becomes very flexible and further increase of $\lambda\ell$ does not change the displacements.

The bending moment and shear forces are shown in Figure 5.9 and 5.10, respectively. It may be noted that the bending moment and shear forces almost disappear as $\lambda\ell$ increases, since with an increase in $\lambda\ell$ the bending stiffness of the beam becomes negligible. For $\lambda\ell = 1.0$, the bending moment and shear forces are very large as can be expected for rigid beams.

Problems related to a central concentrated load has also been examined for relative rigidities equal to 1, 4, 10 and 50. The displacements of the beam are plotted in Figure 5.11.

5.9.4 Effect of Load Location

The effects of the location of the load (ξ) on the beam-deflections, bending moments and shear forces have also been studied. The value of $\lambda\ell$ is kept constant. For a concentrated load, the variation of displacements is shown in Figure 5.12; the corresponding results for flexural moments and shear forces are shown in Figures 5.13 and 5.14, respectively. One can observe that as the load moves to the edge of the beam, the displacements and the shearing forces increase, but the bending moments decreased. The maximum bending moment and shearing force is always under the load.

A set of curves has also been developed to examine the effect of a concentrated moment on the beam deflections, bending moments and shear forces. The results are shown in Figures 5.15, 5.16 and 5.17. It can be noted that when the concentrated moment moves to the left edge of the beam, the -ve displacements, +ve bending moments and the shearing forces increase. The maximum bending moment and shearing force are always under the concentrated moment.

5.10 Comments

1. The example presented in section 5.9.1 demonstrates that either of the two different combination approaches - the equivalent finite element approach or the equivalent boundary element approach - can be applied to the solution of the problem presented here. One can note also from the examples given that the least square symmetrization technique used with the equivalent finite element approach is valid.

2. The equivalent finite element approach is in essence a stiffness method and can easily be incorporated into the existing finite element program. The equivalent finite element approach requires the inversion of the non-banded G matrix. The equivalent boundary element approach does not require such an inversion; however the equations obtained are unsymmetrical.

3. The equivalent boundary element approach, can be applied only if the loading is distributed, that is it can be specified as tractions on the nodes. Concentrated loads must therefore be converted into equivalent distributed loading. Concentrated loads and couples can be

handled directly by the equivalent finite element approach. Distributed loading should be converted into equivalent nodal forces.

4. The advantage of the boundary element method is its ability to represent the semi-infinite soil domain by a straight line [4]. This method is therefore very effective for the soil interaction problems.

5. One can note from the analysis procedure described here for the soil beam interaction problem that compatibility of displacements and forces at the interface of the finite element region and the boundary element region is assured only at the nodes. Between the nodes there is no compatability because the displacement function used for the beam element is a 3rd order polynomial, while that for the boundary element region it is only a first order polynomial.

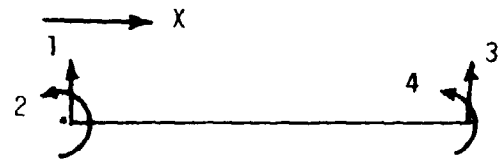

(a)

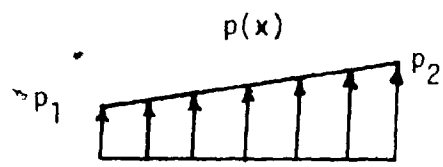

(b)

Figure 5.1 Beam Element

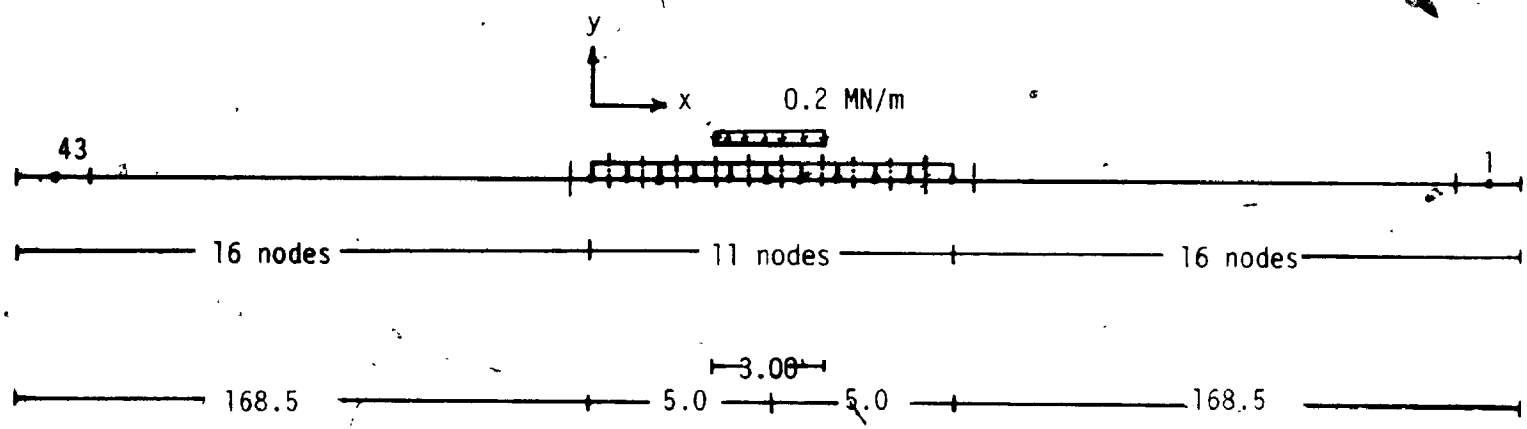

Equivalent Finite Element App.

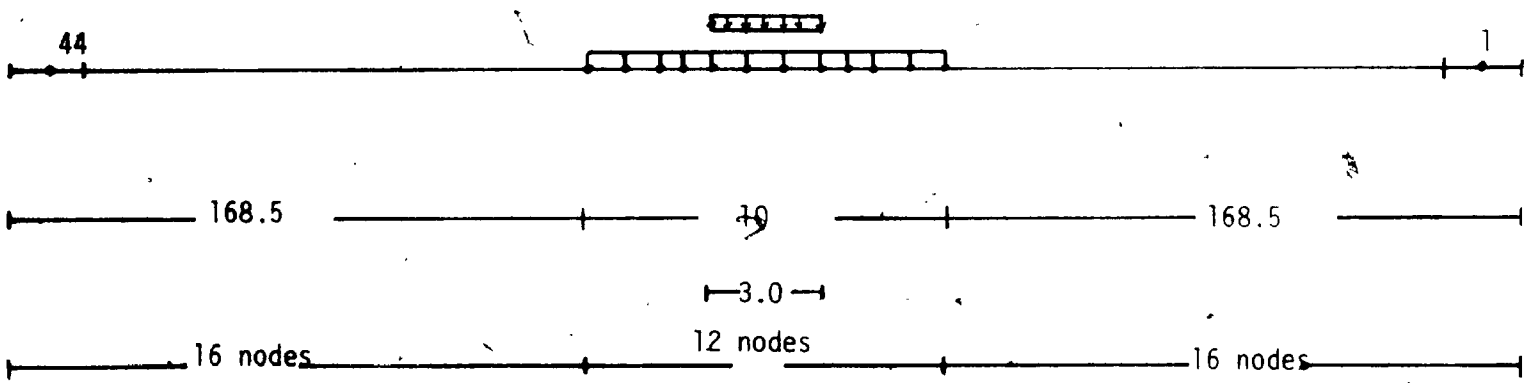

Equivalent Boundary Element App.

Figure 5.2 Geometry of the Problem Solved by Using Equivalent Finite Element Approach and Equivalent Boundary Element Approach

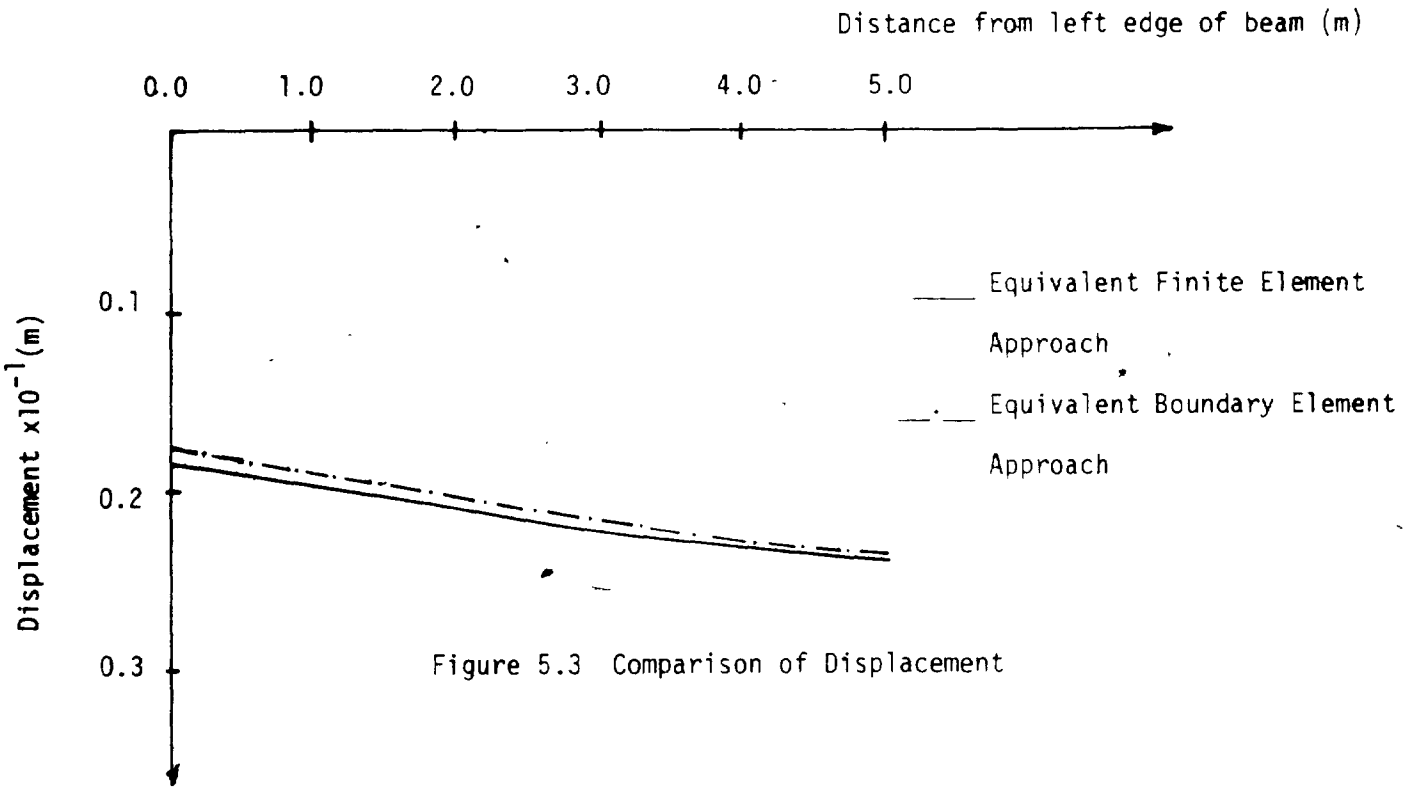

Figure 5.3 Comparison of Displacement

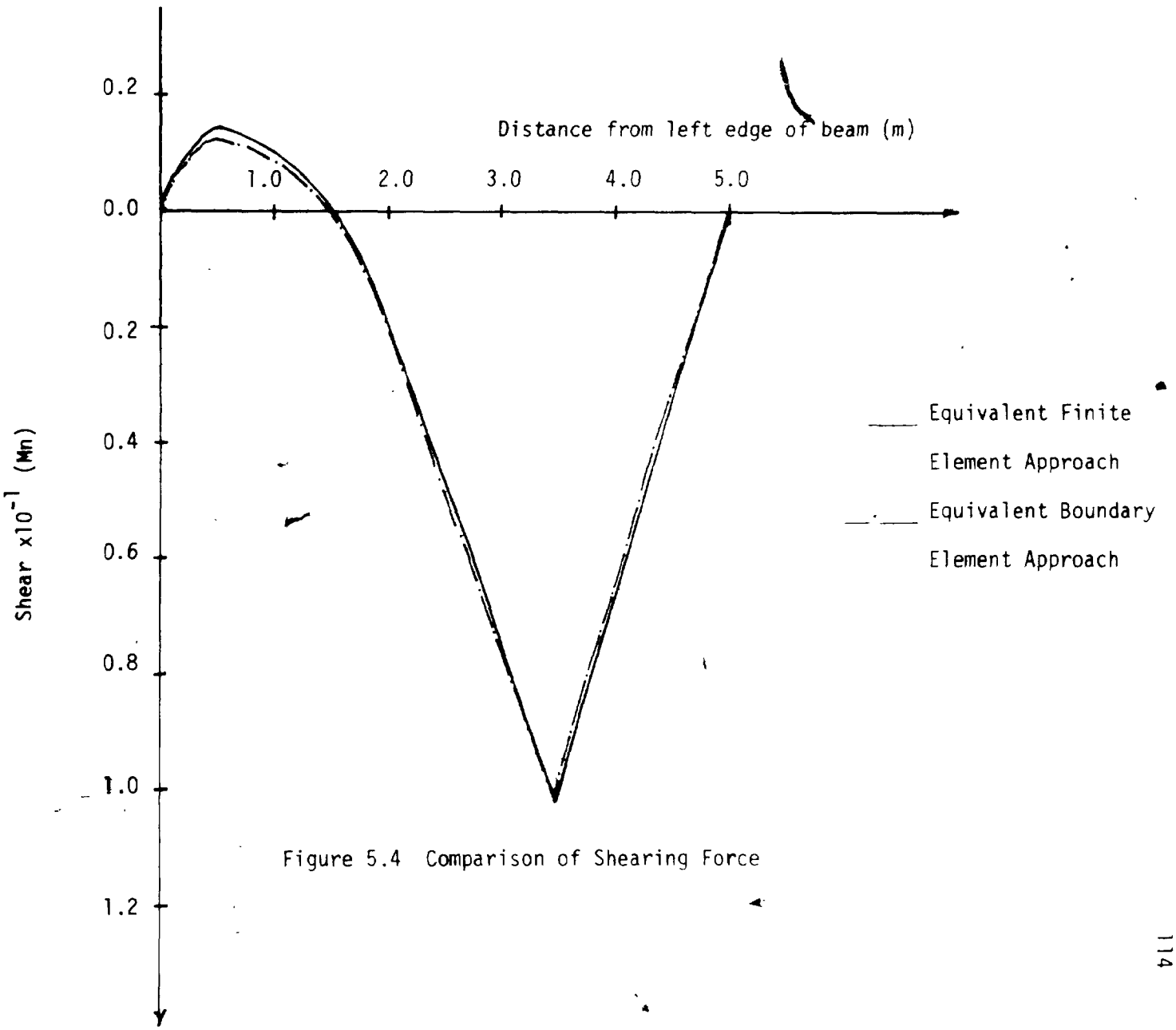

Figure 5.4 Comparison of Shearing Force

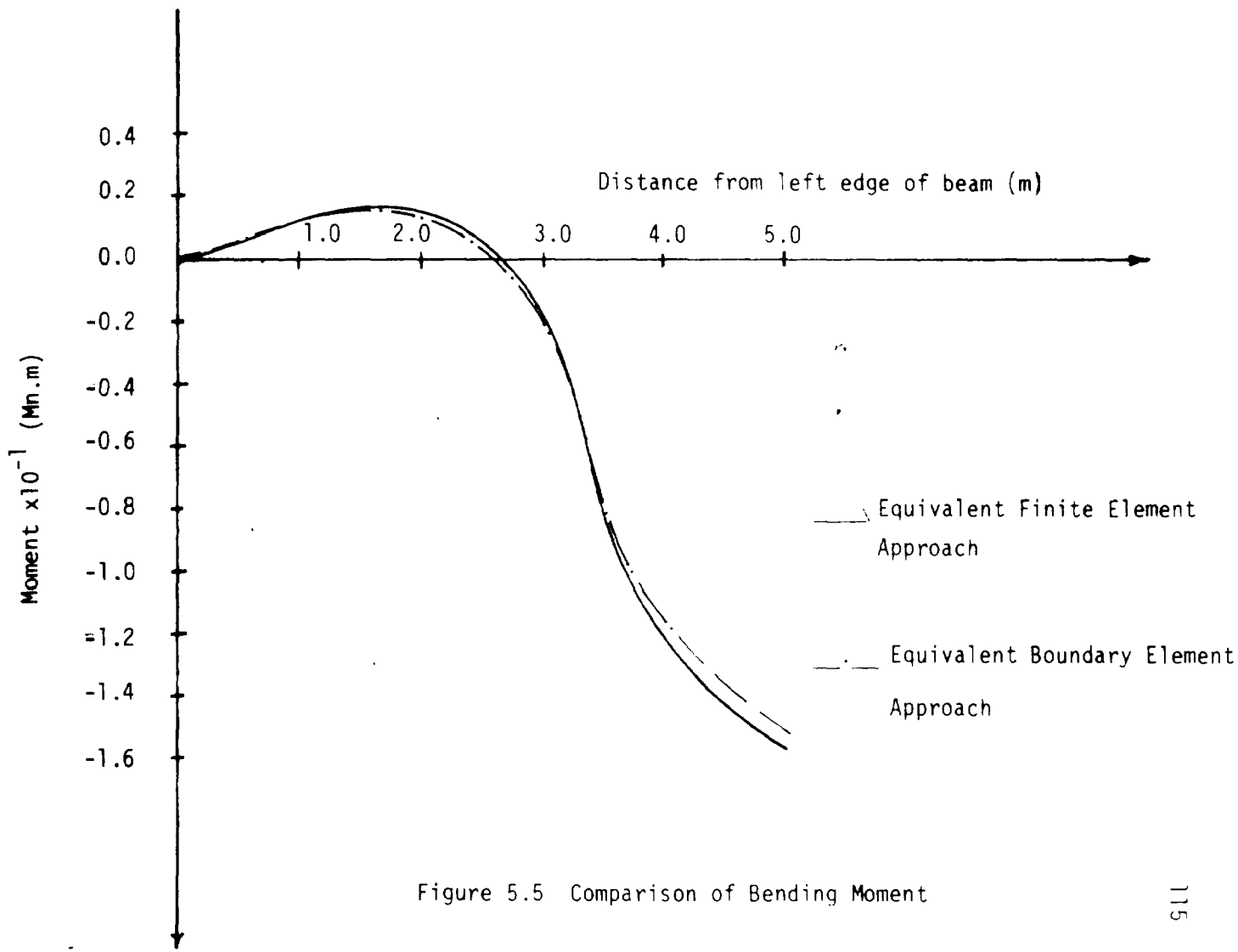

Figure 5.5 Comparison of Bending Moment

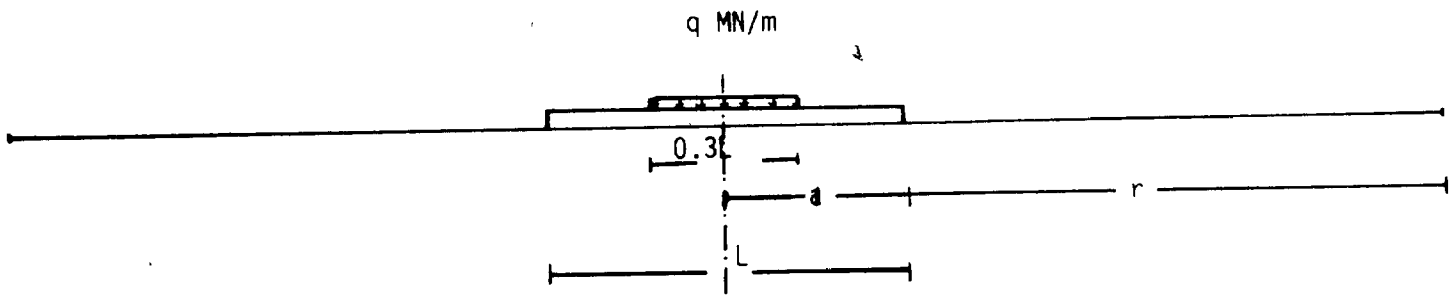

$q = 0.2$ MN/m

$L = 10.0$ m

$h = 0.4$m , $b = 2.0$m

$E_s = 88$ MN/m^2, $\nu_s = 0.3$

$E_b = 13786.0$ MN/m^2

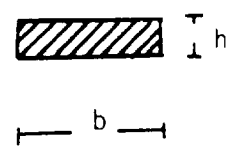

Cross-section of beam

Figure 5.6 Geometry of the Problem Solved by Equivalent Finite Element Approach

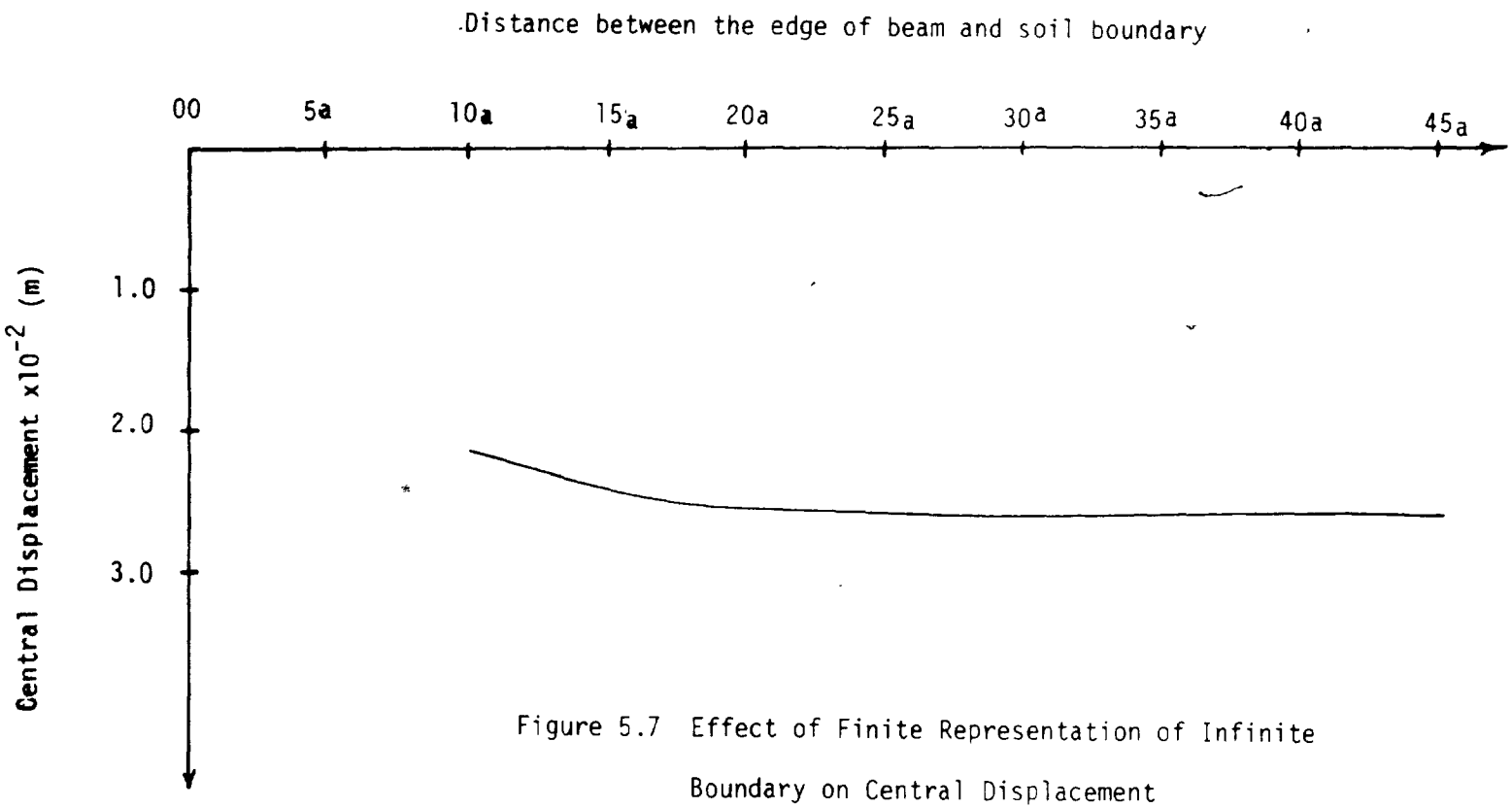

Figure 5.7 Effect of Finite Representation of Infinite Boundary on Central Displacement

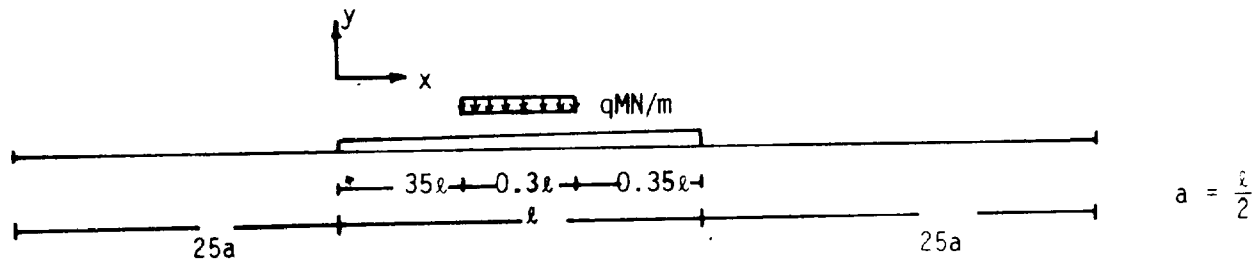

Figure 5.8a

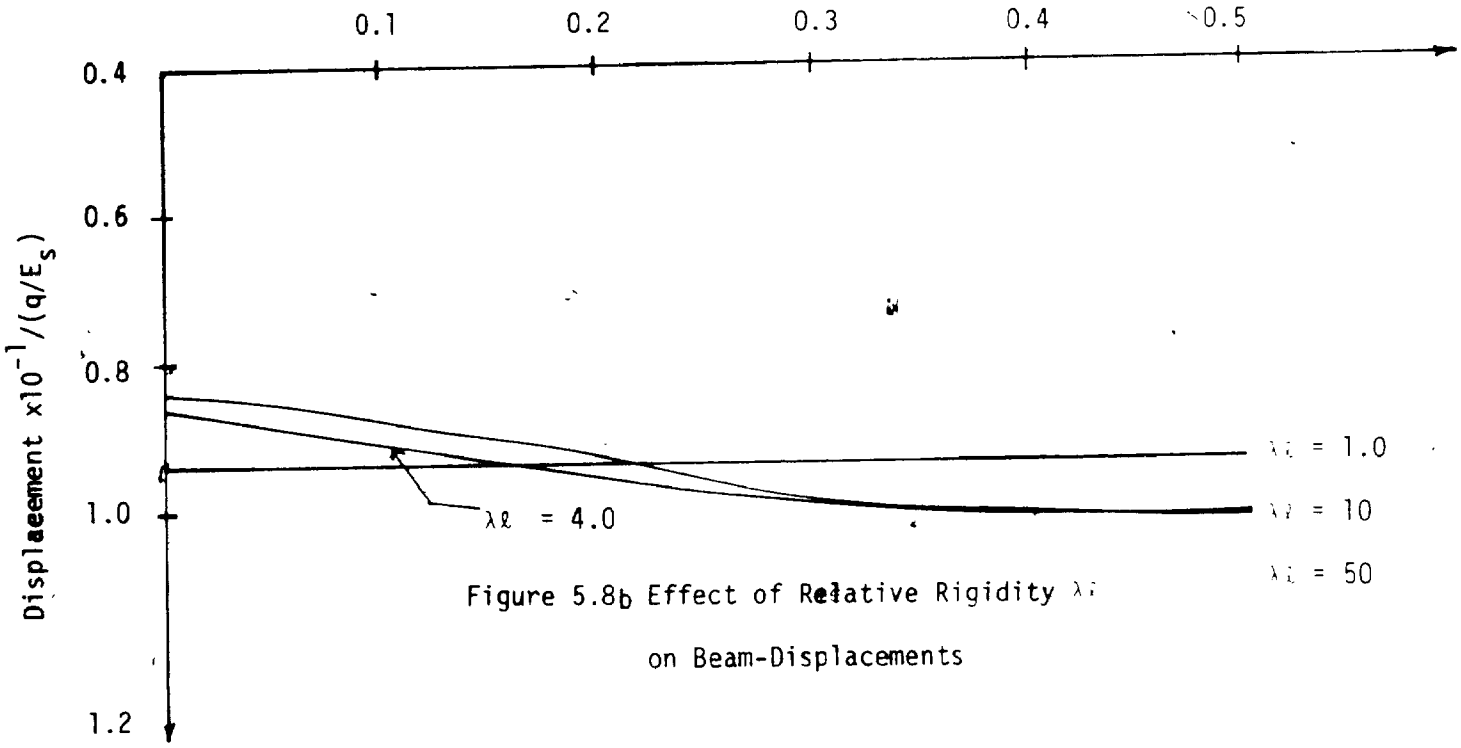

Figure 5.8b Effect of Relative Rigidity λℓ on Beam-Displacements

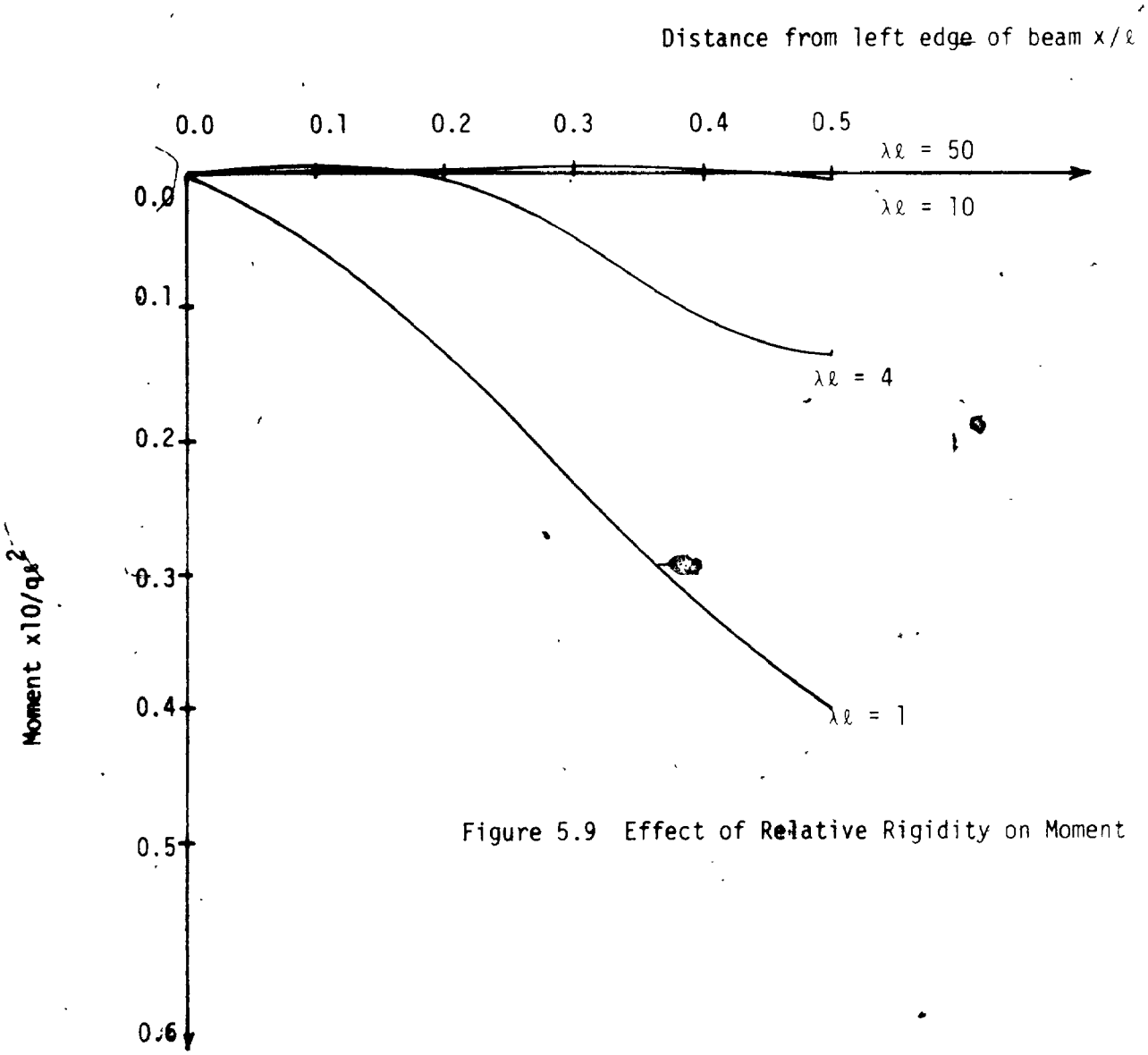

Figure 5.9 Effect of Relative Rigidity on Moment

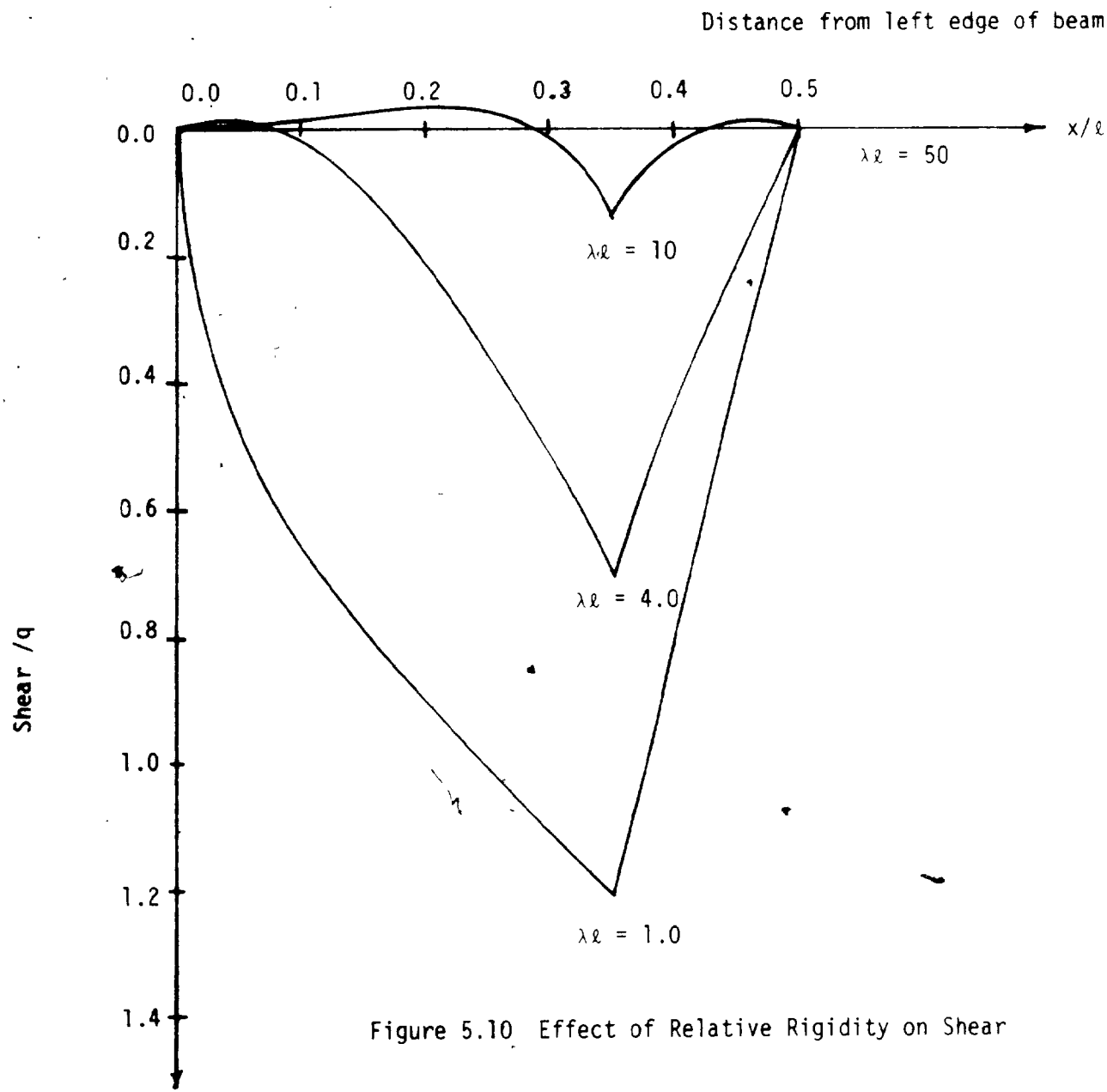

Figure 5.10 Effect of Relative Rigidity on Shear

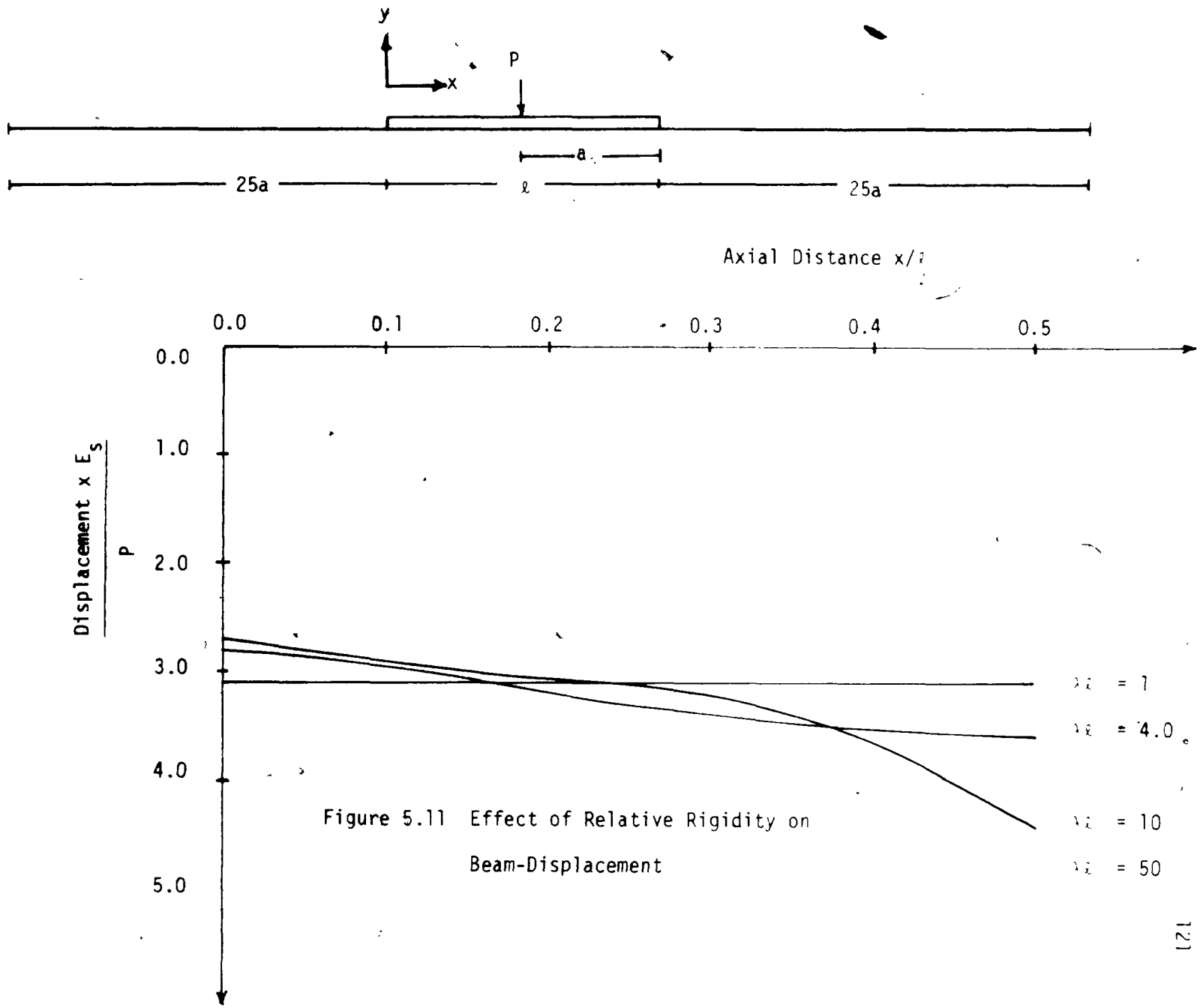

Figure 5.11 Effect of Relative Rigidity on Beam-Displacement

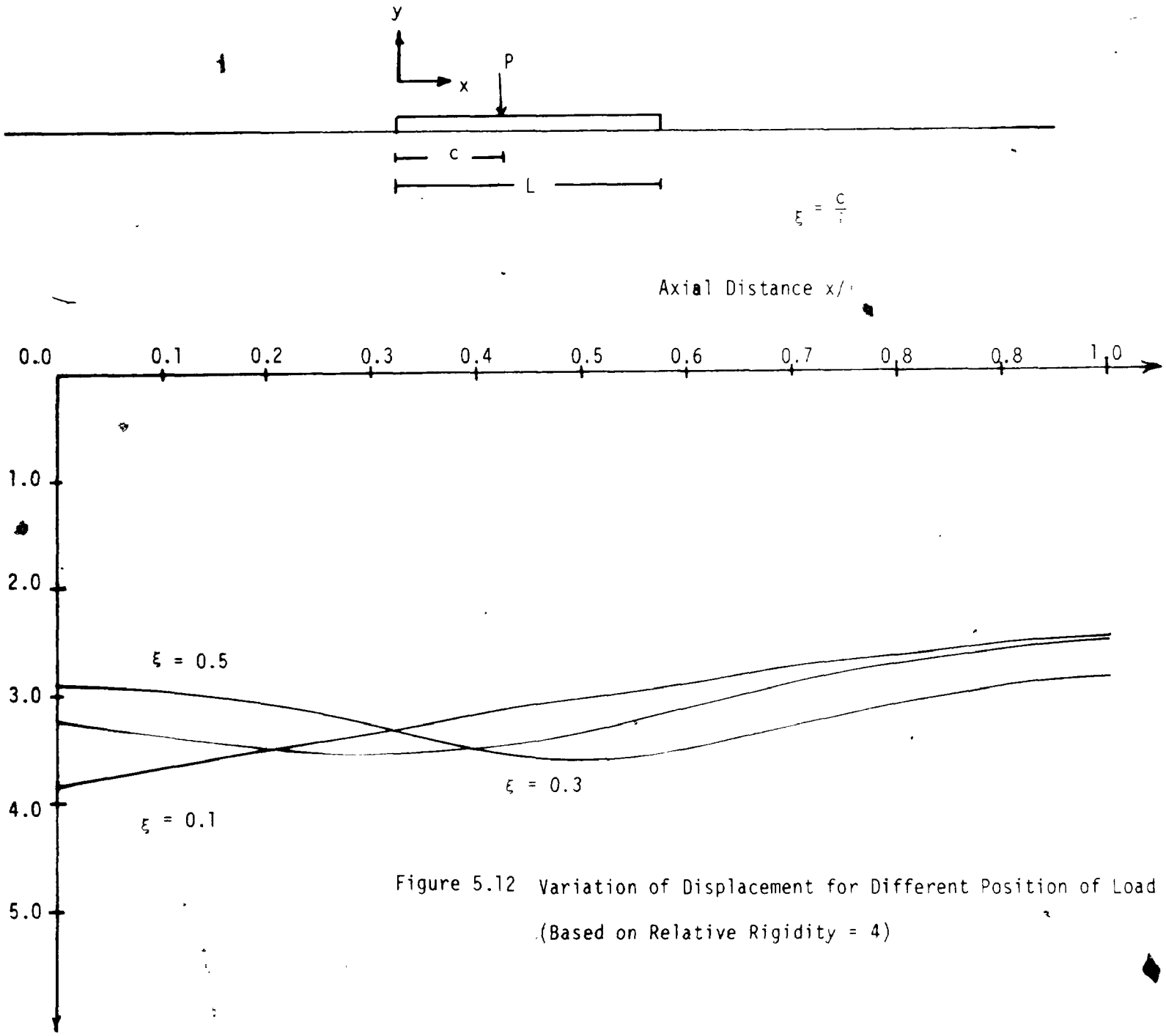

Figure 5.12 Variation of Displacement for Different Position of Load (Based on Relative Rigidity = 4)

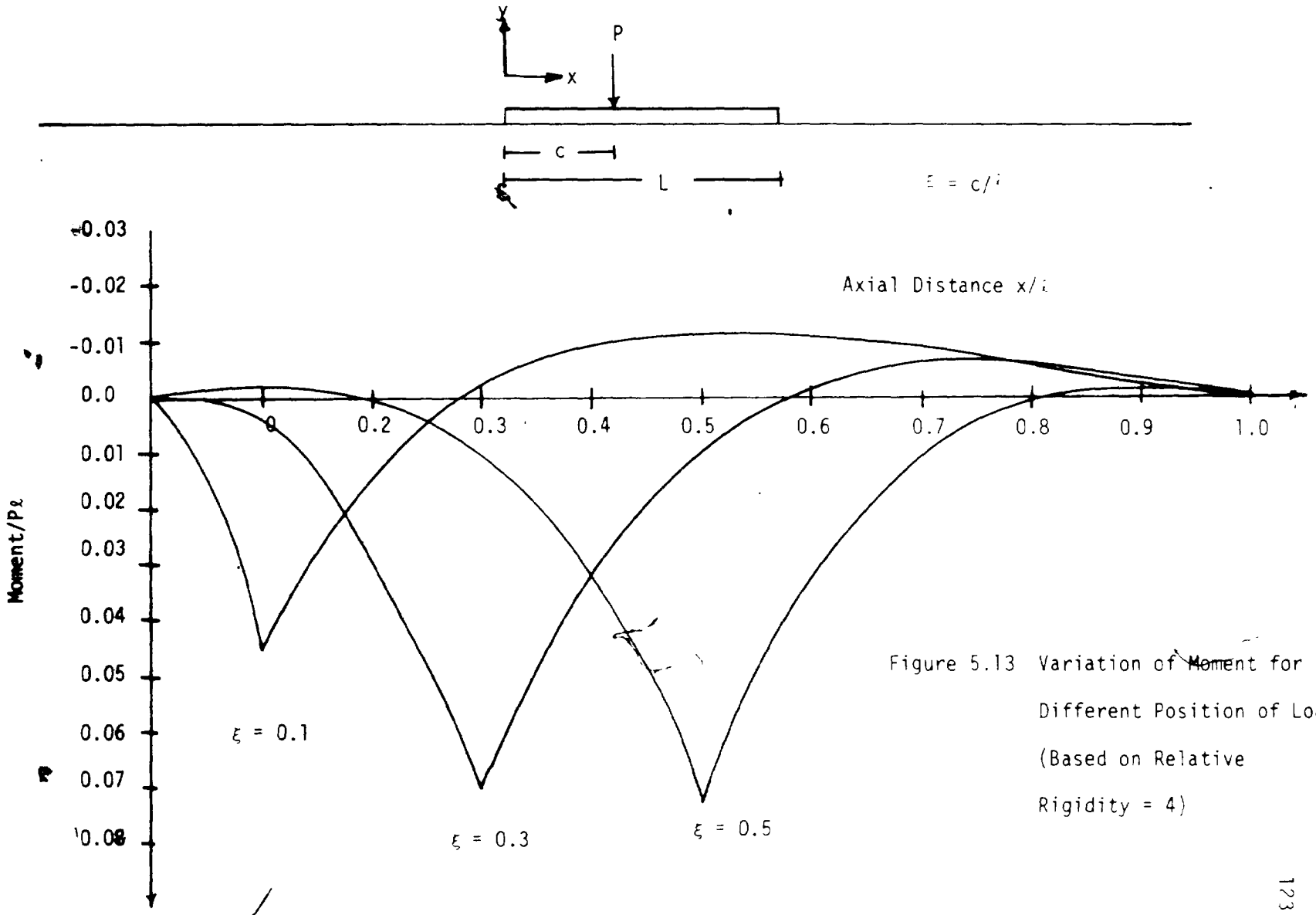

Figure 5.13 Variation of Moment for Different Position of Load (Based on Relative Rigidity = 4)

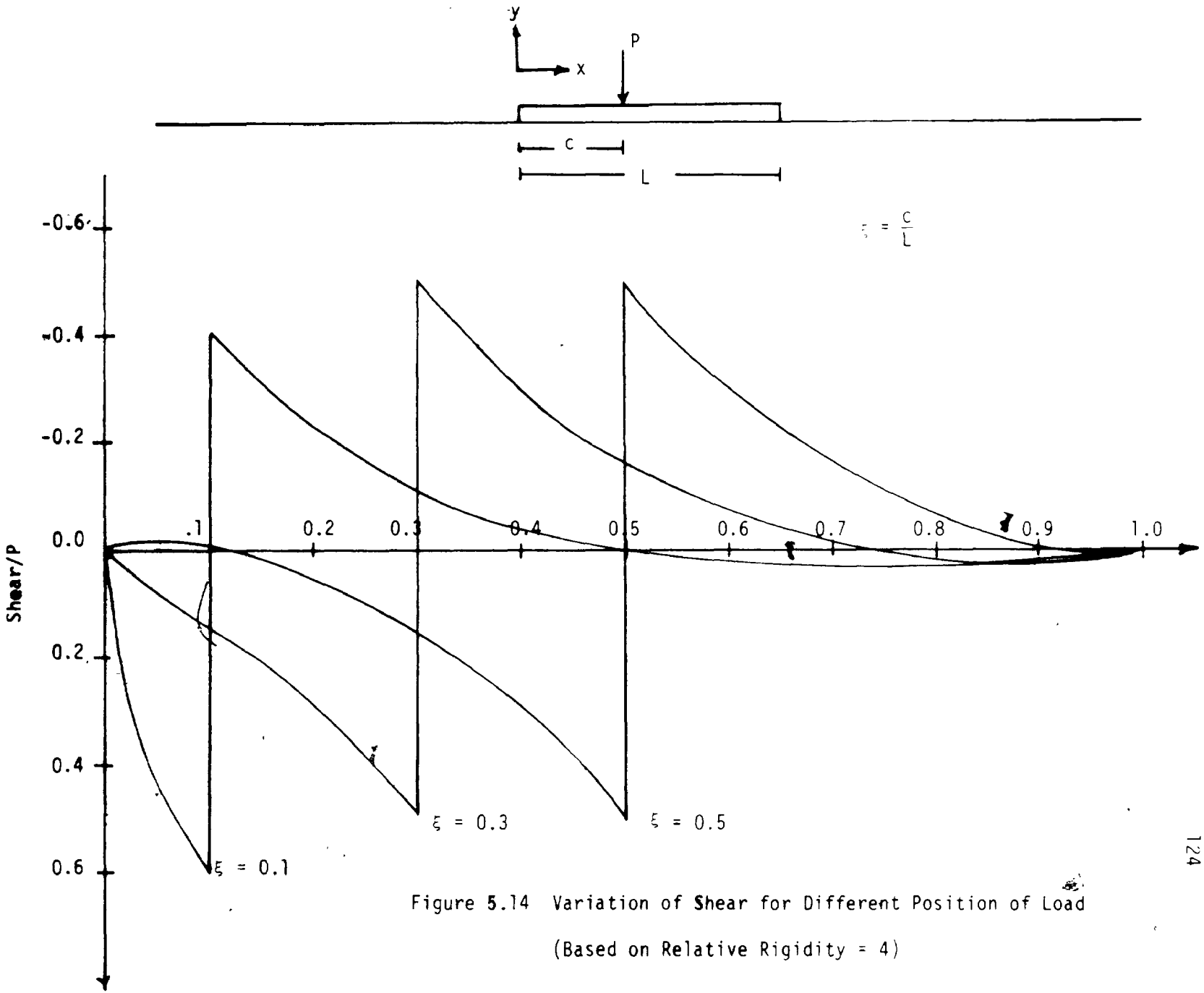

Figure 5.14 Variation of Shear for Different Position of Load

(Based on Relative Rigidity = 4)

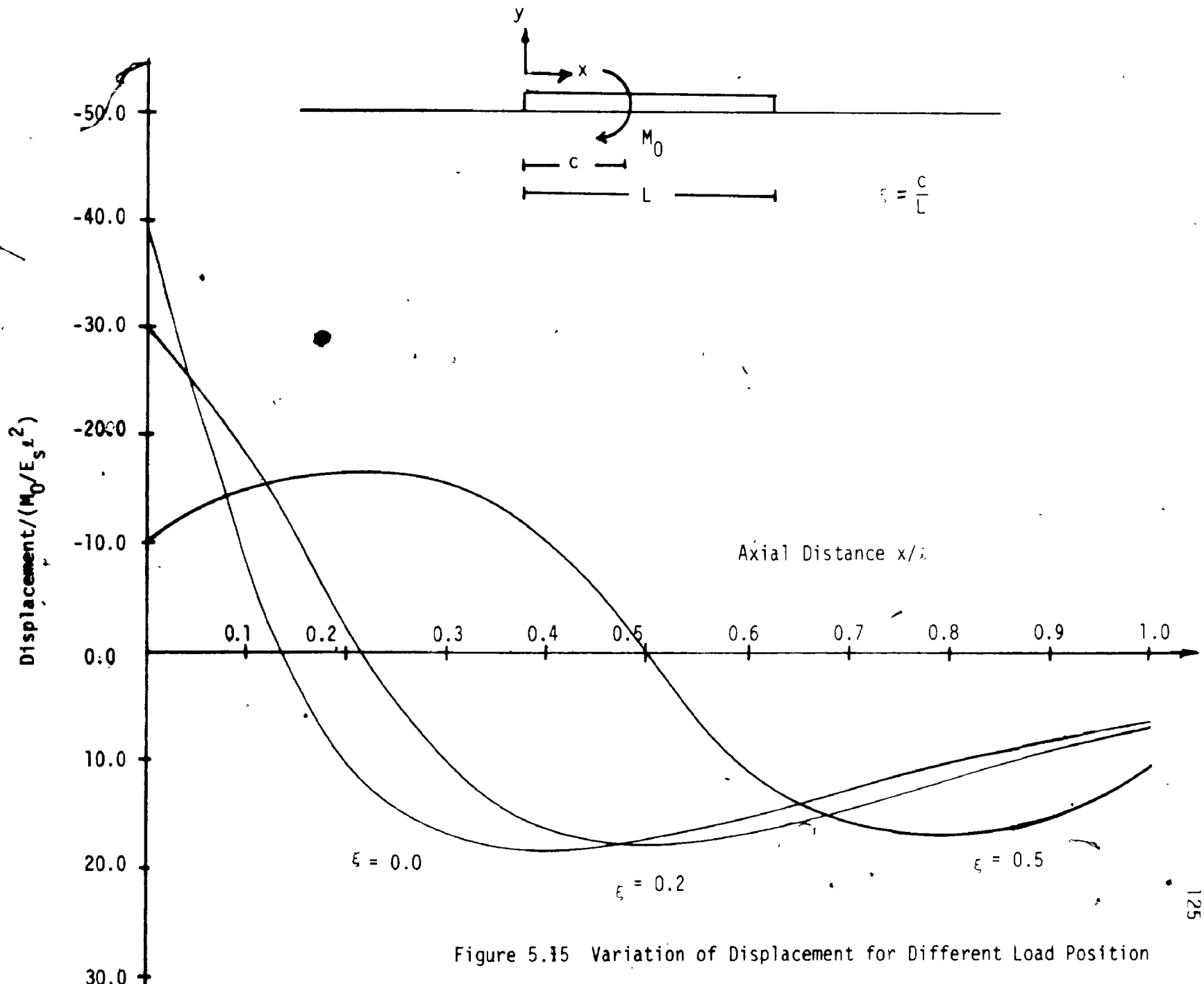

Figure 5.15 Variation of Displacement for Different Load Position

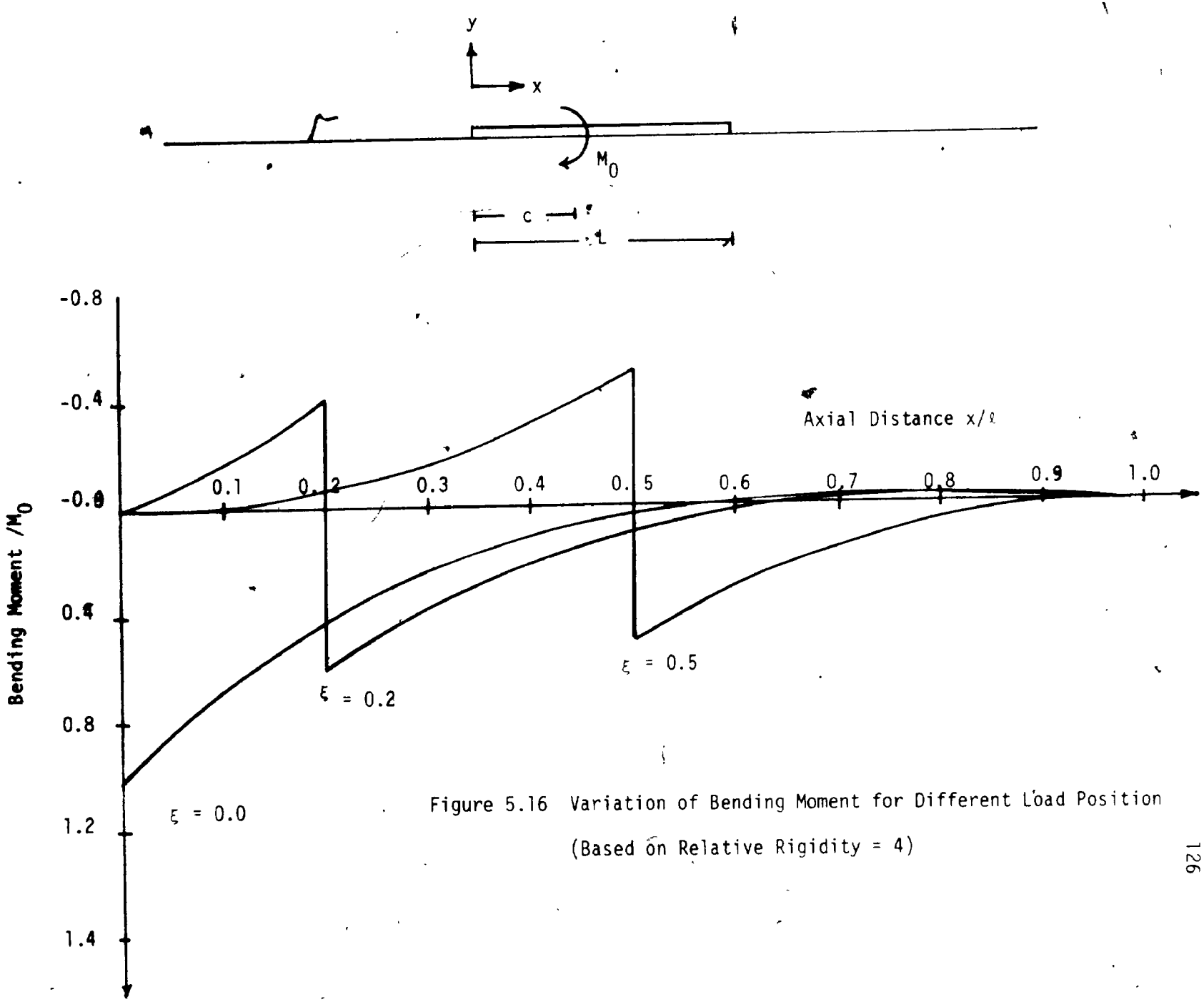

Figure 5.16 Variation of Bending Moment for Different Load Position

(Based on Relative Rigidity = 4)

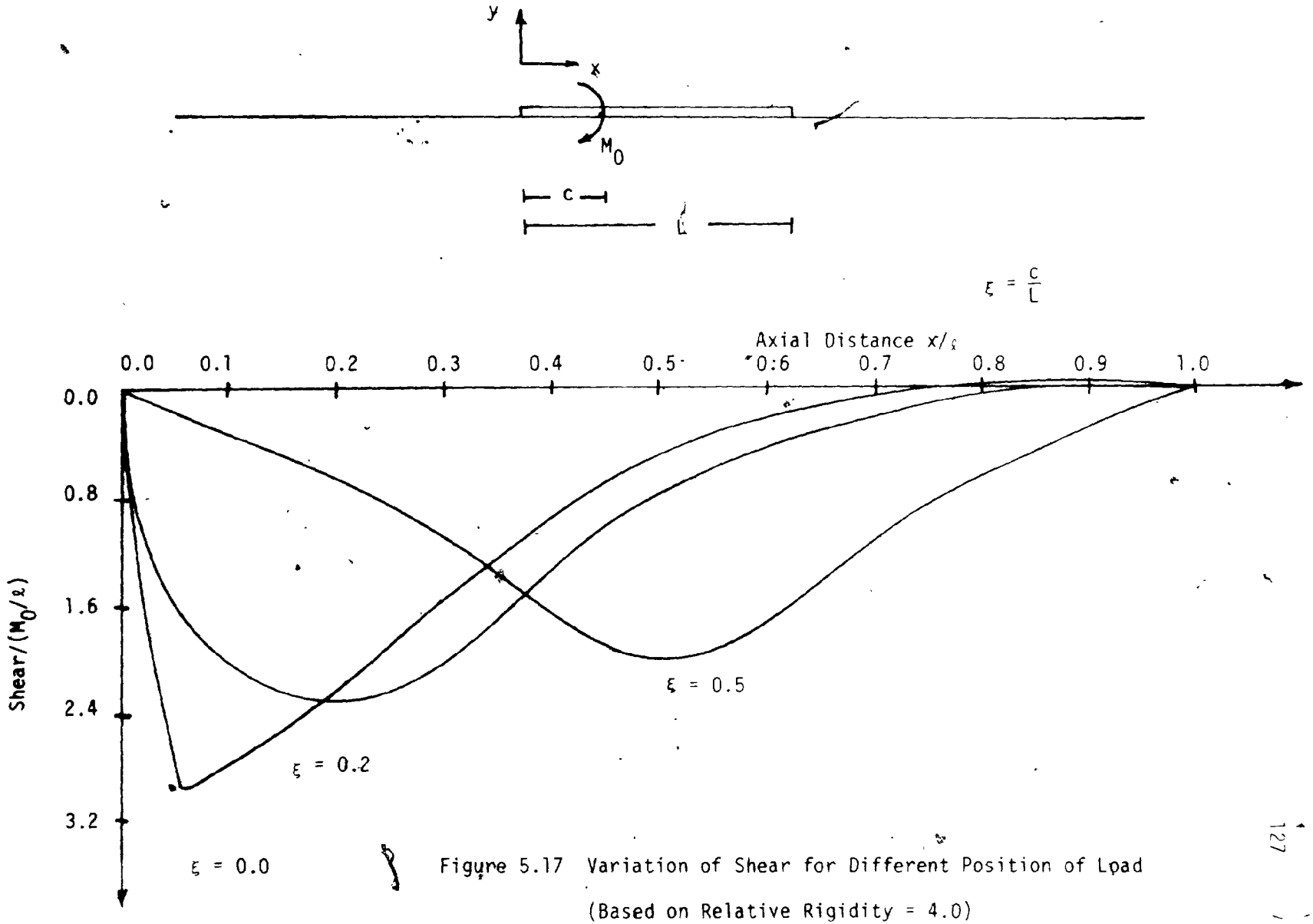

Figure 5.17 Variation of Shear for Different Position of Load

(Based on Relative Rigidity = 4.0)

TABLE 5.1

Combined Effect of Flexural Stiffness and the Shape of Foundation

Shape of Foundation	Flexural Stiffness EI	ω
Circular	0	0.96
	∞	0.89
Square	0	0.95
	∞	0.88
Rectangular	0	
L:B = 1.5		0.94
= 2		0.92
= 3		0.88
= 5		0.82
= 10		0.71
= 100		0.37
= 1000		0.163
= 10000		0.066

TABLE 5.2

Comparison of the Displacements Obtained by Using Equivalent Finite Element Approach and Equivalent Boundary Element Approach

Distance from Left Edge of Beam (m)	Displacement "Y" (m)	
	Equivalent F.E. Approach	Equivalent B.E. Approach
0.0	-0.185×10^{-1}	-0.173×10^{-1}
1.0	-0.197×10^{-1}	-0.187×10^{-1}
2.0	-0.211×10^{-1}	-0.202×10^{-1}
3.0	-0.226×10^{-1}	-0.218×10^{-1}
4.0	-0.238×10^{-1}	-0.232×10^{-1}
5.0	-0.243×10^{-1}	-0.238×10^{-1}

$E_s = 88\ MN/m^2$

$E_b = 13786\ MN/m^2$

$\nu_s = 0.3$

$b = 2.0m$

$h = 0.4m$

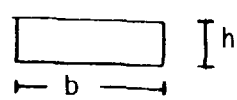

cross-section of the beam

TABLE 5.3

Effect of Finite Representation of Infinite Boundary

Distance from Edge of Beam to Soil Boundary (m)	Central Displacement (m)	Central B.M (MN.m)
10 a	- 0.0215	- 0.15815
15 a	- 0.0241	- 0.15797
20 a	- 0.0255	- 0.15792
28 a	- 0.026	- 0.15786
36 a	- 0.0259	- 0.15784
41 a	- 0.0259	- 0.15784

CHAPTER 6

SUMMARY AND CONCLUSIONS

6.1 Summary and Conclusions

As a result of the present work, the following major conclusions are drawn.

1. From the analysed case studies, it has been demonstrated that the boundary element methods can be efficiently applied to problems in elastostatics. Further, it is equally effective in dealing with both infinite and finite bodies. The results obtained are found to be in good agreement with the available closed form solution.

2. An advantage of the boundary element method is that the boundary at infinity can be modelled without truncating the domain at some arbitrary distance from the region of interest.

3. Another important advantage of the boundary element method is that the values of the functions under consideration are calculated for internal points of the domain only where they are needed.

4. From the point of view of numerical analysis, the boundary element method simplifies the problem by reducing a problem over the domain to one over the boundary. This means the dimension of the problem is reduced by one. This can greatly simplify the development of computer programs and the assembly of input data.

5. Since the discretization covers only the boundary rather than the domain, the system of equations is much smaller.

6. A disadvantage of the boundary element method is that the

coefficient matrices of the resulting equations are usually fully populated and unsymmetrical. This may result in a loss of computational efficiency in certain applications.

7. The boundary element method can be combined with the finite element method to deal with situations where the application of one method alone will be inefficient. For example, the boundary element method is best used for modelling infinite domains while the finite element method is used to advantage in modelling finite regions containing inhomogeneous or anisotropic material properties. When both types of regions coexist, a combination of the two methods will be useful.

8. The combination of boundary element and finite element methods can be used to study the behaviour of beams on elastic half-space. Two different analytical approaches as described in this work can be used; both give similar results.

9. In studying the behaviour of the beam on elastic half-space, the soil region is represented by boundary elements. The length of the boundary should be sufficiently large to provide an adequate model.

10. The effect of increased relative rigidity of the beam soil system is to increase the deflection of the beam. The flexural moments and shear forces are, however, decreased.

11. When relative rigidity of the beam exceeds a value 10, the beam becomes very flexible and a further increase in relative rigidity does not change the bending moment and displacements of the beam.

6.2 Recommendations for Further Research

The following recommendations are made for further research:

1. The solution of the beam on an elastic half-space presented here considers prismatic beams having free ends. Non-prismatic beams with varying cross-sections, different end conditions and more complex load patterns, can be handled with slight extensions in the computer programs developed for this.

2. The study beam-analysis carried out for this thesis assumes the soil parameters to be constant throughout the half-space. The work can be extended to the analysis of beams resting on soils with varying properties such as layered continuum by dividing the soil into subregions.

3. The fundamental solution used in the analyses of the beams is the Kelvin solution. Use of Mindlin solution for a semi-infinite space is likely to make the analysis more efficient and should be studied.

4. The combination of boundary and finite element methods may also be applied to the study of

a) rectangular foundations

b) arbitrary-shaped raft foundations

c) axisymmetric foundation.

Appendix A

The fundamental solutions for the two dimensional case are given by

$$u^*_{ji} = \frac{1}{8\pi G(1-\nu)} \left[(3-4\nu)\ln\left(\frac{1}{r}\right)\Delta_{ji} + \frac{\partial r}{\partial x_j}\cdot\frac{\partial r}{\partial x_i}\right], \text{ and}$$

$$p^*_{ji} = -\frac{1}{4\pi(1-\nu)r}\left[\frac{\partial r}{\partial n}\left\{(1-2\nu)\Delta_{ji} + 2\frac{\partial r}{\partial x_i}\cdot\frac{\partial r}{\partial x_j}\right\}\right.$$

$$\left. - (1-2\nu)\left\{\frac{\partial r}{\partial x_j}\cdot n_i - \frac{\partial r}{\partial x_i}\cdot n_j\right\}\right]$$

The first integral in Equation 2.18 can be represented in matrix form as follows

$$\int \begin{bmatrix} p^*_{11} & p^*_{12} \\ p^*_{21} & p^*_{22} \end{bmatrix} \begin{Bmatrix} u_1 \\ u_2 \end{Bmatrix} d\Gamma$$

Consider the integral $\int_\Gamma p^*_{11}\, u_1\, d\Gamma$.

Since p^*_{11} has a singularity at r=0, the integral has to be derived in a special manner. Consider that the boundary Γ is smooth and is divided into two segments; the first segment centred around point (P) on the boundary being denoted by s^* and the second segment by $\Gamma - s^*$, (Figure 2.6b). Now draw a semi-circle on segment s^*. The integral $\int p^*_{11}\, u_i$ is evaluated on the boundary formed by $\Gamma - s^*$ and the perimeter of the semi-circle. The boundary s^* is then allowed to shrink to zero. The resulting limiting value of the integral gives $\int_\Gamma p^*_{11}\, u_1\, d\Gamma$.

On the semi-circle $\frac{\partial r}{\partial n} = 1$, therefore

$$\int_\Gamma p^*_{11} \cdot u_1 \, d\Gamma = \int_\Gamma - \frac{1}{4\pi(1-\nu)r} \left[(1-2\nu) + 2 \left(\frac{\partial r}{\partial x_1}\right)^2\right] d\Gamma$$

Now since

$$r^2 = x_1^2 + x_2^2$$

$$2r \frac{\partial r}{\partial x_1} = 2x_1 \text{ and } \frac{\partial r}{\partial x_1} = \frac{x_1}{r} = \cos\theta. \quad \text{Thus}$$

$$\int_\Gamma p^*_{11} u_1 \, d\Gamma = u_1 \int_{-\theta_1}^{\pi-\theta_1} - \frac{1}{4\pi(1-\nu)r} \left[(1-2\nu) + 2\cos^2\theta\right] r d\theta + u_1 \int_{\Gamma-s^*} p^*_{11} \, d\Gamma$$

$$= u_1 \int_{-\theta_1}^{\pi-\theta_1} - \frac{1}{4\pi(1-\nu)} \left[2-2\nu + \cos 2\theta\right] d\theta + u_1 \int_{\Gamma-s^*} p^*_{11} \, d\Gamma$$

$$= - \frac{u_1}{4\pi(1-\nu)} \left[(2-2\nu)\theta + \frac{\sin 2\theta}{2}\right]_{-\theta_1}^{\pi-\theta_1} + u_1 \int_{\Gamma-s^*} p^*_{11} \, d\Gamma$$

$$= - \frac{1}{2} u_1 + \int_{\Gamma-s^*} p^*_{11} \, d\Gamma$$

Next consider the integral $\int_\Gamma p^*_{12} u_2 \, d\Gamma$

Since $\frac{\partial n}{\partial x_i} = \frac{\partial n}{\partial r} \cdot \frac{\partial r}{\partial x_i} = \frac{\partial r}{\partial x_i}$ on the semi-circle

$$\int_{\Gamma} p_{12}\, u_2\, d\Gamma = u_2 \int - \frac{1}{4\pi(1-\nu)r}\left[2\frac{\partial r}{\partial x_1} \cdot \frac{\partial r}{\partial x_2}\right] d\Gamma + u_2 \int_{\Gamma - s^*} p^*_{12}\, d\Gamma$$

$$= u_2 \int_{-\theta_1}^{\pi-\theta_1} - \frac{1}{4\pi(1-\nu)r}\,[2 \sin\theta \cos\theta]\, r d\theta + u_2 \int_{\Gamma - s^*} p^*_{12}\, d\Gamma$$

$$= -u_2 \int_{-\theta_1}^{\pi-\theta_1} \frac{1}{4\pi(1-\nu)} \sin 2\theta\, d\theta + u_2 \int_{\Gamma - s^*} p^*_{12}\, d\Gamma$$

$$= \frac{u_2}{4\pi(1-\nu)} \left[\frac{\cos 2\theta}{2}\right]_{\theta_1}^{\pi-\theta_1} + u_2 \int_{\Gamma - s^*} p^*_{12}\, d\Gamma$$

$$= u_2 \int_{\Gamma - s^*} p^*_{12}\, d\Gamma$$

also

$$\int_{\Gamma} p^*_{21}\, u_1\, d\Gamma = \int_{\Gamma - s^*} p^*_{21}\, u_1\, d\Gamma$$

In a similar manner it can be proved that the $\int_{\Gamma} p^*_{22}\, u_2\, d\Gamma$

$$= -\frac{1}{2} u_2 + \int_{\Gamma - s^*} p^*_{22}\, u_2\, d\Gamma$$

Thus, the first integral in Equation 2.18 becomes,

$$\int_{\Gamma} \begin{bmatrix} p^*_{11} & p^*_{12} \\ p^*_{21} & p^*_{22} \end{bmatrix} \begin{Bmatrix} u_1 \\ u_2 \end{Bmatrix} d\Gamma = \begin{bmatrix} -\frac{1}{2} & 0 \\ 0 & -\frac{1}{2} \end{bmatrix} \begin{Bmatrix} u_1 \\ u_2 \end{Bmatrix} + \int_{\Gamma - s^*} \begin{bmatrix} p^*_{11} & p^*_{12} \\ p^*_{21} & p^*_{22} \end{bmatrix} \begin{Bmatrix} u_1 \\ u_2 \end{Bmatrix} d\Gamma$$

The second integral in Equation 2.18 can be represented in matrix form as follows:

$$\int \begin{bmatrix} u_{11}^{*} & u_{12}^{*} \\ u_{21}^{*} & u_{22}^{*} \end{bmatrix} \begin{Bmatrix} p_1 \\ p_2 \end{Bmatrix} d\Gamma$$

Consider the integral $\int_{\Gamma} u_{11}^{*} \, p_1 \, d\Gamma$

since $\frac{\partial r}{\partial x_1} = \cos\theta$,

$$\int_{\Gamma} u_{11}^{*} \, p_1 \, d\Gamma = \frac{p_1}{8\pi G(1-\nu)} \lim_{r\to 0} \int_{s^*} [(3-4\nu)\ln\frac{1}{r} + 2\cos^2\theta] \, r d\theta + p_1 \int_{\Gamma - s^*} u_{11}^{*} \, d\Gamma$$

$$= \frac{-p_1(3-4\nu)}{8\pi G(1-\nu)} \lim_{r\to 0} \theta r \ln r + p_1 \int_{\Gamma - s^*} u_{11}^{*} \, d\Gamma$$

$$= \frac{-p_1(3-4\nu)}{8\pi G(1-\nu)} \lim_{r\to 0} \frac{\ln r}{\frac{1}{r}} \theta + p_1 \int_{\Gamma - s^*} u_{11}^{*} \, d\Gamma$$

using L'Hopital's rule

$$\therefore \int_{\Gamma} u_{11}^{*} \, p_1 \, d\Gamma = \frac{p_1(3-4\nu)}{8\pi G(1-\nu)} \lim_{r\to 0} \frac{\frac{1}{r}}{\frac{1}{r^2}} \theta + p_1 \int_{\Gamma - s^*} u_{11}^{*} \, d\Gamma$$

$$= \frac{p_1(3-4\nu)}{8\pi G(1-\nu)} \lim_{r\to 0} r\theta + p_1 \int_{\Gamma - s^*} u_{11}^{*} \, d\Gamma$$

$$= p_1 \int_{\Gamma - s^*} u_{11}^{*} \, d\Gamma$$

Next consider the integral $\int_{\Gamma} u_{12}^{*} p_2 \, d\Gamma$

$$\int_{\Gamma} u_{12}^{*} p_2 \, d\Gamma = \frac{p_2}{8\pi G(1-\nu)} \lim_{r \to 0} \int_{s^*} 2 \cos^2\theta \, r d\theta + p_2 \int_{\Gamma - s^*} u_{12}^{*} \, d\Gamma$$

$$= p_2 \int_{\Gamma - s^*} u_{12}^{*} \, d\Gamma$$

Also

$$\int_{\Gamma} u_{21}^{*} p_1 \, d\Gamma = p_1 \int_{\Gamma - s^*} u_{21}^{*} \, d\Gamma$$

In a similar manner it can be proved that the $\int_{\Gamma} u_{22}^{*} p_2 \, d\Gamma$

$$= \int_{\Gamma - s^*} u_{22}^{*} p_2 \, d\Gamma$$

Appendix B

The elements of the matrix [G] are in general obtained by a numerical integration using the Gaussian Quadrature. However when z coincides with an analytical technique is used to derive the submatrix given by the following expression for constant boundary element.

$$\begin{bmatrix} G_{11} & G_{12} \\ G_{21} & G_{22} \end{bmatrix} = \int \begin{bmatrix} u^*_{11} & u^*_{12} \\ u^*_{21} & u^*_{22} \end{bmatrix} d\Gamma$$

The detailed derivation for the various terms in the above submatrix follows:

$$G_{11} = \frac{1}{8\pi G(1-\nu)} \left[(3-4\nu) \int_\Gamma \ln\left(\frac{1}{r}\right) d\Gamma + \int_\Gamma \left(\frac{\partial r}{\partial x_1}\right)^2 d\Gamma\right]$$

$$= \frac{1}{8\pi G(1-\nu)} \left[2(3-4\nu) \int_0^R \ln\left(\frac{1}{r}\right) dr + 2 \int_0^R \cos^2\theta dr\right]$$

$$= \frac{1}{8\pi G(1-\nu)} \left[2(3-4\nu) \left[r \ln \frac{1}{r} + r\right]_0^R + 2 R \cos^2\theta\right]$$

$$= \frac{R}{4\pi G(1-\nu)} \left[(3-4\nu)(1-\ln R) + \frac{r_1^2}{4R^2}\right]$$

$$G_{12} = \frac{2}{8\pi G(1-\nu)} \int_0^R \frac{\partial r}{\partial x_1} \cdot \frac{\partial r}{\partial x_2} \, d\Gamma$$

$$= \frac{2}{8\pi G(1-\nu)} \int_0^R \sin\theta \cos\theta \, dr = \frac{2R \sin\theta \cos\theta}{8\pi G(1-\nu)}$$

$$= \frac{r_1 \, r_2}{16R\pi G(1-\nu)} = G_{21}$$

$$G_{22} = \frac{1}{8\pi G(1-\nu)} \left[2(3-4\nu) \int_0^R \ln \frac{1}{r} \, d\Gamma + 2 \int_0^R \left(\frac{\partial r}{\partial x_2}\right)^2 d\Gamma \right]$$

$$= \frac{R}{4\pi G(1-\nu)} \left[(3-4\nu)\,(1-\ln R) + \frac{r_2^2}{4R^2}\right]$$

The definitions for r_1 and r_2 and θ are given in Figure 2.8.

Appendix C

The element of the matrix represented by the first integral in Equation 2.18 were derived in Appendix A where the boundary was assumed to be smooth. Even when the boundary is not smooth, a procedure similar to that given in Appendix A can be used. This time however the limits of integration are not $-\theta_1$ to $\pi-\theta_1$ but depend on the angle included between the two sides forming the corner as shown in Figure 2.9b.

Consider the integral $p^*_{11}\, u_1\, d$. If the fundamental solution is substituted in the integral it is seen that

$$\int_\Gamma p^*_{11}\, u_1\, d\Gamma = u_1 \int_{-(\pi-\frac{\alpha}{2}-\gamma)}^{\pi-\frac{\alpha}{2}+\gamma} -\frac{1}{4\pi(1-\nu)r}\left\{(1-2\nu) + 2\left(\frac{\partial r}{\partial x_1}\right)^2\right\} d\Gamma + \int_{\Gamma-s^*} u_1\, p^*_{11}\, d\Gamma$$

$$= u_1 \int_{-\pi+\frac{\alpha}{2}+\gamma}^{\pi-\frac{\alpha}{2}+\gamma} -\frac{1}{4\pi(1-\nu)r}\left\{(1-2\nu) + 2\cos^2\theta\right\} r\, d\theta + \int_{\Gamma-s^*} u_1\, p^*_{11}\, d\Gamma$$

$$= -\frac{u_1}{4\pi(1-\nu)}\left[(2-2\nu)\theta + \frac{\sin 2\theta}{2}\right]_{\pi-\frac{\alpha}{2}+\gamma}^{\pi-\frac{\alpha}{2}+\gamma} + \int_{\Gamma-s^*} u_1\, p^*_{11}\, d\Gamma$$

$$= -\frac{u_1}{4\pi(1-\nu)}\left[(2-2\nu)\left\{\pi - \frac{\alpha}{2} + \gamma + \pi - \frac{\alpha}{2} - \gamma\right\}\right.$$

$$\left. + \frac{1}{2}\left\{\sin(2\pi - \alpha + 2\gamma) - \sin(-2\pi + \alpha + 2\gamma)\right\}\right] + \int_{\Gamma-s^*} u_1\, p^*_{11}\, d\Gamma$$

$$= -\frac{u_1}{4\pi(1-\nu)}\left[2(1-\nu)(2\pi-\alpha)+\frac{1}{2}\{(\sin 2\gamma\cos\alpha - \cos 2\gamma\sin\alpha)\right.$$

$$\left. - (\sin\alpha\cos 2\gamma + \cos\alpha\sin 2\gamma)\}\right] + \int_{\Gamma-s^*} u_1\, p^*_{11}\, d\Gamma$$

$$= -\frac{1}{4\pi(1-\nu)}\left[2(1-\nu)(2\pi-\alpha) - \sin\alpha\cos 2\gamma\right] + \int_{\Gamma-s^*} u_1\, p^*_{11}\, d\Gamma$$

$$= -\frac{2\pi-\alpha}{2\pi} + \frac{1}{4\pi(1-\nu)}\sin\alpha\cos 2\gamma + \int_{\Gamma-s^*} u_1\, p^*_{11}\, d\Gamma$$

$$= -\left(1-\frac{\alpha}{2\pi} - \frac{1}{4\pi(1-\nu)}\sin\alpha\cos 2\gamma\right) + \int_{\Gamma-s^*} u_1\, p^*_{11}\, d\Gamma$$

Next consider the integral $\int p^*_{12}\, u_2\, d\Gamma$. It is easily seen that,

$$\int_{\Gamma} p^*_{12}\, u_2\, d\Gamma = u_2 \int_{-(\pi-\frac{\alpha}{2}-\gamma)}^{\pi-\frac{\alpha}{2}+\gamma} -\frac{1}{4\pi(1-\nu)r}\left(2\frac{\partial r}{\partial x_1}\cdot\frac{\partial r}{\partial x_2}\right) d\Gamma + \int_{\Gamma-s^*} p^*_{12}\, u_2\, d\Gamma$$

$$= u_2 \int_{-\pi+\frac{\alpha}{2}+\gamma}^{\pi-\frac{\alpha}{2}+\gamma} -\frac{1}{4\pi(1-\nu)r}(2\sin\theta\cos\theta)\, r d\theta + \int_{\Gamma-s^*} p^*_{12}\, u_2\, d\Gamma$$

$$= -u_2 \int_{-\pi+\frac{\alpha}{2}+\gamma}^{\pi-\frac{\alpha}{2}+\gamma} \frac{1}{4\pi(1-\nu)}\sin 2\theta\, d\theta + \int_{\Gamma-s^*} p^*_{12}\, u_2\, d\Gamma$$

$$= \frac{u_2}{4\pi(1-\nu)} \left[\frac{\cos 2\theta}{2}\right]_{-\pi + \frac{\alpha}{2} + \gamma}^{\pi - \frac{\alpha}{2} + \gamma} + \int_{\Gamma - s^*} p^*_{12}\, u_2\, d\gamma$$

$$= \frac{u_2}{4\pi(1-\nu)} \sin 2\gamma \sin\alpha + \int_{\Gamma - s^*} p^*_{21}\, u_1\, d\Gamma$$

In a similar manner it can be shown that

$$\int_{\Gamma} p^*_{22}\, u_2\, d\Gamma = -\left(1 - \frac{\alpha}{2\pi} + \frac{1}{4\pi(1-\nu)} \cos 2\gamma \sin\alpha\right) u_2$$

$$+ \int_{\Gamma - s^*} p^*_{22}\, u_2\, d\Gamma$$

The first integral in Equation 2.18 thus becomes:

$$\int \begin{bmatrix} p^*_{11} & p^*_{12} \\ p^*_{21} & p^*_{22} \end{bmatrix} \begin{Bmatrix} u_1 \\ u_2 \end{Bmatrix} d\Gamma = - \begin{bmatrix} c_{11} & c_{12} \\ c_{21} & c_{22} \end{bmatrix} \begin{Bmatrix} u_1 \\ u_2 \end{Bmatrix}$$

$$+ \int_{\Gamma - s^*} \begin{bmatrix} p_{11} & p_{12} \\ p_{21} & p_{22} \end{bmatrix} \begin{Bmatrix} u_1 \\ u_2 \end{Bmatrix} d\Gamma$$

where

$$c_{11} = 1 - \frac{\alpha}{2\pi} - \frac{1}{4\pi(1-\nu)} \sin\alpha \cos 2\gamma$$

$$c_{12} = c_{21} = \frac{-1}{4\pi(1-\nu)} \sin 2\gamma \sin\alpha$$

$$c_{22} = 1 - \frac{\alpha}{2\pi} + \frac{1}{4\pi(1-\nu)} \cos 2\gamma \sin\alpha$$

Appendix D

The elements of a submatrix of [G] applicable to coincident points j and z were derived for the constant element case in Appendix B. A similar derivation applies to the case of linear element.

Refer to Figure 2.12 which shows an element MF and the local coordinate system x_1 and x_2 Now define,

$$\phi_1 = 1 - \frac{x}{\ell} \text{ and } \phi_2 = \frac{x}{\ell} \text{ and } r = x$$

The elements of the submatrix [G] are then given by the following expression,

$$[G] = \begin{bmatrix} G^F_{11} & G^F_{12} \\ G^F_{21} & G^F_{22} \end{bmatrix} + \begin{bmatrix} G^B_{11} & G^B_{12} \\ G^B_{21} & G^B_{22} \end{bmatrix}$$

where

$$\begin{bmatrix} G^F_{11} & G^F_{12} \\ G^F_{21} & G^F_{22} \end{bmatrix} = \int_{\Gamma_J} \phi_1 \begin{bmatrix} u^*_{11} & u^*_{12} \\ u^*_{21} & u^*_{22} \end{bmatrix} d\Gamma \quad \text{and}$$

$$\begin{bmatrix} G^B_{11} & G^B_{12} \\ G^B_{21} & G^B_{22} \end{bmatrix} = \int_{\Gamma_{J-1}} \phi_2 \begin{bmatrix} u^*_{11} & u^*_{12} \\ u^*_{21} & u^*_{22} \end{bmatrix} d\Gamma$$

The derivation of these elements follows.

$$G_{11}^{F} = \frac{1}{8\pi G(1-\nu)} \left[(3-4\nu) \int_0^{\ell} \ln\left(\frac{1}{r}\right) \phi_1 \, dr + \int_0^{\ell} \left(\frac{\partial r}{\partial x_1}\right)^2 \phi_1 \, dr \right.$$

$$= \frac{1}{8\pi G(1-\nu)} \left[(3-4\nu)\left\{ \int_0^{\ell} \ln\left(\frac{1}{r}\right) dr - \frac{1}{\ell} \int_0^{\ell} \ln\left(\frac{1}{r}\right) r \, dr \right\} \right.$$

$$\left. + \cos^2\phi \int_0^{\ell} dr - \frac{1}{\ell} \int_0^{\ell} r dr \right]$$

$$= \frac{1}{8\pi G(1-\nu)} \left[(3-4\nu)\left\{ \ell(1-\ln\ell) - \frac{\ell}{4}(1-2\ln\ell) \right\} \right.$$

$$\left. + \cos^2\phi \left\{ \ell - \frac{1}{\ell}\left(\frac{\ell}{2}\right)^2 \right\} \right]$$

$$= \frac{1}{8\pi G(1-\nu)} \left[(3-4\nu) \left\{ (1-\ln \ell) - \frac{1}{4}(1-2\ln\ell) \right\} + \frac{r_1^2}{2\ell^2} \right]$$

$$G_{12}^{F} = \frac{1}{8\pi G(1-\nu)} \left[\int_0^{\ell} \frac{\partial r}{\partial x_1} \cdot \frac{\partial r}{\partial x_2} \cdot \phi_1 \, dr \right]$$

$$= \frac{1}{8\pi G(1-\nu)} \sin\theta \cos\theta \left(\ell - \frac{\ell}{2}\right)$$

$$= \frac{r_2 \, r_1}{16\pi G(1-\nu)\ell} = G_{21}^{A}$$

$$G_{22}^{F} = \frac{1}{8\pi G(1-\nu)} \left[(3-4\nu) \int_0^{\ell} \ln\left(\frac{1}{r}\right) \phi_1 \, dr + \int_0^{\ell} \left(\frac{\partial r}{\partial x_2}\right)^2 \phi_1 \, dr \right.$$

$$= \frac{\ell}{8\pi G(1-\nu)} \left[(3-4\nu) \{(1-\ln(\ell)) - \frac{1}{4}(1-2\ln(\ell))\} \right.$$

$$+ \frac{r_2^2}{2\ell^2}$$

$$G_{11}^{B} = \frac{1}{8\pi G(1-\nu)} \left[(3-4\nu) \int_0^{\ell} \ln\left(\frac{1}{r}\right) \phi_2 \, dr + \int_0^{\ell} \left(\frac{\partial r}{\partial x_1}\right)^2 \phi_2 \, dr \right.$$

$$= \frac{1}{8\pi G(1-\nu)} \left[(3-4\nu)\{ \int_0^{\ell} \frac{1}{\ell} \ln\left(\frac{1}{r}\right) dr\} + \frac{\cos^2\theta}{\ell} \int_0^{\ell} r dr \right.$$

$$= \frac{1}{8\pi G(1-\nu)} \left[(3-4\nu)\{ \frac{\ell^2}{4\ell}(1-2\ln\ell)\} + \frac{\cos^2\theta}{\ell} \cdot \frac{\ell^2}{2} \right]$$

$$= \frac{\ell}{8\pi G(1-\nu)} \left[(3-4\nu)\{ \frac{1}{4}(1-2\ln(\ell)\} + \frac{r_1^2}{2\ell^2} \right]$$

$$G_{12}^{B} = \frac{1}{8\pi G(1-\nu)} \sin\theta \cos\theta \left(\frac{\ell^2}{2\ell}\right) = \frac{\ell \sin\theta \cos\theta}{16\pi G(1-\nu)}$$

$$= \frac{r_2 \, r_1}{16\pi G(1-\nu)} = G_{21}^{B}$$

$$G^B_{22} = \frac{1}{8\pi G(1-\nu)} \left[(3-4\nu) \int_0^{\ell} \ln\left(\frac{1}{r}\right) \phi_2 \, dr + \int_0^{\ell} \left(\frac{\partial r}{\partial x_2}\right)^2 \phi_2 \, dr \right.$$

$$= \frac{\ell}{8\pi G(1-\nu)} \left[(3-4\nu) \left\{\frac{1}{4} (1-2\ln(\ell))\right\} + \frac{r_2^2}{2\ell^2} \right]$$

The definitions for r_1 and r_2 are given in Figure 2.12.

REFERENCES

1. Boissenot, J.M., Lochat, J.C. and Watson, J.O., "Etude par Equations Integrals d'une Eprouvette CT15, Revue de Physique Appliquée 9 (1974) 611-615.

2. Bowes, W.H. and Russell, L.T., "Stress Analysis by the Finite Element Method for Practicing Engineers", D. C. Heath and Company, 1975.

3. Brebbia, C.A., "The Boundary Element Method for Engineers", Pentech Press, London, 1978.

4. Brebbia, C.A., "Recent Advances in Boundary Element Methods", Pentech Press, London, 1978.

5. Brebbia, C.A. and Georgiou, P., "Combination of Finite and Boundary Elements for Elastostatics", Appl. Math. Modelling, 1979, Vol.3, June

6. Brady, B.H.G. and Bray, J.W., "The Boundary Element Method for Determining Stresses and Displacements Around Long Openings in a Triaxial Stress Field", Int. J. Roch. Mech. Min. Sci. & Geomech. Abstr. Vol.15, pp.21-28, Pergamon Press, 1978.

7. Cruse, T.A., "Numerical Solutions in Three-Dimensional Elastostatics, Int. J. Sol. Struct. 5 (1969), 1259-1274.

8. Cruse, T.A. and Vanburen, "Three-Dimensional Elastic Stress Analysis of a Fracture Specimen with an Edge Crack", Int. J. Fract. Mech. 7, 1.15 (1971).

9. Fredholm, "Solution d'un Foundamental de la théoriede L'élasticite. Arkiv fur Mathematik Astronomé und Fysik, 3, 1-8, (1905).

10. Hetenyi, M., 1946, "Beams on Elastic Foundation", University of Michigan Press.

11. Iyenger, Sundara Raja, K. T., 1965, "Matrix Analysis of Finite Beams on Elastic Foundations", Inst. of Eng. Journal (India), July.

12. Iwanczewska, A. and Lewandowki, J., 1968, "Oblicazanie Konstrukcji na sprezystym Podlozu", Arkady, Warsaw.

13. Jaswan, M.A. and Ponter, A.R., "Integral Equation Method in Potential Theory, 1, Proc. Roy. Soc. A 273 (1963).

14. Just, D.J., Starzewski, K. and Ronan, P.B. (1971). Finite Element Method of Analysis of Structures Resting on Elastic Foundations, Proc. Symposium on Foundation Structure Interaction, University of Birmingham, England.

15. Kumar, V. and Mukherjee, S. Int. J. Mech. Sci., 1977, 19, 713.

16. Love, A.E., "A Treatise on the Mathematical Theory of Elasticity", 4th ed., Dover, New York, 1944, 245.

17. McDonal, B.H. and Wexley, A., IEEE Trans. on Microwave Theory Techniques, MTT-20, No.12, December 1972.

18. Mei, C. Proc. X Symposium Noval Hydrodyn, 1975.

19. Mendelson, A., "Boundary Integral Methods in Elasticity and Plasticity NASA TN D-7418, November 1973.

20. Mukherjee, S. Int. J. Solids, Struct. 1977, 13, 331.

21. Osias, J.R. et. al., In Proc. First Symp. Numer. Analysis Appl. Eng. Sci. Versailles, France, 23-27, May 1977.

22. Rizzo, F. J., "An Integral Equation Approach to Boundary Value Problems of Classical Elastostatics, Quart. Appl. Math. 25 (1967) 83-95.

23. Selvadurai, A.P.S., "Elastic Analysis of Soil-Foundation Interaction", Elsevier Scientific Publishing Company, 1979.

24. Smith, G.D., "Numerical Solution of Partial Differential Equations. Finite Difference Methods". Clarendon Press, Oxford, 1978.

25. Symm, G.T., "Integral Equation Method in Potential Theory, 2, Proc. Roy. Soc. A275 (1963).

26. Swedlow, J.L. and Cruse, T.A., "Formulation of Boundary Integral Equation for Three-Dimensional Elasto-plastic Flow", Int. Journal Solids Structures, 1971, Vol.7, 1973.

27. Telles, J.C.F. and Brebbia, C.A., "Research Notes on the Application of the Boundary Element Method to Plasticity" Appl. Math. Modelling, 1979, 3, 466, December.

28. Timoshenko, S.P. and Goodiev, J.N., "Theory of Elasticity", Third Edition, McGraw Hill, 1970.

29. Zienkiewicz, O.C. et. al., Int. J. Numer. Meth. Eng., 1977, 11, 355.

30. Zienkiewicz, O.C., 1971, "The Finite Element Method in Engineering Science", McGraw-Hill, New York.

END

23 12 8 1

FIN